2009

ROLE OF OXIDATIVE STRESS AND T CELL HOMING IN THE DEVELOPMENT OF MURINE SYNGENEIC GRAFT-VERSUS-HOST DISEASE

Jacqueline Perez-Rodriguez
University of Kentucky, jprjackie@yahoo.com

ABSTRACT OF DISSERTATION

Jacqueline Perez-Rodriguez

The Graduate School

University of Kentucky

2009

ROLE OF OXIDATIVE STRESS AND T CELL HOMING IN THE DEVELOPMENT OF MURINE SYNGENEIC GRAFT-VERSUS-HOST DISEASE

ABSTRACT OF DISSERTATION

A dissertation submitted in partial fulfillment of the
requirements for the degree of Doctor of Philosophy in the
Graduate Center for Toxicology
at the University of Kentucky

By

Jacqueline Perez-Rodriguez

Lexington, Kentucky

Director: Dr. J.Scott Bryson, Associate Professor of Department of Medicine

Lexington, Kentucky

2009

ABSTRACT OF DISSERTATION

THE ROLE OF OXIDATIVE STRESS AND T CELLS IN THE DEVELOPMENT OF MURINE SYNGENEIC GRAFT-VERSUS-HOST-DISEASE

Syngeneic graft-versus-host disease (SGVHD) is induced by reconstituting lethally irradiated mice with syngeneic BM cells followed by a 21 day treatment with the immunosuppressive agent cyclosporine A (CsA). Clinical symptoms of the disease appear 2-3 weeks following cessation of CsA therapy and disease-associated inflammation occurs primarily in the colon and liver.

The development of SGVHD is a complex process resulting from the cooperative interaction of multiple effector cell populations including NK cells, T cells and macrophages. T_H1 cytokines (IL-12, TNF-α, IFN- γ), produced by these effector cells, serve as inflammatory mediators contributing to the pathogenesis of SGVHD. The SGVHD conditioning agents, irradiation and CsA, are both required for the development of disease and contribute to the production of oxidative stress. Time course studies revealed increased reactive oxygen and nitrogen species (ROS/RNS), as well as, increased colon mRNA levels for TNF-α and iNOS in CsA-treated versus control BMT animals. Since ROS/RNS are known to mediate CsA toxicity, studies were undertaken to determine the effect of oxidative stress on the induction of SGVHD. *In vivo* treatment with the antioxidant MnTBAP caused a reduction in colon mRNA levels for iNOS and TNF-α, as well as delayed disease development, suggesting a role for oxidative stress in the development of SGVHD.

In addition, $CD4^+$ T cells have been shown to play an important role in the inflammatory response observed in the gut of SGVHD mice. Time course studies revealed significant increases in the migration of $CD4^+$ T cells as early as day 14 post-BMT into the colon of CsA mice as well as significant elevated mRNA levels of cell adhesion molecules. Homing studies revealed that a labeled $CD4^+$ T cell line, generated from SGVHD mice, migrated in larger numbers into the gut of CsA-treated mice compared to control animals. This study demonstrated that $CD4^+$ T cells responsible for the pathogenesis observed in murine SGVHD are present early after BMT in colons of CsA-treated mice, suggesting that during the 21 days of immunosuppression therapy functional mechanisms are in place that result in increased homing of effector cells to colons of CsA-treated mice.

Key Words: Reactive Oxygen/Nitrogen Species (ROS/RNS), Manganese (III) meso-tetrakis (4-benzoic acid) porphyrin (MnTBAP), Cell Adhesion Molecules (CAM), β_7 integrin, T cell homing

Jacqueline Perez-Rodriguez

Student's Signature

9/22/2009

Date

ROLE OF OXIDATIVE STRESS AND T CELL HOMING IN THE DEVELOPMENT OF MURINE SYNGENEIC GRAFT-VERSUS-HOST DISEASE

By

Jacqueline Perez-Rodriguez

J. Scott Bryson

Director of Dissertation

David K. Orren

Director of Graduate Studies

9/22/2009

Date

RULES FOR THE USE OF DISSERTATIONS

Unpublished dissertations submitted for the Doctor's degree and deposited in the University of Kentucky Library are as a rule open for inspection, but are to be used only with due regard to the rights of the authors. Bibliographical references may be noted, but quotations or summaries of parts may be published only with the permission of the author, and with the usual scholarly acknowledgments.

Extensive copying or publication of the dissertation in whole or in part also requires the consent of the Dean of the Graduate School of the University of Kentucky.

A library that borrows this dissertation for use by its patrons is expected to secure the signature of each user.

Name	Date

DISSERTATION

Jacqueline Perez-Rodriguez

The Graduate School

University of Kentucky

2009

ROLE OF OXIDATIVE STRESS AND T CELL HOMING IN THE DEVELOPMENT OF MURINE SYNGENEIC GRAFT-VERSUS-HOST DISEASE

DISSERTATION

A dissertation submitted in partial fulfillment of the
requirements for the degree of Doctor of Philosophy in the
Graduate Center for Toxicology
at the University of Kentucky

By

Jacqueline Perez-Rodriguez

Lexington, Kentucky

Director: Dr. J.Scott Bryson, Associate Professor of Department of Medicine

Lexington, Kentucky

2009

DEDICATION: ALONDRA J. GONZALEZ-PEREZ

ACKNOWLEDGMENTS

The following dissertation, while an individual work, benefited from the insights and direction of several people. First, I would like to thank my mentor, Dr. J. Scott Bryson for accepting me into his laboratory and guiding me through the correct path for the last four years. He has taught me to be a better investigator, a better communicator and has pushed me to be independent. This dissertation would not be possible without his support.

I would also like to thank the other members of my committee, Dr. Alan Kaplan, Dr. Donald Cohen and Dr. Willem De Villiers for their support, instructive comments and encouragement at every stage of this period study. I appreciate all of their time and provided insights that guided and challenged my thinking, making possible this final dissertation.

I would also like to thank the help of my co-worker and friend Dr. Ja A. Brandon for his continued conversations, suggestions and assistance throughout these years. Thank you Dr. Maria Bruno for your help in related experimental and written aspects of my project. I would also like to thank Dr. Mary Vore for providing on-going support and encouragement throughout this entire process. Their support and help made this experience a positive one.

Finally, I would like to thank the important assistance from my family and friends, specially my mother Dulce, my father Hery, my brother Erie, my sister Sandra, my aunt Rochy, my husband Angel and my beloved daughter Alondra. I am who I am because of them. Thanks for your continuous support and bearing by my side through the difficult times. They instilled in me the determination to work toward my goals. Thank you for all you have done. I love you very much.

TABLE OF CONTENTS

Acknowledgments....iii

List of Tables....vii

List of Figures....viii

Chapter One: Introduction

1.1 Bone Marrow Transplantation....1

1.2 Allogeneic graft-versus-host disease....5

1.3 Syngeneic graft-versus-host disease....9

1.4 Role of T cells in SGVHD....11

1.5 Proinflammatory mediators and SGVHD....15

1.6 Oxidative Stress and SGVHD....16

1.7 Lymphocyte homing to inflammatory sites....19

Chapter Two: Material and Methods

2.1 Mice....27

2.2 Induction of SGVHD....27

2.3 Evaluation of SGVHD....28

2.4 *In vivo* treatment with the antioxidant MnTBAP....29

2.5 *In vivo* neutralization of TNF-α....30

2.6 Isolation of peripheral lymphoid cells....30

2.7 Treatment of lymphocytes with DCFH-DA....31

2.8 Isolation of immune cells from the colon....31

2.9 Flow cytometry analysis....33

2.10 Immunohistochemical staining....34

2.11 Real Time Reverse Transcription-Polymerase Chain Reaction (RT-PCR) for cytokine message....35

2.12 Measurement of plasma NO....36

2.13 SG6 cell line....38

2.14 Determination of Protein content using Bio-Rad assay 39
2.15 Labeling of SG6 cells with (CFSE) 40
2.16 In vivo homing of labeled SG6 cells 40
2.17 Statistics 41
Chapter Three: Role of oxidative stress in SGVHD
3.1 Synopsis 51
3.2 Determination of intracellular reactive oxygen species 52
3.3 Increased NO production in CsA-treated mice 53
3.4 Reduction of Oxidative Stress during CsA therapy alters the development of SGVHD 54
3.5 Decreased iNOS and TNF-α mRNA levels after MnTBAP therapy during CsA treatment 55
3.6 Effect of MnTBAP treatment during CsA therapy on generation of oxidative stress 56
3.7 Reduction of Oxidative Stress post-CsA therapy alters the development of SGVHD 56
3.8 Summary 58
Chapter Four: Role of T cell homing in SGVHD
4.1 Synopsis 73
4.2 Enhanced $CD4^+\alpha\beta TCR^+$ T cells in colons of CsA-treated mice compared to control BMT 74
4.3 Increased Proinflammatory Mediators and Cell Adhesion Molecules (CAM) during SGVHD 75
4.4 Increased homing of labeled SGVHD T cells into the colons of CsA-treated mice 77
4.5 $CD4^+$ T cell migration into the liver 79
4.6 Summary 80

Chapter Five: Discussion

5.1 Synopsis 94

5.2 Role of oxidative stress in SGVHD 95

5.3 Role of T cell homing in SGVHD 102

5.4 Proposed mechanism underlying oxidative stress and T cell role in the pathogenesis observed in murine SGVHD 108

5.5 Future directions 110

Apendendix

Reagent preparation 113

References 116

Vita 128

LIST OF TABLES

Table 2.1 SGVHD Grading scale for colon and liver tissues 43

Table 2.2 Antibodies used for FACs analysis..... 46

Table 2.3 Antibodies used for immunohistochemistry (IHC) analysis..... 47

Table 2.4 Real Time RT-PCR reaction conditions for mRNA analysis 48

Table 2.5 Polymerase chain reaction (PCR) primers and conditions 49

LIST OF FIGURES

Figure 1.1 CsA inhibition of the calcineurin signaling pathway in T cells 23
Figure 1.2 Nitric oxide generation from L-arginine oxidation 24
Figure 1.3 Generation and detoxification of ROS/RNS 25
Figure 1.4 Attachment of T cells to the endothelium and extravasation 26
Figure 2.1 The induction of murine syngeneic graft-versus-host disease 42
Figure 2.2 In vivo treatment with the antioxidant MnTBAP..... 44
Figure 2.3 In vivo neutralization of TNF-α 45
Figure 3.1 Elevated ROS in mice treated with CsA compared to control BMT 59
Figure 3.2 Increase reactive nitrogen species in CsA-treated mice 60
Figure 3.3 Increased levels of nitrotyrosine in the colons of CsA-treated mice..... 61
Figure 3.4 MnTBAP treatment delayed the development of SGVHD 62
Figure 3.5 MnTBAP therapy resulted in decreased colonic iNOS and TNF-α 64
Figure 3.6 MnTBAP therapy did not reduce IL-12 or IFN-γ mRNA levels..... 65
Figure 3.7 Reduced nitrotyrosine staining after antioxidant therapy..... 66
Figure 3.8 Delayed SGVHD after MnTBAP treatment post-CsA..... 67
Figure 3.9 MnTBAP therapy reduced mRNA levels of iNOS 69
Figure 3.10 Decreased RNS in colon of CsA-treated mice after MnTBAP therapy 70
Figure 3.11 Colon pathology was not altered by MnTBAP treatment 71
Figure 3.12 Migration of T cells into the colon was not reduced by MnTBAP 72
Figure 4.1 Enhanced numbers of $CD4^+$ IEL and LPL isolated from CsA-treated animals 81
Figure 4.2 Elevated CD4 expression in colonic tissue of CsA-treated mice compared to control BMT..... 82
Figure 4.3 Increased production of TNF-α in colonic tissue of CsA-treated mice..... 83
Figure 4.4 Elevated levels of CAM mRNA in the colon of CsA-treated mice compared to control BMT 84

Figure 4.5 Increased presence of MAdCAM-1 in colonic tissue of CsA-treated mice compared to control BMT 86
Figure 4.6 SGVHD induction results in increased production of proinflammatory chemokines in the colon 87
Figure 4.7 SGVHD T cell line express a $CD4^+\beta_7integrin^+$ phenotype 89
Figure 4.8 SGVHD $CD4^+$ T cell line proliferate against bacterial-Ag pulsed DC 90
Figure 4.9 Increased homing of $CD4^+$ T cells into the gut of CsA-treated mice 91
Figure 4.10 Elevated $CD4^+$ T cell expression in liver tissue of SGCHD mice 92
Figure 4.11 MAdCAM-1 expression post-BMT in liver tissue 93
Figure 5.1 Role of oxidative stress and T cell homing in SGVHD 112

CHAPTER ONE: INTRODUCTION

1.1 Bone Marrow Transplantation

Bone marrow transplantation (BMT) is a medical procedure that was first applied in 1968 to treat severe combined immunodeficiency diseases (SCID). In these studies bone marrow (BM), taken from a major histocompatibility complex (MHC)-matched donor, was able to correct the immunological deficiency of a patient with Wiscott-Aldrich Syndrome (WAS) [1]. Since its first successful use, BMT/hematopoietic stem cell transplantation (HCT) has been used as a treatment of choice for many diseases (i.e. leukemia, aplastic anemia, immune deficiency disorders, etc.). The major complications of BMT, graft rejection and graft-versus-host disease (GVHD) are the direct consequence of human leukocyte antigen (HLA) (in mouse major histocompatibility complex, (MHC)) polymorphisms. The major HLA are essential components of the immune system and have different functions. HLA class I antigens (A, B and C) present to T cells peptides that are derived from endogenous cell components (or of viral origin), which are produced from digested proteins that are broken down in the proteosomes. $CD8^+$ killer T cells are activated by the foreign antigens presented by HLA class I antigens and are the effector cells responsible for the destruction of intracellular pathogens. HLA class II antigens (DP, DQ and DR) present exogenous antigens derived from outside of the cell to $CD4^+$ T helper cells [2]. Helper T cells can be classified as to the types of cytokines they produce and the nature of the adaptive immune response they generate. $CD4^+$ T helper 1 (T_H1) cells enhance cellular immune responses against intracellular pathogens via the production of interferon γ (IFN-γ), that enhances macrophage activation and killing [2,

3]. T_H2 cells are involved in enhancing humoral immune responses via the production of interleukin 4 (IL-4) and IL-5 [2, 3]. Finally, a recently described population of T helper cells, T_H17 cells, secrete IL-17 and participate in the response against extracellular pathogens [4, 5].

The immune system uses the histocompatibility antigens to differentiate self from non-self. Upon infection, antigen presenting cells (APC) recognize the pathogen by their surface receptors (i.e toll like receptors (TLR)/pattern recognition receptors) and allow binding by common constituents in the cell surface of the pathogen (i.e lipids, carbohydrates, peptides or nucleic acids). This interaction allows the APC to engulf the foreign pathogen through a process called phagocytosis. The ingested pathogen is contained within a vesicle called phagosome that fuses with lysosomes, which are acidified organelles containing degradative enzymes, to form a phagolysosome. Lysosomal enzymes degrade the pathogen into small pieces. After encountering the pathogen and taking it up in infected tissue, the APC becomes activated/mature and carries pathogen antigens to peripheral lymphoid organs where they present them to T lymphocytes [2]. This process allows for the digestion of proteins into small peptides, which are then presented by self MHC class II to T helper cells or MHC class I to $CD8^+$ T cells. This allows for immune responses to take place and elimination of the pathogen. As the response is generated in the context of self-MHC, known as MHC restriction, self-reactivity is avoided. As T cells mature in the thymus, they first recognize peptides bound to self MHC expressed by thymic APC. Immature T cells, capable of binding to self-peptide-self MHC complexes at a proper affinity, undergo positive selection. If these immature T cells have high affinity and/or cross reactivity for these self-peptides/MHC

complexes they are eliminated by negative selection to avoid autoimmunity. Mature T cells exit the thymus and migrate to the periphery where they encounter APC with foreign-peptide-self MHC antigens and initiate an immune response. If on the other hand, they encounter APC expressing self-peptides they do not react, a concept known as self tolerance which prevents autoimmunity. However, if these T cells react to MHC molecules, that they did not encounter during thymic development, it can lead to alloreactivity. More than 1% of T cells can be activated by foreign (allogeneic) MHC molecules [2]. This is a very high percentage relative to that observed in an immune response to nominal antigen where the frequency of reactive T cells is on the order of 1:50,000–300,000 T cells in unprimed individuals and ~1:1000–10,000 T cells in primed individuals [6, 7].

The two major complications of allogeneic BMT are graft rejection and GVHD which develop when T cells from one individual recognizes the other's individuals MHC as foreign and respond against it [2, 8]. MHC polymorphisms are not the only donor-host disparities that are involved in graft rejection. Differences in minor histocompatibility antigens (miHA) can also cause the graft to be rejected slowly as well as to induce GVHD [2, 9, 10]. Minor histocompatibility antigens are peptides derived from allogeneic proteins that exist in various isoforms and can affect the fate of a graft by provoking cell-mediated immune responses [9, 11]. In mice and other species there are at least 30 such antigens [12]. While $CD4^+$ and $CD8^+$ participate in the immune response directed against MHC antigens, $CD8^+$ T cells are mainly responsible for immunity directed against miHA [13, 14].

Bone marrow transplants are classified based on the source of the donor marrow: syngeneic if the BM is from an identical twin, autologous if it is isolated from the patient or allogeneic if it is isolated from a HLA-matched sibling or unrelated donor. Allogeneic BM recipients usually receive pretransplant conditioning regimens which include high doses of chemotherapy and/or irradiation [15-18]. This therapy allows for the maximal destruction of the abnormal cells causing the disease, typically malignant cells, as well as, to eliminate the recipient's hematopoietic/immune system that is required to avoid immune responses against the donor cells and to allow proper engraftment, i.e. prevent graft rejection [19, 20]. Alloantigens associated with the MHC molecules (Human: HLA-A, B, C, DR, DQ; Mouse: H-2, I-E, I-A and miHA) are the major target of alloreactive T cells that mediate patient immune reactivity against the donor BM underlying graft rejection and GVHD after BMT [20, 21]. Most transplants preferentially take place between donor and recipients that are HLA-matched siblings over HLA-matched unrelated donors to reduce the possibility of graft rejection. During graft rejection, the host's immune system initiates an effective response in which T lymphocytes recognize the allo-MHC antigens as foreign and attack the transplanted tissue and destroy it [2]. Because of this destructive immune response, tissues from the patient and from potential donors must be typed and matched as completely as possible before transplants are performed to reduce the probability of graft rejection. Santos et al. described three prerequisites for an effective conditioning to take place. First, the regimen must suppress the recipient's immunity to avoid graft rejection. Second, it must create a "space" in the marrow microenvironment to allow establishment and growth of hematopoietic progenitors. And third, for patients with malignant diseases, the conditioning must have

an antitumor effect to eradicate residual tumor cells [22]. Thus, unless the recipient and donor are identical twins, all recipients receiving BMT should undergo immunosuppressive therapy.

1.2 Allogeneic graft-versus-host disease

Graft-versus-host disease remains a major complication following allogeneic BMT. In 1967, Billingham described three requirements for GVHD to take place: First, the graft must contain immunologically competent cells (which are now known to be T cells); second, the recipient must express tissue antigens that are not present in the transplant donor; and third, the patient must be incapable of mounting an effective response to eliminate the transplanted cells [23]. GVHD takes place when T cells in the graft respond to HLA proteins on host cells and the frequency of this disease is directly related to the degree of mismatch that exists between HLA proteins [24]. Reports show that GVHD occurs in 25-60% of patients who receive BM from an HLA-identical related donor and in 45-70% of recipients from matched unrelated donor [15, 25, 26]. As a consequence, approximately 50% of patients who might benefit from BMT cannot find a suitable match related or unrelated donor to be able to benefit from this therapeutic option. Ferrara et al. has described the pathophysiology of GVHD as a multifaceted process that occurs in three stages [17, 27]: (1) preconditioning regimens (i.e. high doses of chemotherapy) results in damage to host tissues leading to increased proinflammatory rmed inces, such as tumor necrosis factor-alpha (TNF-α) and interleukin-1 (IL-1), amplified expression of adhesion molecules and MHC antigens in target organs (intestine, liver skin) [28-31] allowing the migration of effectors cells to the site of inflammation; (2) recognition of alloantigens on host APC by donor T cells, results in T

cell proliferation, differentiation and secretion of T_H1 cytokines (IFN-γ and IL-2); and (3) effector cell activation (i.e. macrophages, natural killer cells, cytotoxic T lymphocytes) that act in concert with the cytokines described above to cause further tissue injury. Finally, it has been demonstrated that mature alloreactive T cells that contaminate the marrow and which are responsible for the second stage of this disease are able to initiate two forms of GVHD: acute and chronic [17].

In clinical GVHD, the acute phase is observed during the first 100 days post-transplant and is considered the major challenge of patients because of its high association with morbidity and mortality [32]. This stage is associated with damage to the liver (cholestatic hyperbilirubinaemia), skin and mucosa (maculopapular skin rash) and gastrointestinal (GI) tract (nausea, anorexia, watery and/or bloody diarrhea and severe abdominal pain) [26, 27]. The chronic phase normally occurs after 100 days and it adversely influences long-term survival. In addition to the organs damaged by acute GVHD, the chronic phase also affects nails, mouth, eyes, muscles, connective tissues, lung, kidneys, heart, marrow and female genitalia [27, 33]. Severity of acute GVHD is scored by the extent of involvement of the three main target organs (skin, liver and GI): grades are I (mild), II (moderate), III (severe), and IV (very severe). Severe GVHD has poor prognosis, with 25% long-term survival (5 years) for grade III disease and 5% for grade IV [34]. The relationship between acute and chronic GVHD is controversial. While some findings support the idea that the chronic phase is an extension of the acute stage [35, 36], others suggest that they appear separately [37, 38]. Atkinson et al. reported that acute and chronic are different diseases but share similar risk factors (HLA disparity,

female → male transplant, recipient age, etc.) and that the major risk factor for chronic GVHD is the prior occurrence of acute GVHD [36].

Mouse models have been important in the classification and understanding of the processes underlying GVHD. Different effector cells have been associated with the development of GVHD depending on the type of mismatch involved in the transplant. When donor and recipient differ at MHC Class II, $CD4^+$ T cells have been reported to be the effector cells responsible for the disease process [21, 39]. Conversely, when donor and recipient differ at MHC Class I, $CD8^+$ T cells are associated with disease induction [21, 40]. Meanwhile, the effector cells that cause GVHD in miHA mismatch models depends on the combination of strains used [41]. When the type of T_H immunity that was involved in the development of GVHD was analyzed, acute GVHD was dominated by a T_H1 response while the T cell response during chronic GVHD is driven primarily by a T_H2 type, characterized by the production of IL-4 and IL-10 cytokines [42, 43] and the production of autoantibodies [44]. Although the work is ongoing, recent studies within the last year or so have demonstrated a role for T_H17 immunity in the development of GVHD [45, 46].

Many approaches have been used over the years to minimize GVHD following BMT. One strategy includes T cell depletion (TCD) from the donor inoculum which has been reported to decrease GVHD but this treatment has been associated with increased rates of graft failure and relapse [25, 47, 48]. Reisner et al. demonstrated that depletion of T cells, with soybean or peanut agglutination, from mouse bone marrow and spleen cells suspensions resulted in successful reconstitution of lethally irradiated mice without complications due to GVHD [47]. In 1981, Valera et al. reported that *ex vivo* depletion of

T cells, with the use of monoclonal antibody against Thy 1.2, in a murine transplant model receiving MHC-mismatched BM prevented GVHD, indicating a role for T cells in this disease [48]. Due to the success of studies in animal models, human clinical trials using various methods of TCD have been used [25, 49]. These trials confirmed the low incidence of GVHD observed in animal models but was also accompanied by other limitations (i.e. graft rejection, delayed immune reconstitution, increased rate of disease relapse) that did not improve overall survival. Another approach that has been used to control GVHD after BMT includes the use of immunosuppressive drugs such as cyclosporine A (CsA), prednisone, and methotrexate. These agents by themselves typically fail to completely diminish GVHD but therapies using drug combination has led to better prognosis [50, 51]. One problem is their lack of specificity since they affect many immune responses indiscriminately, causing the patients to be more susceptible to opportunistic infections as well as causing toxicity to several organs [52].

Graft-versus-host disease remains the major limitation of allogeneic BMT since it causes significant morbidity and mortality in patients undergoing such treatment [32]. The efficacy of allogeneic BMT has been accredited to an allogeneic graft-versus-tumor (GVT) response that is associated with the development of GVHD [53]. However, because of the toxicities and risks associated with this procedure only a few patients can benefit from allogeneic BMT. Meanwhile, autologous BMT is less toxic and does not lead to GVHD development since the use of autologous stem cells eliminates donor anti-recipient alloreactivity. Nonetheless, an increase in relapse is associated with this method, presumably due to the lack of an allogeneic GVT response [32], suggesting that T cells present in the donor marrow graft are necessary to mediate this response. Thus, the

manipulation of the system during the post-transplantation period following autologous BMT in order to induce a GVT response, could be beneficial to patients without the allogeneic BMT limitations.

1.3 Syngeneic graft-versus-host disease (SGVHD)

Syngeneic GVHD was described by Glazier et al. as a GVHD-like syndrome that developed in rats following syngeneic BMT and cyclosporine A (CsA) treatment [16]. In the rat SGVHD model pathology was observed in the intestine, liver, skin and tongue that was similar to that observed in allogeneic GVHD. Due to these similarities in pathology and the use of BMT, this disease was termed CsA-induced syngeneic GVHD. Further studies revealed that upon cessation of CsA therapy, an acute phase occurred during rat SGVHD that was characterized by the infiltration of lymphocytes, mainly $CD8^+$ T cells and destruction to the epithelium in target organs. This response was followed by a chronic phase that consisted of further damage to the epidermis (fibrosis and scleroderma) and dominated by $CD4^+$ T cells [54].

Syngeneic GVHD can be induced in mice by reconstituting lethally irradiated animals with syngeneic BM cells followed by a 21 day treatment with immunosuppressive agent cyclosporine A (CsA) [55]. Clinical symptoms of the disease, which include weight loss and diarrhea, appear 2 to 3 weeks after cessation of CsA therapy. Similar to acute GVHD in murine models, SGVHD-associated inflammation occurs primarily in the colon and liver [55]. Three conditions are required for the induction and development of SGVHD: First, the recipient must have a thymus. Second, the thymus must be in the field of irradiation. Previous work has shown that

thymectomized animals do not develop SGVHD [56]. Third, animals have to be irradiated for optimal induction of the disease. Disease does not develop in normal animals treated with CsA alone [57] or following adoptive transfer of T cells from diseased animals into secondary recipients that are not irradiated [57, 58]. Finally, CsA therapy is required for disease induction since animals undergoing syngeneic BMT that do not receive CsA treatment have been shown not to develop SGVHD [16].

As mentioned above, CsA is an immunosuppressive drug that has been used clinically [59] and experimentally [18] to prevent graft rejection following solid organ transplantation and to prevent GVHD following allogeneic BMT. This immunosuppressive drug is derived from *Tolypocladium inflatum*, a soil fungus. It blocks T-cell proliferation by inhibiting the phosphate activity of calcineurin, a Ca^{2+}-activated enzyme. Calcineurin is an important phosphatase involved in signaling transmission from the T cell receptor (TCR) to the nucleus. Upon its activation, calcineurin dephosphorylates nuclear factor of activated T cells (NFAT), rendering it active and capable of migrating into the nucleus to induce the transcription of NFAT-dependent genes. CsA inhibition of the calcineurin signaling pathway in T cells ultimately inhibits the clonal expansion of activated T cells [2, 60](**see Figure 1.1**). CsA has various biological effects on T cells, including the downregulation of proinflammatory cytokines [61, 62]. Studies have shown that CsA can impair T cell function by blocking the production of IL-2 in activated T lymphocytes, observed by decreased levels of IL-2 mRNA [63, 64]. In addition, *in vitro* studies have shown that CsA can reduce the production of IL-15 and TNF-α through the upregulation of IL-10 in cell culture of rheumatoid synovial fibroblasts [62]. And inhibition of IL-15-induced IL-17 production

in $CD4^+$ T cells have been reported after CsA treatment [61]. Long-term treatment with CsA results in toxicities in the kidney and liver. CsA therapy has been shown to cause tubular injury, with interstitial cell proliferation, extracellular matrix deposition and the infiltration of macrophages into the interstitium of the kidney [65]. CsA treatment has also been reported to affect liver pathology by causing hepatocyte damage, necrosis [66, 67] and cholestasis [68]. CsA induced hepatotoxicity includes impairment of antioxidant enzymes [66, 67] as well as disorganization of the canalicular bile salt export pump transporter mechanism [69]. Finally, CsA treatment has been shown to affect the thymus and consequently T cell maturation [70]. There is evidence that CsA therapy in animals leads to damages of the thymic architecture and the medullary region [71] that may affect negative selection of immature thymocytes and has been proposed to mediate the development of SGVHD following lethal irradiation, syngeneic BMT and treatment with CsA [70].

1.4 Role of T cells in SGVHD

The role of T cells as an effector cell population has been well established in the rat model of SGVHD. Various studies have demonstrated the role of $CD4^+$ as well as $CD8^+$ T cells in the induction and development of rat SGVHD [56, 72]. The disease in the rat model is characterized by an early acute phase mediated by $CD4^-CD8^+$ T cells, that takes place within the first week after the cessation of CsA treatment, followed by a chronic phase that is dominated by double positive T cells ($CD4^+CD8^+$) [54]. Finally, rat SGVHD can be adoptively transferred into secondary irradiated animals by T cells isolated from diseased animals [57, 72].

The major effector cells in rat SGVHD were originally described as cytotoxic $CD8^+$ T lymphocytes that were specific for MHC class II antigens [73]. It is interesting that the $CD8^+$ autoreactive T cells promiscuously recognize MHC class II molecules [74]. This observed association is aberrant in that $CD8^+$ T cells typically recognize antigen in the context of MHC class I molecules. It was later shown that these effector cells were specific for the class II-associated invariant chain peptide CLIP [73]. This peptide is generated during the trafficking of MHC class II to the surface of the cell. The invariant chain binds to the newly synthesized MHC class II molecules and blocks the binding of peptides and unfolded proteins in the endoplasmic reticulum and during the transport of the MHC class II molecule into acidified endocytic vesicles. In these vesicles, proteases cleave the invariant chain, leaving the CLIP peptide attached to the binding groove of the MHC class II molecule. Endocytic antigens (pathogens and their proteins) are degraded to peptides in the endosome but cannot bind to MHC class II molecules that are occupied by the CLIP peptide. Once CLIP is bound to the MHC class II molecule, it cannot bind other peptides thus inhibiting their upload and delivery to cell surface were they can be presented to effector cells [2, 75]. For CLIP to be removed from the binding groove of the MHC class II molecule it requires the action of the MHC like-molecule, DM (HLA-DM for human and H-2M for mouse), which is encoded in the MHC locus and resides in the endosome. DM catalyses the dissociation of CLIP and stabilizes the MHC class II molecule so it can interact with antigenic peptides in the endosome. Once a stable peptide/MHC class II complex forms, DM disassociates and the complex transits to the cell surface of MHC class II expressing cells [75]. Further characterization revealed that the reactivity of $CD8^+$ autoreactive T cells from SGVHD rats with MHC class II

molecules bearing CLIP was based on the specific interaction of the N-terminal flanking region of CLIP/MHC class II and the Vβ segment of the TCR to initiate a pathogenic immune response. Fischer et al. demonstrated that the $CD8^+$ autoreactive T cell population in rat SGVHD predominantly expresses Vβ 8.3/8.5 TCR and adoptive transfer of these cells ($V\beta\ 8.5^+CD8^+$ T cells) could promote SGVHD in secondary recipients [76]. However, clonal analysis of these regions revealed that not only the N-terminal flanking region on CLIP could stimulate T cells but that the C-terminal region presented in the context of class II could also activate SGVHD T cells. However, only the cells that were specific for the N-terminal region of CLIP were pathogenic *in vivo*, while clones requiring the C-terminal region were nonpathogenic [74]. It is interesting to note that the pathogenic CLIP-reactive T cell clones have the ability to produce T_H1 cytokines (IL-2 and IFN-γ), that mediate the acute phase of the disease, while the nonpathogenic C-terminal-reactive clones produced T_H2 cytokines (IL-4 and IL-10), that are associated with the chronic disease stage [77]. These studies demonstrated that an autoreactive, pathogenic $CD8^+$ T cell response was associated with the generation of rat SGVHD. However, while the induction protocol and tissue pathology were similar between the rat and mouse models of SGVHD, data will be presented demonstrating that the effector mechanisms underlying the murine model of SGVHD appear to be very different from that observed in the the rat model of this inducible disease.

Immunohistochemical (IHC) analysis has demonstrated an increased presence of $CD4^+$ and $CD8^+$ T cells in the colonic lesions of mice with SGVHD [78]. However, murine SGVHD appear not to be mediated by $CD8^+$ T cells, since cytotoxic T cell responses were not demonstrated in this disease model [79]. Recently, the role of $CD4^+$ T

cells in the development of murine SGVHD was clearly established [58, 78]. First, as described above, IHC analysis revealed an increased presence of $CD4^+$ T cells in the SGVHD colon. Upon isolation and characterization of immune cells from the colons of SGVHD mice, it was shown that increased numbers of $CD4^+$ T cells were present in the colons of diseased animals compared to BMT control and normal mice [78]. The percentage and numbers of $CD8^+$ T cells did not change between the diseased and control animals. To determine if the increase in $CD4^+$ T cells in the colons of SGVHD mice was functional, *in vivo* T cell depletion studies were employed. The use of a monoclonal antibody (mAb) cocktail against T cells during the post-CsA period failed to inhibit disease [80] and subsequent analysis revealed that antibody treatment was able to remove peripheral $CD4^+$ T cells but not colonic T cells [78]. Thus, Ab therapy after cessation of CsA therapy failed to eliminate T cells from the colons of treated animals and did not alter disease induction. Expanding on these studies, specific mAb against $CD4^+$ or $CD8^+$ T cells were utilized following myeloablative conditioning and during the 21 days of CsA therapy period to inhibit T cell migration into the gut and to determine the role of these T cell subsets in the development of SGVHD. Treatment during this period specifically removed $CD4^+$ or $CD8^+$ by day 21 post-BMT. Depletion of $CD4^+$ T cells, but not $CD8^+$ cells, significantly reduced the induction of clinical symptoms as well as pathology associated with murine SGVHD [78]. These findings were supported by additional experiments demonstrating that $CD4^+$ T cells isolated from SGVHD mice were capable of inducing disease when adoptively transferred into irradiated secondary recipients [58]. Taken together, these studies demonstrated that the presence of $CD4^+$ T cells in the colons of CsA-treated mice during the induction period is critical for disease

development. In addition, Bryson et al. [58] have shown that $CD4^+$ T cells isolated from the spleen and mesenteric lymph nodes from SGVHD had increased proliferative responses against dendritic cells (DC) pulsed with a bacterial lysate prepared from the cecum of normal mice. $CD4^+$ T cells from SGVHD mice did not respond against syngeneic/self APC (unpulsed DC or splenic APC), or DC pulsed with self epithelial antigens, nominal protein antigens or food-derived antigens, demonstrating a specificity for bacterial antigens. With the similarity between SGVHD-intestinal inflammation and murine models of colitis and the dependency of colitis models on bacterial specific T cells [81, 82], we hypothesized that bacterial-specific $CD4^+$ T cells may mediate the induction of murine SGVHD. Thus, based on the phenotype of the major effector cells, as well as, putative antigen specificity, it is clear that while SGVHD is induced via similar protocols, the T cell response is demonstrably different in the rat and mouse.

1.5 Proinflammatory mediators and SGVHD

Previous studies demonstrated significantly higher levels of mRNA for the T_H1 cytokines IL-12, interferon-γ (IFN-γ) and TNF-α in target organs of mice that had developed SGVHD. *In vivo* depletion of IL-12 [80], as well as TNF-α [83], inhibited the development of the disease suggesting a role for T_H1 cytokines in the development of murine SGVHD [80]. The role of macrophages in this inducible disease was documented by Flanagan et al. [83]. Activated macrophages were present in SGVHD mice. These animals were more responsive to sublethal doses of LPS relative to control animals. As macrophages are a major source of IL-12 and TNF-α and are responsive to LPS and other bacterial products through interaction with toll-like receptors [84] it was concluded that activated macrophages play a major role in the development of SGVHD. Thus, activation

of macrophages could lead to an increased release of proinflammatory cytokines, resulting in enhanced production of IL-12 and TNF-α, cytokines which were shown to contribute to the development of murine SGVHD [80, 83].

1.6 Oxidative Stress and SGVHD

Both radiation and CsA are required for the development of SGVHD [57, 85] and participate in the induction of oxidative stress [65, 86-88]. Radiation allows for the elimination of regulatory cells that are present in normal mice and are capable of modulating the induction as well as the adoptive transfer of SGVHD [58, 73]. Irradiation is also required to prolong the alterations in thymic architecture induced by CsA treatment which has been proposed in the rat model to alter thymocyte maturation resulting in the generation of self-reactive T cells [71]. Finally, it has been demonstrated that cell killing by ionizing radiation is mediated primarily through the induction of oxidative stress [89-91]. Several toxicities are also associated with the use of CsA immunosuppression. CsA-associated side effects include damage to the vascular endothelium via the production of reactive oxygen species (ROS) [86-88, 92]. Administration of CsA to rats has been shown to cause overproduction of ROS, measured by increased levels of 2',7'-dichlorofluroscein (DCF) and malondialdehyde (MDA) as well as increased RNS shown by elevated iNOS and nitrotyrosine levels [87, 88]. Also, CsA-induced oxidative stress has been shown to activate some transcriptional factors, such as nuclear factor kappa B (NF-kB), leading to the activation of gene transcription of proinflammatroy molecules, including ROS/RNS mediators [93].

In addition to the generation of ROS by conditioning agents, oxidative signals can also be induced by cytokines. Tumor necrosis factor-α, is a prime example and is regulated transcriptionally by NF-κB, which is a ubiquitous transcription factor implicated in the induction of many cytokines and adhesion molecules involved in immune and inflammatory responses [27, 94]. The NF-κB family of transcription factors is composed of five members: p65 (REL-A), REL-B, cytoplasmic c-REL, p50 and p52 which function as homo- or heterodimers. NF-κB dimers are sequestered in the cytoplasm in an inactive form which is bound to the inhibitor molecule IκB. Tumor necrosis factor-α signaling mediates the phosphorylation of IκB via a kinase complex leading to the polyubiquitination and proteosome-mediated degradation of the inhibitor and allowing for the release of the NF-κB factors. Free NF-κB dimers can then translocate to the nucleus and activate gene transcription of proinflammatory molecules [95, 96].

The development of SGVHD is a multi step process resulting from the cooperative interaction of various effector cell populations, including NK cells [80], T cells [78, 97] and macrophages [83], along with T_H1 cytokines that result as a consequence of the preconditioning regimes during the induction the disease [80, 83]. However, the mechanism of action of these proinflammatory cytokines in SGVHD remains unclear. A possible mechanism could be via their stimulation of oxidative stress, including the production of nitric oxide (NO) [98]. Nitric oxide is a ubiquitous molecule needed for normal physiologic functions but it is also associated with several pathologic diseases including GHVD [98-102]. Nitric oxide is generated from L-arginine through an oxidation reaction that is catalyzed by NO synthase (NOS)(**see Figure 1.2**). It can be

produced via constitutive and inducible forms of the NO synthase (iNOS, NOS2) enzyme. The constitutively expressed forms are found in vascular endothelial cells (eNOS, NOS-3) or in neuronal cells (nNOS, NOS-1). The inducible form of NOS (iNOS) can be expressed in many cell types including macrophages, neutrophils, endothelial cells and hepatocytes; it also has immunosuppressive properties that may play a role in the downregulation of immune responses [98]. It is known that activated macrophages have the ability to produce large amounts of nitric oxide (NO), via the iNOS (NOS2) enzyme [103] . Since studies revealed a role for macrophages in SGVHD, due to IL-12 secretion, and they are known to produce NO, the contribution of this inflammatory mediator to the development of murine SGVHD was studied during the active disease period (after cessation of CsA therapy). The functional role for NO was determined by the treatment of mice with the iNOS inhibitor aminoguanidine (AG) [104]. Inhibition of iNOS resulted in the abrogation of clinical symptoms, tissue pathology and cytokine (IL-12 and IFN-γ) levels associated with the development SGVHD [100]. Nitric oxide has also been studied in animal models of allogeneic GVHD. Inhibition of iNOS also resulted in reduced development of pathophysiology (i.e. tissue injury, intestinal pathology, reduced lethality) associated with allogeneic GVHD [104, 105]. Hongo et al. studied the role of NO during the early stages of GVHD induction (days -2 up to 14 post-BMT) and concluded that NO had a protective effect during this period since enhanced mortality was observed in mice when NO was inhibited by treatment with AG [106]. Similar results were obtained by Drobyski et al. in which inhibition of iNOS, with the administration of NG-methyl-L-arginine (L-NMA), after allogeneic BMT, resulted in significant decreased survival, likely due to decreased engraftment [98].

By itself, NO is a weak free radical but in combination with other ROS, like superoxide (O_2^-), it can result in the formation of peroxynitrite ($OONO^-$), a very toxic and reactive product capable of mediating several cytotoxic processes [107](**see Figure 1.3**). *Data presented in this dissertation will address the involvement of oxidative stress in the development of murine SGVHD and will be discussed in Chapter 3.*

1.7 Lymphocyte homing to inflammatory sites

Homing of naïve lymphocytes from their site of origin, either bone marrow or thymus, into lymph nodes and peripheral tissues is governed by their lymphocyte trafficking properties, which include tissue-specific adhesion and chemokine interactions [2, 108-113]. Migration into the inflamed gut requires lymphocyte trafficking through the mesenteric lymph nodes (MLN), an important site of the mucosal immune system [114]. Naïve T cells enter the MLN via high endothelial venules (HEV) and are able to encounter foreign antigens by their interaction with dendritic cells (DC) that resided in the intestinal tract and have processed gut-associated antigens, and transported them back to the MLN. As a consequence, these lymphocytes interact with these gut-antigen presenting DC, become activated and express surface markers (i.e. L-selectin, $\alpha_4\beta_7$) that change the migratory behavior of these activated effector cells. This acquired gut-homing phenotype enables them to reach the site of inflammation where they can exert their effect [2, 114, 115]. Proinflammatory chemokines, released by the tissue along with their corresponding receptors, found on active lymphocytes form an important axis that directs lymphocytes to the gut. Specific chemokines and their receptors, including CCL20, CCL5, CCR5, CCR6 among others, have been previously associated with inflamed

intestines observed in inflammatory bowel diseases (IBD) as well as murine models of colitis [111, 112].

The recruitment of leukocytes from the vascular compartment into the extravascular space is crucial for the development of inflammatory responses. This movement involves cell adhesion interactions that are regulated by several ligands known as cell adhesion molecules (CAM) which are expressed in the surface of endothelial cells and leukocytes [110, 113, 116, 117]. Mucosal vascular addressins are tissue-specific endothelial cell adhesion molecules for circulating lymphocytes. They are expressed on the surface of vascular endothelial cells and serve as receptors to which ligands expressed on the surface of activated lymphocytes bind, thus allowing leukocyte homing to specific tissues [118]. Mucosal addressin cell adhesion molecule-1 (MAdCAM-1) is an example of one of these vascular addressins that is expressed in mucosal endothelium lining blood vessels and serves to guide the entry of lymphocytes into mucosal lymphoid tissues such as the gut. MAdCAM-1 plays a critical role in mucosal immunity and is up-regulated during inflammation in the gut [116, 117]. It binds to integrin $\alpha_4\beta_7$ expressed on the surface of activated T lymphocytes allowing their migration into the gut where they can initiate an inflammatory response [2, 116, 117]. It has been shown that lymphocytes expressing $\alpha_4\beta_7$ migrate in a selective manner to sites of MAdCAM-1 expression [109]. Other examples of adhesion molecules include intercellular adhesion molecule-1 (ICAM-1) and vascular adhesion molecule-1 (VCAM-1) which are both expressed on the endothelium and bind to integrins expressed on the surface of activated lymphocytes. Lymphocyte function-associated antigen-1 (LFA-1) is the ligand for ICAM-1 and has a major role in T cell activation and migration of both naïve and effector T cells out of the

blood. VCAM-1 binds to integrin $\alpha_4\beta_1$, also known as VLA-4, thus allowing for the extravasation of effector T cells [2, 116]. It has been reported that TNF-α, and other proinflammatory mediators, can induce VCAM-1, ICAM-1 [119] and MAdCAM-1 upon inflammatory responses [120]. Oxidative stress induced by immune responses as a consequence of irradiation treatment and/or cytokine production can also induce CAM expression [121].

The interaction of blood lymphocytes with the endothelium involves multiple steps that account for their specificity. First, selectins on the T lymphocyte cells bind to sulfated carbohydrates on proteins such as vascular addressins (i.e. GlyCAM, ICAM-1, MAdCAM-1) that are expressed on endothelial cells. This allows for lymphocyte contact and weak interaction with the endothelium which initiates rolling of the lymphocyte along the endothelium surface. This step is crucial to initiate the cascade that leads to stronger interactions to allow for lymphocyte migration into the tissue. The second step consists of the actions of activating factors (i.e. chemokines), found in the environment, that bind to proteoglycan molecules on the endothelium walls and to receptors in the T lymphocyte cell, triggering rapid intracellular signaling in the leukocyte. This interaction leads to the activation of preexisting cell surface integrins (i.e. LFA-1, β_7, α_4) on the T cell that increases its affinity for cell adhesion molecule receptors (i.e. ICAM-1, MAdCAM-1, VCAM-1) which are expressed on endothelial cells, mediating firm arrest of the cell on the vessel wall. The interaction between receptor and counterligand allows for the fourth step known as diapedesis/extravasation in which the lymphocyte migrates through the vessel wall into the tissue [2](**see Figure 1.4**). The expression of these vascular addressin on the endothelium serves as a mark point to signal the presence of

infection attracting effector cells to the site of inflammation. Their interaction with integrins expressed on activated lymphocytes allows for the entry, in large numbers, of these effector cells into the infected tissue where they can conduct an inflammatory response. As increased numbers of $CD4^+$ T cells were observed in the colon of CsA-treated, BMT mice at the end of the SGVHD induction period, and the migration of these cells to the colon during this period was shown to be essential for the development of this disease [78], *the data presented in Chapter 4 will examine the role of T cell homing into the gut at the early stages after BMT in the development of SGVHD.*

Figure 1.1 CsA inhibition of the calcineurin signaling pathway in T cells

Adapted from Steinbach et al. [122]

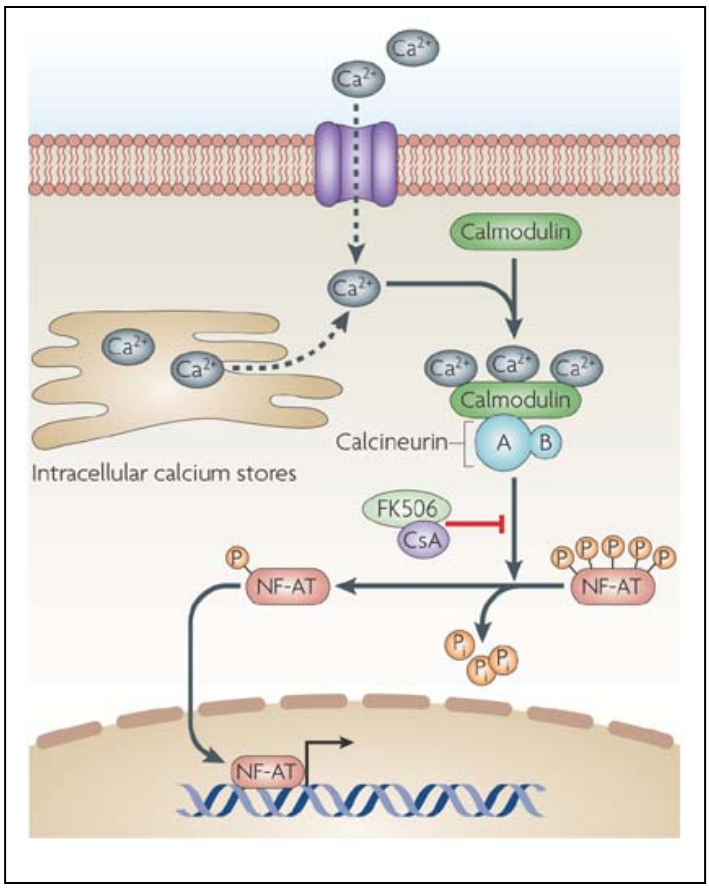

Figure 1.1 CsA inhibition of the calcineurin signaling pathway in T cells. Activation of T cell receptor (TCR) triggers increases in Ca^{2+} which activates calmodulin and allows its binding to calcineurin. The calcineurin catalytic subunit (A), when bound to the regulatory subunit (B) and calmodulin–Ca^{2+} complex, dephosphorylates nuclear factor of activated T-cells (NF-AT) in the cytoplasm, leading to nuclear migration of this transcription factor and the subsequent activation of various cellular processes. The dephosphorylation of NF-AT is inhibited by cyclosporine A (CsA) and FK506.

Figure 1.2 Nitric oxide generation from L-arginine oxidation

Adapted from Vallance et al. [123]

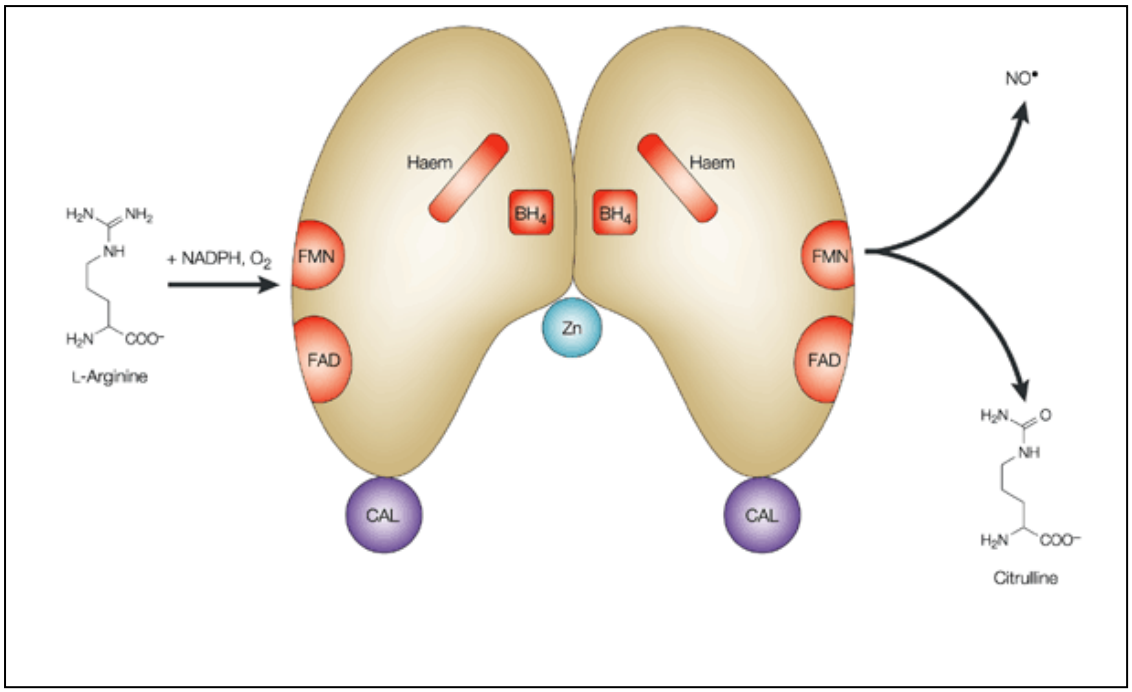

Figure 1.2 Nitric oxide generation from L-arginine oxidation. For enzymatic activity, nitric oxide synthase (NOS) enzymes must dimerize and bind the cofactors tetrahydrobiopterin (BH_4), haem, flavin mononucleotide (FMN) and flavin adenine dinucleotide (FAD). On binding calmodulin (CAL), the active enzyme catalyses the oxidation of L-arginine to citrulline and nitric oxide (NO) and requires molecular oxygen and NADPH as co-substrates. Each NOS dimer coordinates a single zinc (Zn) atom.

Figure 1.3 Generation and detoxification of ROS/RNS

Adapted from Griendling et al. [124]

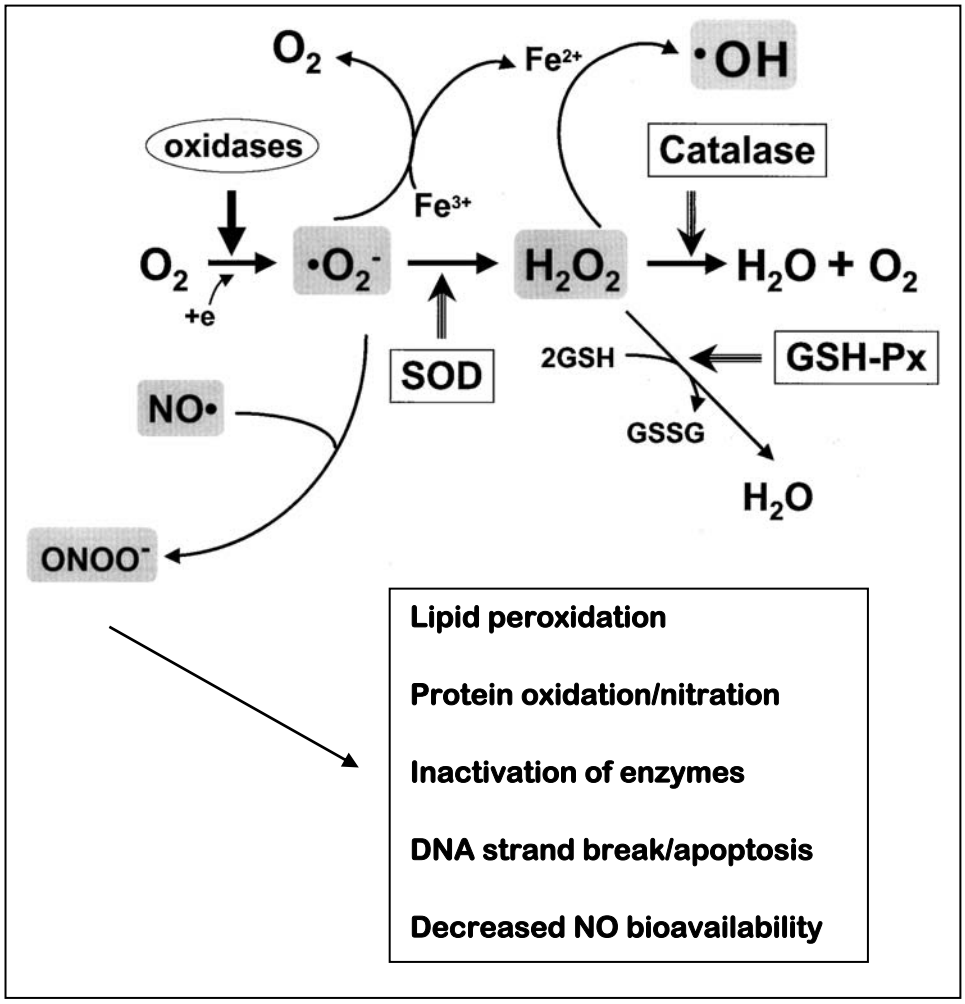

Figure 1.3 Generation and detoxification of ROS/RNS. Oxidases convert oxygen to superoxide ($\bullet O_2^-$) which can react rapidly with nitric oxide (NO•) to form peroxynitrite ($ONOO^-$) and cause downstream cellular damages. $\bullet O_2^-$ can also be dismutated to hydrogen peroxide (H_2O_2) by superoxide dismutase (SOD). H_2O_2 can be converted to H_2O by catalase or glutathione peroxidase (GSH-Px) or to hydroxyl radical (•OH) after reaction with Fe^{2+}.

Figure 1.4 Attachment of T cells to the endothelium and extravasation

Adapted from Kunkel et al. [125]

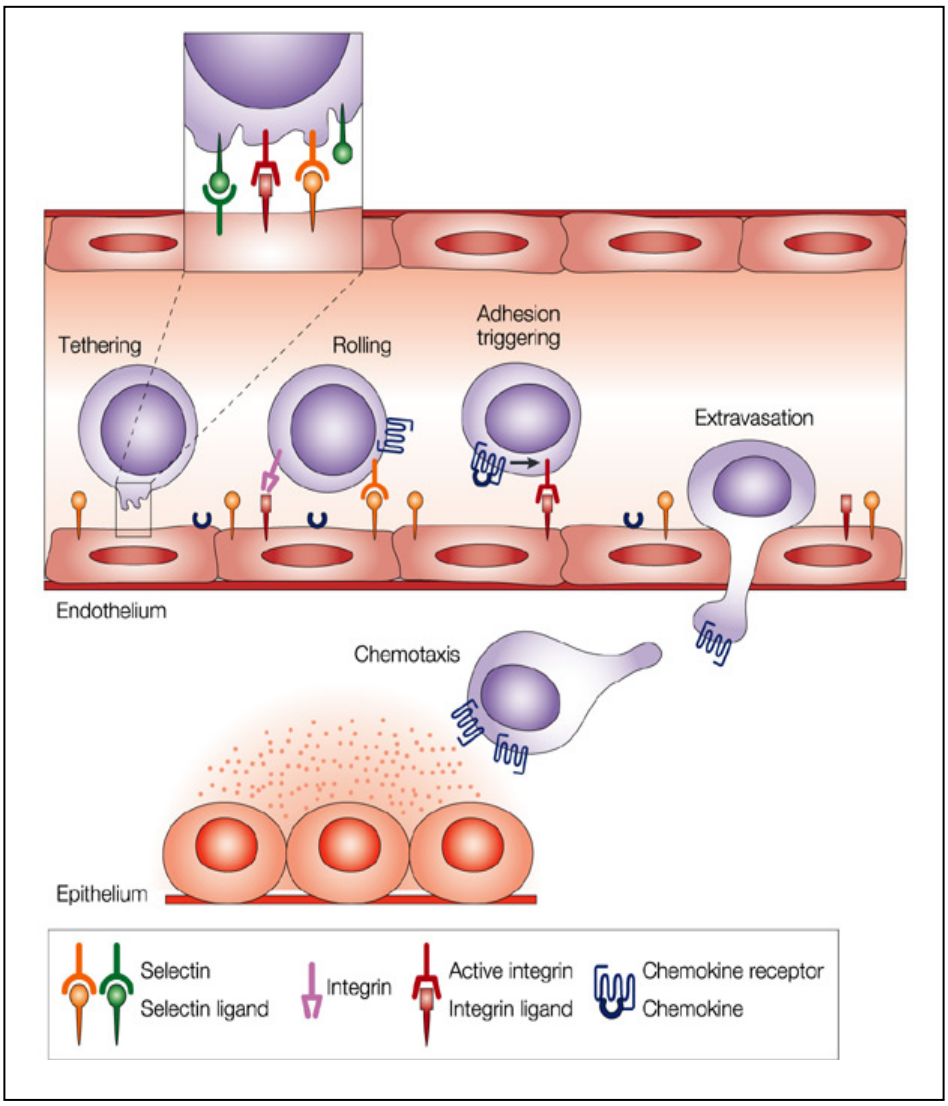

Figure 1.4 Attachment of T cells to the endothelium and extravasation. Integrins present on the surface of T cells mediate adhesion to the endothelium via their interaction with CAM. The multiple steps involved in T cells attachment to the endothelium includes: (1) tethering, (2) rolling, (3) adhesion and (4) diapedesis/extravasation.

CHAPTER TWO: MATERIAL AND METHODS

2.1 Mice

C3H/HeN mice were purchased from Harlan Sprague-Dawley (Indianapolis, IN) at 20–21 days of age and were used within 1 week of arrival. The mice were given acidified water and fed autoclaved lab food *ad libitum* and were housed in sterile microisolator cages (Lab Products, Maywood, NJ). The animal used protocols were reviewed and approved by the University of Kentucky Institutional Animal Use and Care Committee.

2.2 Induction of SGVHD

Bone marrow (BM) was isolated from the femurs and tibias of syngeneic age-matched mice. The donor BM suspensions were prepared in RPMI 1640 (Cellgro, Herndon, VA) supplemented with 5ml of penicillin/streptomycin/glutamine (100X; (Gibco-Invitrogen, Grand Island, NY)(**see Appendix A** for solution preparation). The resulting cell suspensions were resuspended in cytotoxic medium (RPMI 1640 containing penicillin/streptomycin/glutamine and 0.3% BSA Fraction V (Gibco-Invitrogen)) to a final concentration of 5 x 10^7 cells/ml. BM cells were treated with monoclonal antibody (mAb) against Thy1.2 (HO-13-4, 1:20; American Type Culture Collection, ATCC No. TIB-99, Rockville, MD) to deplete $Thy1^+$ cells, for 60 minutes on ice. Anti-Thy1.2-treated BM cells were then washed three times with cytotoxic medium and treated with a 1:10 dilution of Low Tox-M rabbit complement (Cedarlane Laboratories, Westbury, NY) at a concentration of 5 x 10^7 cells/ml for 1 hour in 37°C water bath. After incubation, cells were washed three times with cytotoxic medium. Cell count was performed by

diluting cells 1:100 in cytotoxic medium with the adition of 5% acetic acid (Baxter; Stephens Scientific, Riverdale NJ, USA) then counted on a hemacytometer. The cell viability was determined by trypan blue exclusion. Removal of donor BM $Thy1^+$ cells is required for disease development because in the presence of these autoregulatory cells development of SGVHD is reduced or inhibited depending on the strain of mice used [97]. Recipient mice were lethally irradiated with 900 cGy in a Mark I ^{137}Cs irradiator (J.L. Shepard and Associates, Glendale, CA) 4-6 hours before transplant. Irradiated mice were reconstituted with 5 x 10^6 T cell-depleted BM cells (ATBM) intravenously (i.v.) in 0.1 ml PBS via tail vein injection. Beginning on the day of transplantation, groups of mice were injected intraperitoneally (i.p.) daily for 21 days with 0.1 ml of either 15 mg/kg CsA in the diluent olive oil (Sigma-Aldrich, St. Louis, MO) or diluent alone (**Figure 2.1**). CsA was purchased through the Division of Laboratory Animal Resources, University of Kentucky.

2.3 Evaluation of SGVHD

Following cessation of CsA, the animals were weighed three times per week and observed for clinical signs of the development of SGVHD (weight loss and diarrhea). Animals that lost weight for three consecutive weighings and/or diarrhea or mortality were considered as positive for the induction of SGVHD. In general, by 2–3 weeks after cessation of CsA therapy, clinical symptoms were evident (**Figure 2.1**) in approximately 80% of the treated animals. Tissue samples were taken from the animals at different times during and post-CsA treatment. For histological evaluation of SGVHD, tissue samples taken from euthanized animals were immediately placed in 10% buffered formalin (Fisher Scientific, Atlanta, GA). Fixed tissues were embedded in paraffin, cut

into 4 to 6 μm tissue sections, mounted on glass slides, and then stained with a standard hematoxylin and eosin (H&E) procedure. All tissue sections were analyzed blind without the knowledge of the treatment category of the animal and graded for inflammation caused by SGVHD using a previously published grading scale [79] (**Table 2.1**).

2.4 *In vivo* treatment with the antioxidant MnTBAP

Mice were lethally irradiated, reconstituted with syngeneic ATBM and treated with either diluent or CsA as described. Treatment with MnTBAP was performed during or post-CsA therapy (**Figure 2.2**). MnTBAP reconstitution was performed following the manufacturer's instructions (Axxora Life Sciences Inc., San Diego, CA.). The black crystalline powder was dissolved in 1 ml 0.1M NaOH, then 9 ml of 1X PBS was added to reach a final stock concentration of 5 mg/ml. The pH was adjusted to 7.4 and the solution was filter sterilized using a 0.2 μm syringe filter. The MnTBAP stock was stored in the dark at 4°C. For MnTBAP therapy during CsA period, treatment began two days prior to BMT when mice were treated i.p. with 10 mg/kg or 20 mg/kg of MnTBAP ending at day 21 post-BMT. Twice a day dosing regimen was used based on the MnTBAP elimination half-time of 9.5 hours [126]. For post-CsA treatment, twice daily (10 mg/kg) antioxidant therapy began at day 21 post-BMT and was given for to 2-3 weeks. Treatment was stopped when the majority of the CsA group (typically >80%) had developed SGVHD. Following cessation of MnTBAP therapy, the animals were monitored for the development of clinical symptoms of SGVHD as described.

2.5 *In vivo* neutralization of TNF-α

To determine the effect of TNF-α on the induction of SGVHD, mice were treated with soluble TNF Receptor-1 (sTNFR-1) (Amgen, Thousand Oaks, CA) during the CsA treatment period (**Figure 2.3**). Four experimental groups were used in which mice received either olive oil, CsA alone, sTNFR-1 only or CsA and sTNFR-1. Several experiments were performed in which mice received sTNFR-1 beginning at different time points: (1) Two days prior to bone marrow transplantation; (2) At day three post-BMT or (3) One week (day 7) post-BMT. The mice received 100 μg of sTNFR-1 i.p. beginning at the indicated times for 4 consecutive days and then every other day through day 21 post-BMT. Moribund animals were euthanatized and counted as mortalities. Animals were then monitored for clinical symptoms of SGVHD, as described previously. At the end of each experiment tissue was collected and analyzed for changes in immune parameters.

2.6 Isolation of peripheral lymphoid cells

At the indicated times after BMT, mice were euthanized by CO_2 inhalation, the spleens were removed and placed into Stomacher bags (Fischer Scientific) containing 10 ml 5% complete medium (RPMI 1640 containing penicillin/streptomycin/glutamine (Gibco), 5% FBS (Atlanta Biologicals, Inc., Norcross, GA, USA) and 5mM 2-mercaptoethanol (2-ME) (Sigma Chemical Co.)). The tissue was homogenized in a Stomacher-80 (Fisher Scientific) to prepare single cell suspensions. The spleen cell suspensions were then treated with 0.83% Tris-buffered ammonium chloride (NH_4Cl), pH 7.2, for 7 minutes at room temperature to lyse the red blood cells. Cells were then

washed once with 5% complete medium and the resulting cell population was diluted in 0.04% trypan blue, counted on a hemacytometer and cell viability was determined by trypan blue exclusion. Isolated lymphoid cells were then stained following flow cytometry procedure described below.

2.7 Treatment of lymphocytes with DCFH-DA

Intracellular ROS were detected using the cellular marker 2',7'-dichloro-dihydrofluroscein diacetate (DCFH-DA) (Molecular Probes, Eugene, OR) following the method of Saito et al. with a slight modification [127]. Briefly, the lymphoid cells were isolated (2 x 10^6 cells/ml), washed once in 5% complete RPMI then resuspended in phosphate-buffered saline (PBS). The cells were incubated with DCFH-DA at a final concentration of 5 μM for 30 minutes at 37°C. Following incubation, the cells were washed twice in PBS and stained for surface markers following the flow cytometry method described below.

2.8 Isolation of immune cells from the colon

Intraepithelial lymphocytes (IEL) and lamina propia lymphocytes (LPL) were isolated according to a modification of the method of Lefrancois and Lycke [128]. Colons were removed from euthanatized mice at different times post- BMT and placed in Petri dishs containing cold calcium and magnesium free (CMF) HBSS (Ca^{2+} and Mg^{2+} free, 100 mM HEPES (Sigma-Aldrich), 250 mM sodium bicarbonate (Fisher Scientific, Pittsburgh, PA), and 2% FBS (HyClone, Logan, UT)). The colons were cleaned by removing debris and all fecal matter. Tissue was cut open longitudinally and then laterally into ~0.5 cm pieces. Colon pieces were transferred into 50 ml conical tube

containing 40 ml cold CMF and kept on ice. Individual colons were pooled within the experimental groups and washed three times in cold CMF. Colon pieces were transferred into a sterile 125 ml Erlenmeyer flask and treated with 20 ml of 37°C CMF solution containing 1 mM dithiothreitol (DTT) (Research Products International, Mt. Prospect, IL) and 1 mM ethylenediamine tetraacetic acid (EDTA) (Sigma-Aldrich) and placed on a shaker for 30 minutes in a 37°C warm room. This step allows detachment of the epithelial cell layer. After incubation, contents of each flask were transferred to 50 ml conical tubes. The tubes then were vortexed for 15 seconds and the supernatant containing cells was collected. CMF-DTT-EDTA was added to the tissue and the step was repeated twice combining the supernatant of both collections. The cell containing supernatant represents the epithelial fraction and contains the IEL. Tubes containing supernatant were centrifuged at 2000 rpm for 10 minutes. The supernatant was discarded and the cell pellet was washed once with 5% complete medium. The IEL were resuspended in 10 ml cold 10% complete medium (RPMI 1640 containing 10% FBS (Atlanta Biologicals, Inc.,) penicillin/streptomycin/glutamine (Gibco), and 5 mM 2-ME (Sigma)) and kept on ice while working with the LPL isolation. LPL suspensions were prepared by treating the de-epithelialized intestinal tissue with 20 ml 10% medium containing 240U/ml collagenase (Sigma) and 2U/ml DNaseI (Roche, IN, USA) on a shaker for 1 hour at 37°C. This allows for further digestion of the tissue and the release of colonic LPL. Supernatant was then collected into 50 ml conical tubes and the step repeated twice collecting both supernatants containing the LPL. Tubes were then centrifuged at 2000 rpm for 10 minutes. The supernatant was discarded and the cell pellet was washed once with 5% complete medium. The pellet containing the LPL was resuspended in 10 ml cold 10%

complete medium and kept on ice. To enrich for T cells, the IEL and LPL suspensions were passed over a 0.2-g nylon wool (Robbins Scientific, Sunnyvale, CA) column and eluted with medium. The entire volume of eluate was collected in a 50 ml conical tube. Tubes were centrifuged at 2000 rpm for 10 minutes and pellet resuspended in 8 ml cold 44% Percoll solution and kept on ice. First, 100% stock Percoll solution was made by diluting 90 ml Percoll (GE Healthcare Bio-Sceinces AB, Uppsala Sweden) with 10 ml of 10X PBS. The appropriate volume of 100% Percoll solution was then added to 5% complete medium to make a 44% and 67% Percoll solutions. Lymphocytes were isolated by density percoll gradient centrifugation by overlaying the IEL and LPL in 44% Percoll solution over 14 ml polystyrene tubes containing 5ml cold 67% Percoll solution. Tubes were centrifuged at 1800 rpm for 30 minutes at room temperature. The cells in the 44/66% Percoll interface were collected and transferred into a 50 ml conical tube. After collection the cells were washed once with cold 5% complete medium and resuspended in 2 ml of 10% complete medium. The resulting cell population was counted using 0.04% trypan blue exclusion and analyzed by flow cytometry, as described below.

2.9 Flow cytometry analysis

Isolated lymphoid cells (1×10^6) from the spleens and colons were placed into 12x75 mm polystyrene tubes (Fisher Scientific) used for flow cytometry analysis and washed once using 2 ml of staining buffer (PBS containing 1% FCS and 0.1% NaN_3). The staining buffer was poured off the cell pellet, leaving approximately 100 µl buffer in the tube. One µg Fc block, an antibody against CD16/CD32 (2.4G2; BD PharMingen, San Diego, CA) was added to each tube to reduce non-specific staining and incubated for 15 minutes on ice. The appropriate labeled antibody (**see Table 2.2**) was added to the

tube to a final concentration of 1μg/tube and incubated on ice for 30 minutes. After incubation, the labeled cells were washed once with PBS containing 0.1% NaN_3 (Sigma) and fixed with 1% paraformaldehyde (Sigma). Staining was analyzed using a BD Biosciences FACS Calibur flow cytometer (San Jose, CA) and 20,000-25,000 cells were analyzed per sample.

2.10 Immunohistochemical staining

To perform immunohistochemistry, tissue was placed in plastic cryostat holder (Sakura Tissue-Tek 4566, Cryomold Intermediate, Torrance CA, USA) embedded in Tissue-Tek Optimal Cutting Temperature (OCT) compound (Sakura Finetek, Torrance CA, USA), snap frozen in liquid nitrogen and stored in a -80°C freezer. Tissues were cut into 10-μm tissue sections, using a cyostat microtome instrument (Microm HM 505N) at -22°C, mounted on glass slides (Superfrost Plus Fisherbrand, Fisher Scientific, PA, USA) and stored in a -20°C freezer. Usually 4-6 slides per tissue was cut with each slide containing 2-3 tissue sections. At the time of staining, tissues were fixed in 3% paraformaldehyde for 15 minutes and washed three times with PBS for 5 minutes each. Slides were treated with blocking solution containing 2mg/ml normal donkey serum (Jackson ImmunoResearch, West Grove, PA), 0.3% Triton X-100 in PBS for 30 minutes at 4°C to block non-specific binding. All incubations were carried out in a dark humidifying chamber (Tupperware container with wet paper towel inside) to prevent drying. After draining the excess blocking solution, slides were randomly selected for incubation with appropriate primary antibody (**see Table 2.3**) in PBS containing 2mg/ml normal donkey serum and 0.3% Triton X-100 at 4°C overnight. After washing twice

with PBS for 30 minutes, sections were incubated with corresponding secondary antibody (**see Table 2.3**) for 1 h and then washed twice for 30 minutes. The MAdCAM staining required a third antibody (Strep-PE) and the procedure was performed following the exact same steps as staining with a secondary antibody. Control staining was performed by omitting the primary antibody during the procedure to control for the specificity of the primary antibody staining. Samples were visualized with a 100x objective and digitized with an AxioCam HR Vision System (Carl Zeiss MicroImaging Inc., Thornwood, NY). For each experiment, three to four animals were evaluated per experimental group and from each organ 4-5 fields were analyzed.

2.11 Real Time Reverse Transcription-Polymerase Chain Reaction (RT-PCR) for cytokine message

Total colon and liver RNA was isolated using Trizol reagent (Invitrogen, Grand Island, NY). Briefly, samples were placed into RNA/DNAse-free 1.5 ml Eppendorf tubes (VWR International, LLC, Batavia, IL), homogenized in 1 ml of Trizol by hand using sample pestles (Reaserch Product International Corp., Mount Prospect, IL) and then incubated for 5 minutes at room temperature. After the tissue was homogenized, 200 µl of chloroform (Sigma St. Louis, MO) was added and the mixture was shaken vigorously by hand and using a vortex mixer (Fisher Scientific). Samples were then centrifuged at 12,000 X g for 15 minutes at 4°C. The clear aqueous top layer was transferred into an RNA/DNAse-free 1.5 ml Eppendorf tube (VWR International, LLC) and 500 µl of isopropanol (Sigma) was added, to precipitate the RNA, and incubated for 10 minutes at room temperature. Tubes were then centrifuged at 12,000 X g for 10 minutes. The

supernatant was removed and the RNA pellet was washed with 1 ml 75% ethanol. Samples were vortexed and centrifuged at 7,500 X g for 5 minutes and the supernatant was discarded. The RNA pellet was resuspended in RNAse-free water, vortexed and stored in a -80°C freezer. The amount of RNA present in each sample was quantified by diluting 4 µl of RNA sample with 96µl of distilled water in a Quartz U.V. cuvette and reading the absorbance at 260 and 280 nm using a SmartSpec^{TM} 3000 Spectrophotometer (Bio-Rad, USA). The A260:A280 ratio should be between 1.8-2.2 for pure RNA, values below this ratio may indicate the presence of co-purified contaminants. One µg of RNA from each group was reversed transcribed into cDNA using the Promega reverse transcription system (Madison, WI)(**see Table 2.4, Panel A** for procedure). The PCR reaction mixture was then prepared by combining 2.5 µl of cDNA with 10 µl of master mix (**see Table 2.4, Panel B)** and 1 µM of appropriate primer (**see Table 2.5**). Real time RT PCR was performed on a Roche Lightcycler (Roche Diagnostics, Indianapolis, IN) and the amount of cytokine message was normalized to GAPDH and calculated by the comparative C_T method.

2.12 Measurement of serum NO

Circulating nitric oxide (NO) levels were determined using a Cayman Chemical Nitrate/Nitrite Colorimetric Assay kit (Alexis Biochemicals, San Diego, CA). The reagents in this kit use nitrate reductase to reduce serum nitrate (NO_3^-) to nitrite (NO_2^-). To measure the production of NO during the induction of SGVHD (day 7-21 post-BMT), normal, control, and CsA-treated mice were euthanized individually by CO_2 inhalation, and blood was obtained by cardiac puncture using a 25-gauge needle. The blood was

allowed to clot overnight at 4ºC and the serum was collected. The serum samples were treated and assayed according to kit instructions. Briefly, samples were placed in 0.45 µM Ultrafree-MC Centrifugal Filter Devices (Millipore Corporation, Bedford, MA) and centrifuged for 2 minutes at 12,000 g using a accuSpin™ Micro (Fisher Scinetific) to remove interfering background absorbance attributable to proteins in the serum. After preparation of serum samples, nitrate in the samples was reduced to nitrite by incubation of 80 µl of sample with 10µl of Nitrate Reductase (Alexis Biochemicals) and 10 µl of Enzyme Cofactor (Alexis Biochemicals) at room temperature for 3 hours. All analyses were carried out in 96-well microtiter plates (Falcon, Becton Dickinson, Franklin Lakes, NJ) in triplicates. A nitrate standard curve was prepared by mixing 0.9 ml of Assay Buffer (Alexis Biochemicals) and 0.1 ml of reconstituted nitrite standard (in Assay Buffer; Alexis Biochemicals). From this solution, eight dilutions were prepared to a final nitrite concentration of 0, 5, 10, 15, 20, 25, 30 and 35 µM. The plate was set up as follow, 200 µl of Assay Buffer was added to blank wells, 100 µl of standard (for all eight dilutions) or 100 µl of serum was added to appropiate wells. The nitrate concentration in the samples was determined by the Griess reaction, by adding 50 µl of Griess reagent R1 (sulphanilamide; Alexis Biochemicals), immediately followed by 50 µl of Griess reagent R2 (*N*-(1-Naphthyl) ethylenediamine; Alexis Biochemicals) to every well. The color was then allowed to develop for 10 minutes, at room temperature, before the absorbance was read at 540 nm using a Vmax microtiter plate spectrophotometer (Molecular Devices Corporation, Menlo Park, CA). A standard curve comparison was used to obtain the relative measurement of nitrite concentration for the serum samples.

2.13 SG6 cell line

The SG6 cell line was established from peripheral lymphoid cells isolated from SGVHD mice exhibiting clinical symptoms of disease (typically 60-80% of CsA-treated animals). Animals were euthanized, the spleen and mesenteric lymph nodes were removed and placed into stomacher bags containing 5% complete medium. After homogenization, the single-cell suspensions of spleen and MLN were pooled and the RBC were removed with Tris ammonium chloride as described. $CD4^+$ T cells were positively selected using CD4 (L3T4) mouse MicroBeads (MACS magnetic beads, Miltenyl Biotech, Auburn, CA, USA) with the cells being selected on an AutoMACS system (Miltenyl Biotech). The purity of the MACS-isolated donor cells was monitored by flow cytometry and found to be > 92% $CD4^+$ T cells. Purified $CD4^+$ T cells (1-2 x 10^6), resuspended in 10% complete medium, were cultured in 24-well, flat-bottomed microtiter plates with 2 x 10^6 (2000cGy) irradiated cecal antigen-pulsed spleenic APC. The cecal antigen was prepared according to the procedure described by Cong et al. [81]. Briefly, the ceca were removed from animals and placed in a Petri dish containing PBS. The cecal contents were collected by low-speed centrifugation and were resuspended in PBS containing DNase I (10 μg/ml) (Sigma-Aldrich). Glass beads equal to 1/5th the volume of the material in the tube were added and the preparation was sonicated for 5 min (15 s on, 15 s off) in a Fisher 550 Dismembrator (Thermo Fisher, Waltham, MA, USA). After sonication, the antigen preparation was centrifuged for 15 min at 10,000 rpm in a Fisher AccuSpin microcentrifuge (Thermo Fisher) to remove debris. The supernatant was removed, filter sterilized, and analyzed for protein content by Bio-Rad assay (Hercules, CA, USA). Spleen cells isolated from normal C3H/HeN mice were cultured

overnight with 200μg cecal antigens, washed, irradiated (2000 cGy) and utilized as described. After 8-10 days of culture the cells were harvested over lympholyte M (Atlanta Biologicals). The viable cells were counted and restimulated as described.

2.14 Determination of Protein content using Bio-Rad assay

Protein levels of cecal Ag preparation was measured by Bio-Rad assay following the standard protocol of the manufacturer. The Bio-Rad Dye reagent was prepared by diluting 1 part Dye Reagent Concentrate with 4 parts of distilled, deionized (DDI) water. The reagent was filtered using a Watman#1 paper to remove particulates. Dilutions were prepared for the bovine γ-globulin protein standard (1.38 mg/ml) and the sample as follow: four dilutions (690 μg/ml, 345 μg/ml, 173 μg/ml and 86.2 μg/ml) of the protein standard and eight dilutions (1:2, 1:4, 1:8, 1:16, 1:32, 1:64, 1:128 and 1:256) of the cecal Ag preparation. One hundred (100) μl of each standard and sample solution was added into a glass test tube. Five ml of the diluted dye reagent was added to each tube and and the tubes were vortexed. The mixture was incubated at room temperature for 5 minutes. After incubation, the absorbance was measured at 595 nm using a SmartSpec^{TM} 3000 Spectrophotometer (Bio-Rad). A standard curve comparison was used to obtain the relative measurement of protein concentration.

2.15 Labeling of SG6 cells with (CFSE)

Cells were labeled with carboxyfluorescein succinimidyl ester (CFSE) according to the manufacturer's instructions (CellTrace™ CFSE Cell Proliferation Kit, Invitrogen, Eugene OR). Briefly, a 5 mM CellTrace™ CFSE stock solution was prepared by the addition of 18µl of DMSO (Sigma) to a vial of CFSE. SG6 cells were labeled by incubating 5 x 10^6 cells with 2.5 µM CFSE in PBS for 6 min at 37°C. After incubation, the cells were washed once with 10% complete medium (RPMI 1640 containing penicillin/streptomycin/ glutamine and 10% FBS (Atlanta Biologicals, Inc., Norcross, GA, USA)). The cell pellet was diluted with 5 volumes of complete medium and the cells were further incubated for 15 minutes at 37°C to remove excess dye. The cells were washed with complete medium and resuspended in PBS for use in homing studies.

2.16 *In vivo* homing of labeled SG6 cells

The *in vivo* migration of SG6 cells labeled with CFSE was analyzed in several tissues of control and CsA mice at day 22 post-BMT. A total of 5 × 10^6 CFSE-labeled cells suspended in 0.1 ml of PBS were injected i.v. into tail vein of olive oil- or CsA-treated mice at day 21 post-BMT. Mice were killed after 24 hours and the distribution of CFSE-labeled SG6 cells in different organs was measured. Tissues were removed from euthanized animals and immediately embedded in Tissue-Tek OCT compound and snap frozen in liquid nitrogen. Samples were cut into 10 µm tissue sections, mounted on glass slides and observed under a fluorescent microscope. Each labeled SG6 cell was counted, in 4-5 microscopic fields, over a 100x magnification. The mean values and their standard

error were determined from two independent experiments containing a total of four animals per experimental group.

2.17 Statistics

Statistical differences between experimental groups were determined using Student's *t* test, Fisher's exact test (induction) and Two way ANOVA analysis of variance. Differences $p<0.05$ were considered statistically different.

Figure 2.1 Induction of murine syngeneic graft-versus-host disease

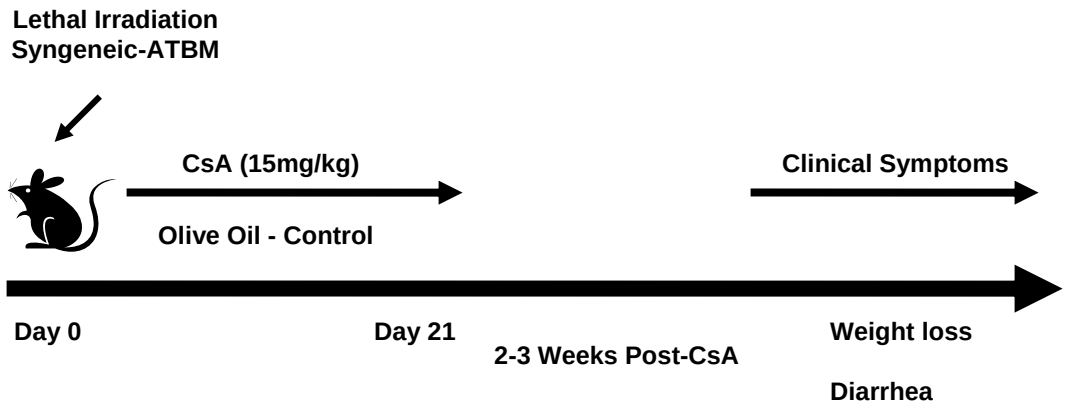

Figure 2.1 Induction of murine syngeneic graft-versus-host disease. C3H/HeN recipient mice were lethally irradiated (900 cGy) and reconstituted with 5 x 10^6 T cell-depleted bone marrow (ATBM) from syngeneic aged-matched mice. Beginning on the day of transplantation, mice were treated daily for 21 days with either 15mg/kg CsA in the diluent olive oil or with the diluent alone. Between 2-3 weeks post-CsA animals begin to develop clinical symptoms (weight loss and/or diarrhea).

Table 2.1 SGVHD Grading scale for colon and liver tissues

Adapted from Bryson et al. [79]

GRADING	COLON	LIVER
+/-	Rare crypt cell necrosis	Minimal lymphocyte infiltrate in portal area; rare bile duct epithelial cell degeneration
1^+	Definite scattered single-cell necrosis in crypts	Sparse, but definite portal lymphocyte infiltrate; occasional necrotic bile duct epithelial cells
2^+	Several necrotic cells in gland, crypt abscesses present	Diffuse infiltrate in portal area; invasion of bile ducts by inflammatory cells
3^+	Confluent destruction of glands	Heavy infiltrate partially obscuring bile ducts; focal bile duct destruction
4^+	Loss of mucosa with formation of granulation tissue and pseudomembranes	All the above plus secondary changes in hepatocytes, bile stasis, hepatocyte necrosis and disordered architecture

Figure 2.2 *In vivo* treatment with the antioxidant MnTBAP

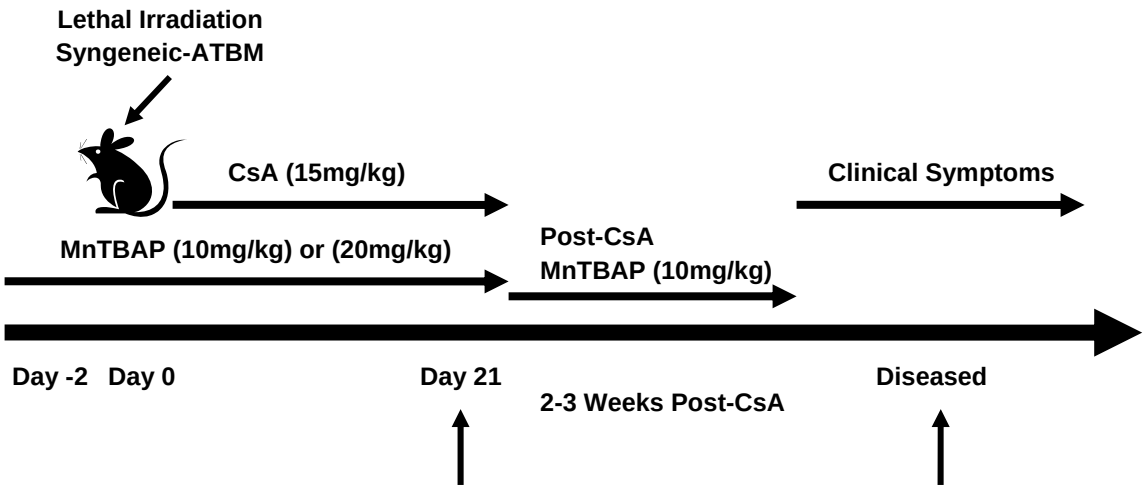

Figure 2.2 *In vivo* treatment with the antioxidant MnTBAP. C3H/HeN recipient mice were induced to develop SGVHD as described. Antioxidant treatment was performed either during or post-CsA therapy. For MnTBAP treatment during CsA period, mice were treated daily for 21 days with either 15mg/kg CsA in the diluent olive oil, the diluent alone, MnTBAP alone or CsA and MnTBAP. For MnTBAP treatment post-CsA, control or CsA-treated mice received MnTBAP starting at day 21 post-BMT for 2-3 weeks. Starting on day 21 post-BMT all mice are monitored for the onset of clinical symptoms (weight loss and/or diarrhea).

Figure 2.3 *In vivo* neutralization of TNF-α

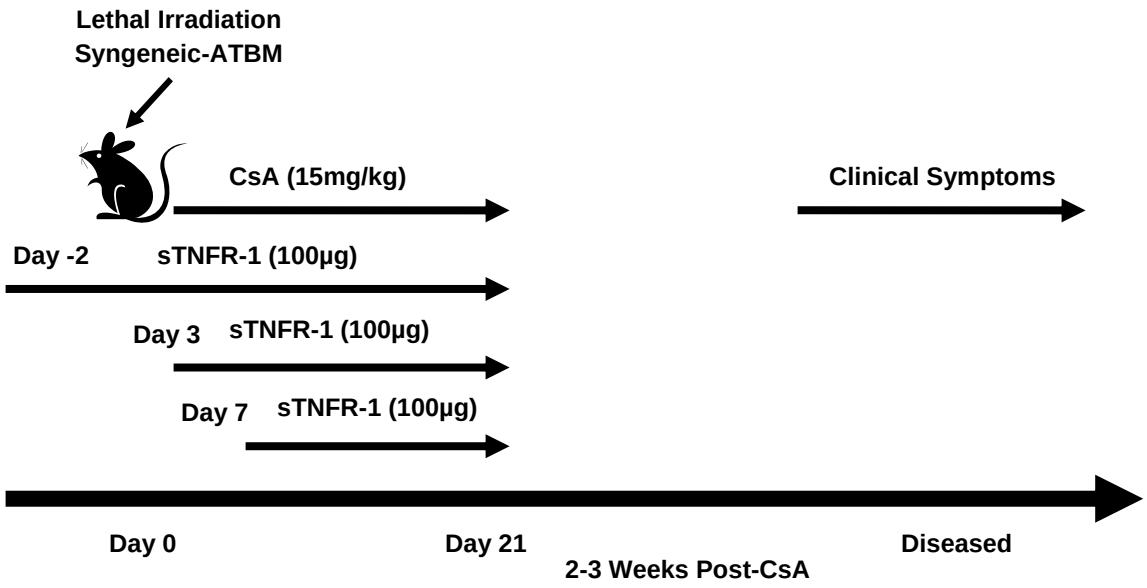

Figure 2.3 *In vivo* neutralization of TNF-α. C3H/HeN mice were induced to develop SGVHD as described previously. Groups of mice received either olive oil, 15mg/kg CsA, 100 µg sTNFR-1 alone or CsA and sTNFR-1. Neutralization of TNF- α started at several time points during the CsA treatment period. Mice were monitored for clinical symptoms of SGVHD (weight loss and/or diarrhea) starting on day 21 post-BMT. Tissue was collected at the end of each experiment for analysis.

Table 2.2 Antibodies used for flow cytometry analysis

ANTIBODY	**SPECIFICITY**	**LABEL**	**MANUFACURER**	**VOLUME ADDED**
Fc block	Fc receptor	None	BD Pharmingen[a]	1 µl
F4/80	Macrophages	APC	BioLegend[a]	1 µl
CD4	T cells	APC	Caltag[b]	1 µl
αβ	TCR	FITC	BD Pharmingen[a]	2 µl
CD62L	Naïve phenotype	PE	BD Pharmingen[a]	5 µl
β_7 integrin	Activated lymphocyte	FITC	BD Pharmingen[a]	1 µl
CD44	Memory phenotype	PE	BD Pharmingen[a]	5 µl

[a] San Diego, CA; [b] Burlingame, CA

Table 2.3 Antibodies used for immunohistochemistry (IHC) analysis

ANTIBODY	SPECIFICITY	LABEL	MANUFACURER	DILUTION
Rabbit Anti-nitrotyrosine	Protein tyrosine nitration	None	Millipore[a]	1:50
Goat Anti-Rabbit IgG	IgG heavy and light chains	Oregon Green 488	Invitrogen[b]	1:1000
Mouse Anti-MAdCAM-1	MECA-367	None	BD Pharmingen[c]	1:1000
Anti-Rat IgG	Rat IgG	Biotin	BD Pharmingen[c]	1:1000
Streptavidin	Biotin	PE	Sigma[d]	1:1000
CD4	L3T4	FITC	eBioscience[c]	1:1000
Anti-Rat IgG	Rat IgG	FITC	eBioscience[c]	1:1000

[a] Temecula, CA; [b] Grand Island, NY; [c] San Diego, CA, [d] St. Louis, MO

Table 2.4 Real Time RT-PCR reaction conditions for mRNA analysis

A. REVERSE TRANSCRIPTION REACTION*	
Reagent[a]	**Volume added per sample**
$MgCl_2$ 25mM	4.0 µl
Buffer 10X pH.8.8	2.0 µl
PCR Nucleotide Mix 10mM	2.0 µl
Oligo (dT) 500µg/ml	1.0 µl
RNasin 40U/µl	0.5 µl
AMV Reverse Transcriptase	0.6 µl
B. PCR REACTION (Master Mix)	
Reagent	**Volume added per sample**
Enzyme Diluent[b]	1.125 µl
dNTP[b] 10X 2mM	1.250 µl
Buffer[b] 10X w/BSA 30 mM $MgCl_2$	1.250 µl
Primer[c]	0.250 µl
Sybr Green[d] 5X	0.625 µl
dH_2O	5.375 µl
Platinum Taq DNA Polymerase[e] 5U/µl	0.125 µl
cDNA	2.500 µl

* After mixing all reagents, 1µg of RNA and dH_2O to 20µl were added. The tubes were then incubated for 30 minutes at 42°C, then for 5 minutes at 95°C and 5 minutes on ice. Samples were stored in -20°C freezer.

[a] Reagents were purchased from Promega Corporation (Madison, WI).
[b] Reagents were purchased from Idaho technology Inc (Salt Lake City, UT).
[c] Reagents were purchased from Integrated DNA technologies (Coralville, IA).
[d] Reagents were purchased from Molecular probes (Eugene, OR).
[e] Reagents were purchased from Invitrogen (Grand Island, NY).

Table 2.5 Polymerase chain reaction (PCR) primers and conditions

PRIMERS*	**SEQUENCE**
GAPDH[a]	Forward 5'-TGCACCACCAACTGCTTA-3' Reverse 5'-GGATGCAGGGATGATGTTC-3'
TNF-α[a]	Forward 5'-CATCTTCTCAAAATT CGAGTGACAA-3' Reverse 5'-TGGGAGTAGACAAGGTACAACCC-3'
iNOS[a]	Forward 5'-TGACGGCAAACATGACTTCAG-3' Reverse 5'-GCCATCGGGCATCTGGTA-3'
SOD-1[a]	Forward 5'-AAGGCCGTGTGCGTGCTGAA-3' Reverse 5'-CAGGTCTCCAACATGCCTCT-3'
GPx[a]	Forward 5'-CCTCAAGTACGTCCGACCTG-3' Reverse 5'-CAATGTCGTTGCGGCACACC-3'
CAT[a]	Forward 5'-GCAGATACCTGTGAACTGTC3' Reverse 5'-GTAGAATGTCCGCACCTGAG -3'
MAdCAM-1[a]	Forward 5'-GACACCAGCTTGGGCAGTGT-3' Reverse 5'-CAGCATGCCCCGTACAGAG-3'
ICAM-1[a]	Forward 5'-GGGACCACGGAGCCAATT-3' Reverse 5'-CTCGGAGACATTAGAGAACAATGC-3'
VCAM-1[a]	Forward 5'-CTGAATACAAAACGATCGCTCAA-3' Reverse 5'-GCGTTTAGTGGGCTGTCTATCTG-3'
CCR5[a]	Forward 5'-CAAGACAATCCTGATCGTGCAA-3' Reverse 5'-TCCTACTCCCAAGCTGCATAGAA-3'
CCL5 [b]	Forward 5'-TGCCCACGTCAAGGAGTATTT-3' Reverse 5'-TCTCTGGGTTGGCACACACTT-3'
CCL20 [c]	Forward 5'-CTGCTGGCTCACCTCTGCA-3' Reverse 5'-CATCGGCCATCTGTCTTGTG-3'

Table 2.5 (Cont.) Polymerase chain reaction (PCR) primers and conditions

[*] All the primers were purchased from Integrated DNA technologies (Coralville, IA).

[a] 95°C for 10 minutes, followed by 50 cycles of 30 seconds at 95°C, 30 seconds at 60°C, 30 seconds at 72°C and 72°C for 10 minutes

[b] 95°C for 10 minutes, followed by 50 cycles of 30 seconds at 95°C, 30 seconds at 64°C, 30 seconds at 72°C and 72°C for 10 minutes

[c] 95°C for 10 minutes, followed by 50 cycles of 30 seconds at 95°C, 30 seconds at 56°C, 30 seconds at 72°C and 72°C for 10 minutes

CHAPTER THREE: ROLE OF OXIDATIVE STRESS IN SGVHD

3.1 Synopsis

Under normal physiological conditions, the production of reactive oxygen species (ROS) as well as reactive nitrogen species (RNS) function as signaling molecules in many processes including cell cycle and metabolism [129, 130]. When the balance between levels of intermediate species is disrupted the harmful effects overcome the beneficial ones interrupting redox homeostasis. For this reason, there are several molecules that exist to counteract the damaging effects of oxidative stress and are known as antioxidants. This group of protective molecules include enzymes like superoxide dismutase (SOD), catalase and glutathione peroxidase (Gpx) [131]. Thus, oxidative stress production can be defined as the imbalance between the generation of free radicals, including their intermediates and the incapacity of antioxidant activity to reduce their effect. Recently, the concept of oxidative stress has been extended to not only ROS, like superoxide radicals and hydrogen peroxide but also includes RNS such as nitric oxide (NO), peroxynitrate and S-nitrosothiols [130]. Nitric oxide reacts with superoxide (O_2^-) to form peroxynitrite ($ONOO^-$), a highly reactive species that induces nitrative and oxidative DNA damage [103, 107]. The role of oxidative stress in the pathophysiology of diseased states [88, 99, 126, 132] has led to the development of metalloporphyrin catalytic antioxidants as possible therapeutic agents. Manganese (III) meso-tetrakis (4-benzoic acid) porphyrin (MnTBAP) is a stable metalloporphyrin that can scavenge a broad spectrum of reactive oxygen and nitrogen species [133-137]. This compound can scavenge peroxynitrite [137], catalyze the dismutation of superoxide [136] and hydrogen

peroxide [135], inhibit lipid peroxidation [134] as well as protect DNA from ROS-mediated damage. MnTBAP has been successfully used to prevent oxidant-induced injury responses by activated macrophages both *in vitro* and *in vivo* [135, 136]. Since it has been implied that ROS is a mediator of CsA toxicity, and CsA treatment is a prerequisite for SGVHD induction, studies were undertaken to investigate the role of oxidative stress in the induction of SGVHD by treating mice with the antioxidant MnTBAP. Tissues from C3H/HeN mice were taken at various time points and analyzed for the presence of oxidative stress as well as proinflammatory cytokine expression and SGVHD induction.

3.2 Determination of intracellular reactive oxygen species

Intracellular ROS production was determined by using the fluorescent probe DCFH-DA. When the diacetate form of DCFH (DCFH-DA) is added to cells, it diffuses across the cell membrane and is hydrolyzed by intracellular esterases to give 2',7'-dichlorofluorescin (DCFH), the oxidation of which yields fluorescent DCF [127] that can be monitored by flow cytometry. DCFH-DA labeled spleen cells were monitored, as an indicator of changes in ROS during SGVHD induction (days 0-21 post-BMT) (**Figure 3.1, A**) as well as during the post-CsA period, when clinical symptoms of disease were evident (**Figure 3.1, B**). Oxidation of DCFH-DA to fluorescent DCF was significantly increased in CsA-treated animals by day 21 post-BMT (P=0.0240; **Figure 3.1, A**) as well as during active disease (P=0.0307; **Figure 3.1, B**) when compared to transplant control mice, demonstrating higher levels of ROS in CsA-treated animals.

3.3 Increased NO production in CsA-treated mice

Since our data demonstrated elevated levels of ROS, we then decided to investigate if increases in RNS could also be detected during the development of SGVHD. Nitric oxide was particularly intriguing because of the relationship that had been identified between NO and gut pathology during allogeneic GVHD [105], as well as in the pathological processes that are associated with the development of murine SGVHD [100]. Real time RT-PCR studies were performed to determine if increases in mRNA for iNOS could be detected in the colon, one of the target organs of SGVHD, during the period of CsA therapy (**Figure 3.2, A**). Increased mRNA for iNOS was present in the colon of CsA-treated animals as early as day 14 (P=0.0262) and at day 21 post-BMT (P=0.0011). As previously published by our group [100], iNOS mRNA levels remain significantly elevated during active disease in colonic tissue of CsA-treated mice compared to BMT control (P=0.0146). Preliminary studies confirmed the PCR findings in that increases in circulating NO were observed in the plasma/serum of SGVHD mice relative to normal or transplant control animals (**Figure 3.2, B**). As another measure of oxidative stress in the tissues of CsA-treated/SGVHD animals we monitored protein tyrosine nitration since it is an important marker of oxidative stress induced by peroxynitrite and other nitric-oxide derived oxidants [99, 130]. Our results show increased nitrotyrosine in colonic tissue of CsA-treated mice compared to control mice by day 21 post-BMT (**Figure 3.3, A**) as well as during disease period (**Figure 3.3, B**), demonstrating increased oxidation mediated by peroxynitrite. Taken together, these results demonstrate that CsA-treated mice produced significantly elevated amounts of

RNS compared to control BMT mice and confirm that increased oxidative stress is generated in mice undergoing CsA therapy.

3.4 Reduction of oxidative stress during CsA therapy alters the development of SGVHD

To determine the role of conditioning-induced oxidative stress on the development of SGVHD, the antioxidant MnTBAP, a stable metalloporphyrin that can scavenge a broad spectrum of reactive oxygen and nitrogen species [133-137], was given to control BMT and CsA mice during the CsA therapy period. C3H/HeN mice were lethally irradiated, reconstituted with syngeneic BM and treated with CsA for 21 days as described. Beginning two days prior to BMT, the mice were treated with MnTBAP, 10 mg/kg twice a day until day 21 post-BMT. Twice a day dosing regimen was performed based on the MnTBAP elimination half-time of 9.5 hours, as indicated by toxicology data [126]. Treatment of CsA mice with MnTBAP was able to significantly delay the induction of SGVHD in these animals compared to the ones that received CsA alone (**Figures 3.4, A, B and C**). Antioxidant therapy during CsA treatment delayed weight loss observed in the CsA-treated mice (**Figure 3.4, A**) as well as delayed development of clinical symptoms of SGVHD (P= 0.0023; **Figure 3.4, B**) and total disease induction (P= 0.0240; **Figure 3.4, C**).

3.5 Decreased iNOS and TNF-α mRNA levels after MnTBAP therapy during CsA treatment

Since the data showed increased levels of iNOS mRNA and RNS in CsA-treated animals compared to control BMT mice during CsA therapy (**Figure 3.2**), studies were undertaken to determine if treatment with the antioxidant MnTBAP was capable of reducing iNOS levels in CsA-treated animals during this time frame after BMT. Real time RT-PCR studies revealed a decrease in iNOS mRNA levels in CsA-treated mice that were treated with MnTBAP (10 mg/kg) at day 21 post-BMT (**Figure 3.5, A**), suggesting that MnTBAP therapy was able to reduce NO production by inhibiting the iNOS enzyme. Similarly, Garcia-Ruiz et al. recently demonstrated that iNOS activity was reduced following MnTBAP therapy in the murine model of non-alcoholic fatty liver disease (NAFLD) [138]. Additionally, TNF-α mRNA levels were analyzed since increased mRNA levels of this proinflammatory mediator in colonic tissue of CsA-treated mice were observed by day 21 post-BMT (refer to Chapter 4 of dissertation; **Figure 4.3**). MnTBAP therapy was able to decrease TNF-α mRNA levels in the colon of CsA-treated mice when compared to CsA mice that did not receive the antioxidant therapy (**Figure 3.5, B**). While there was a clearly identified trend, the reduction in iNOS and TNF-α mRNA levels were not statistically significant ($p \geq 0.05$). The mRNA levels of the proinflammatroy cytokines IL-12 and IFN-γ, which are known to mediate SGVHD [80, 83] were also analyzed by real time RT-PCR at day 21 post-BMT and as shown in **Figure 3.6**, MnTBAP therapy did not reduce their levels in the colonic tissue of CsA-treated mice.

3.6 Effect of MnTBAP treatment during CsA therapy on generation of oxidative stress

Our results demonstrated that treatment of CsA mice with an antioxidant reduced the severity of SGVHD when compared to mice receiving CsA alone. However, the mechanism(s) by which the SOD mimetic exerted its beneficial actions remained unknown. Given that the levels of nitrotyrosine in colonic tissue of CsA-treated mice were elevated when compared to transplanted controls (**Figure 3.3**), we analyzed the levels of this oxidative stress marker in control, CsA and CsA-MnTBAP treated mice at day 21 post BMT (**Figures 3.7**). Immunohistochemistry analysis revealed less nitrotyrosine staining in the colons of CsA mice that also received MnTBAP compared to mice treated with CsA alone (**Figure 3.7, A**). In addition, the quantitative measure of nitrotyrosine staining in colonic tissue revealed that MnTBAP treatment was capable of reducing oxidative stress in a significant manner when compared to mice that were only treated with CsA (**Figure 3.7, B**). These studies demonstrated that treatment with the SOD mimetic reduced production of peroxynitrite in the colon of CsA-treated mice, reducing a potent RNS mediator that has been shown to be unregulated during intestinal inflammation of IBD [99].

3.7 Reduction of oxidative stress post-CsA therapy alters the development of SGVHD

Since our results demonstrated that antioxidant therapy during the 21 days of CsA induction therapy was able to delay disease induction, we analyzed the role of oxidative stress post-CsA therapy in the development of SGVHD. For these experiments, treatment

with the antioxidant MnTBAP was given to BMT control and CsA mice after cessation of CsA therapy. C3H/HeN mice were lethally irradiated and reconstituted with syngeneic BM and treated with CsA for 21 days as described. Beginning on day 21 post-BMT, the mice were treated with MnTBAP 10 mg/kg twice a day for 2-3 weeks until CsA-treated mice were positive for SGVHD (≥ 80%). Treatment of control and CsA-treated mice with MnTBAP in the post-CsA period delayed the development of clinical symptoms of SGVHD (**Figures 3.8, A, B and C**). Antioxidant therapy post-CsA treatment reduced weight loss observed in the CsA-treated mice (**Figure 3.8, A**). Clinical symptoms of SGVHD, including weight loss, diarrhea and/or death were decreased in CsA-treated mice that also received MnTBAP compared to mice that did not receive the antioxidant therapy (P= 0.0050; **Figure 3.8, B**). In addition, total disease induction was significantly reduced by antioxidant therapy post-CsA period (P= 0.0003; **Figure 3.8, C)**. Since iNOS mRNA levels were shown to be up-regulated during SGVHD (**Figure 3.2**), real time RT-PCR analysis was performed to evaluate the effect that MnTBAP therapy had on the generation of iNOS mRNA at this stage of disease. Results showed decreased iNOS mRNA levels after antioxidant treatment in the colon of CsA-treated mice if compared to mice that received CsA alone (**Figure 3.9**). In addition, MnTBAP treatment in the post-CsA period was also capable of reducing nitrotyrosine staining in CsA-treated mice as shown in **Figure 3.10**. These results were not surprising as our group had previously shown that inhibition of iNOS post-CsA therapy decreased SGVHD induction [100]. Interestingly, histological analysis of colonic tissue revealed that MnTBAP treatment post-CsA therapy did not ameliorate disease pathology observed in CsA-treated mice (**Figure 3.11**) and was confirmed by immunohistochemistry analysis of $CD4^+$ T cells in

which migration of these effector cells into the colon of CsA-treated mice was not decreased by antioxidant therapy (**Figure 3.12**).

3.8 Summary

The results presented in this chapter confirm the hypothesis that SGVHD induction results in increased oxidative stress in CsA-treated mice compared to BMT controls. Treatment with a commercially available SOD mimetic, MnTBAP, during the 21 days of CsA therapy as well as post-CsA period resulted in delayed disease induction and clinical symptoms of SGVHD. However, the reduction of proinflammatory mediators and oxidative stress was not enough to completely ameliorate disease induction.

Figure 3.1 Elevated ROS in mice treated with CsA compared to control BMT

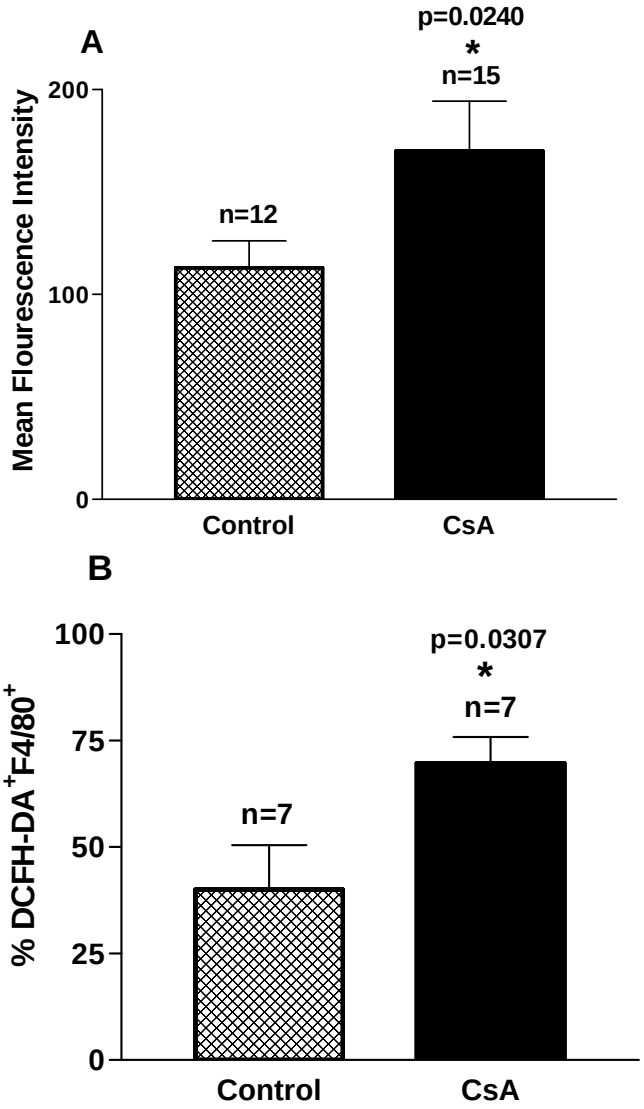

Figure 3.1 Elevated ROS in mice treated with CsA compared to control BMT. Spleen cells from CsA-treated mice produce increased levels of DCFH-DA. Spleens were removed from control and CsA-treated mice at day 21 post-BMT (A) or during active disease (B). Splenocytes were isolated and treated with DCFH-DA, as described and analyzed by flow cytometry. Data presented is pooled from four individual experiments, *n* represents the number of animals per group.

Figure 3.2 Increased reactive nitrogen species in CsA-treated mice

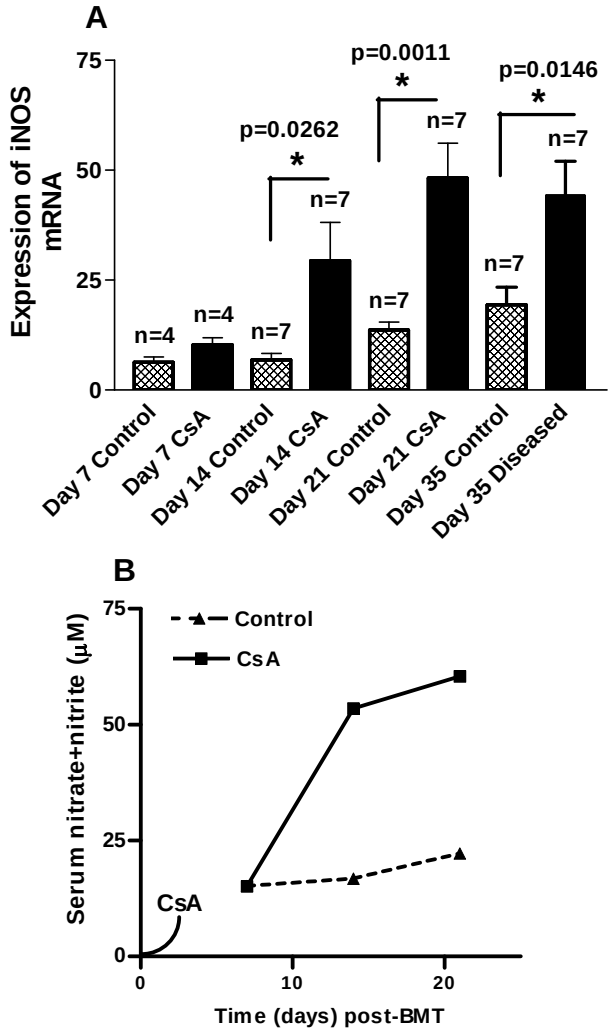

Figure 3.2 Increased reactive nitrogen species in CsA-treated mice. (A) Increased levels of iNOS mRNA in CsA-treated mice. Animals were induced to develop SGVHD as described. Tissue isolated from the colon at several time points was analyzed by real time RT-PCR. Data is representative of two experiments with *n* representing the number of mice. (B) Circulating NO is increased in CsA-treated animals. Normal, control, and CsA-treated BMT recipient mice were bled at several time points during CsA therapy. Serum was collected, and nitrate was reduced to nitrite by nitrate reduction and analyzed for the presence of NO_2^-. Data is representative of one experiment.

Figure 3.3 Increased levels of nitrotyrosine in the colons of CsA-treated mice

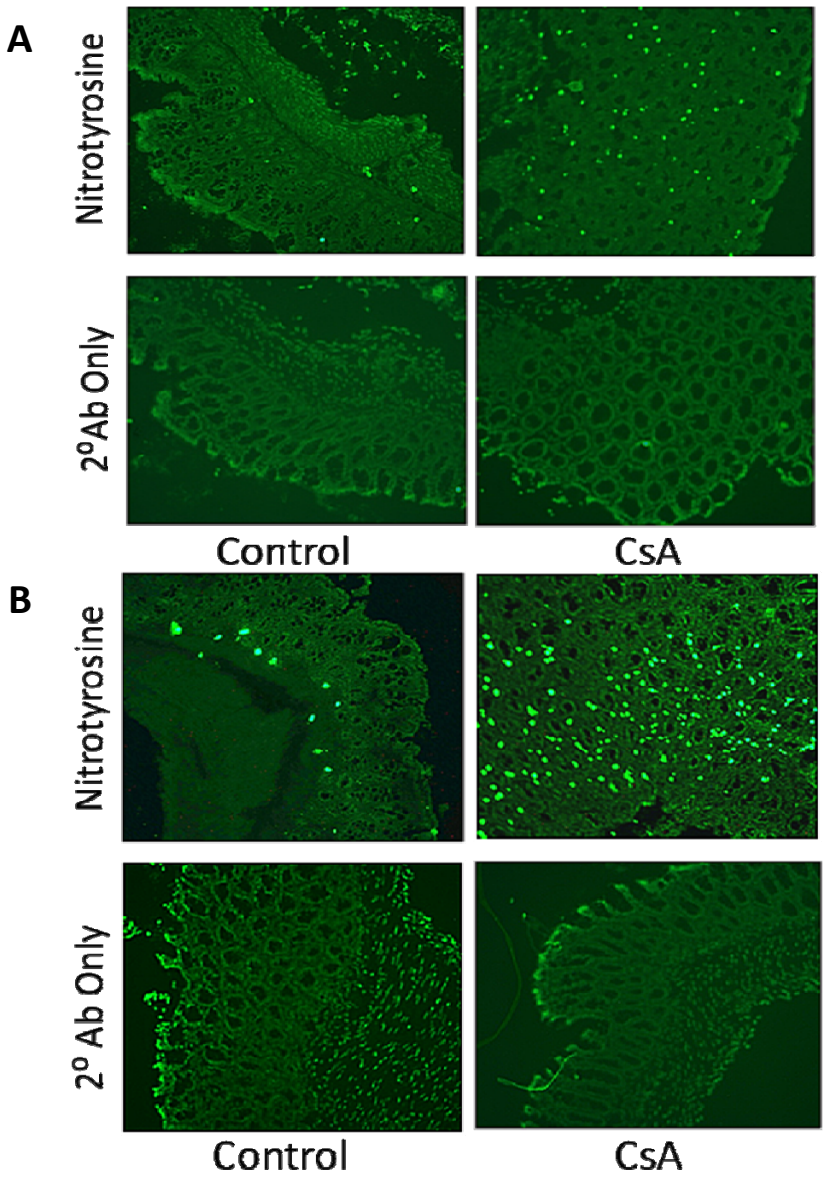

Figure 3.3 Increased levels of nitrotyrosine in the colons of CsA-treated mice compared to transplant controls. Colon tissue was isolated at day 21 post-BMT (A) and during SGVHD (B) and frozen sections analyzed for the presence of nitrotyrosine, a marker of RNS by IHC analysis. Slides were visualized under 100x magnification. The data presented are representative of samples from four mice from two individual experiments.

Figure 3.4 MnTBAP treatment delayed the development of SGVHD

A. Antioxidant therapy reduced weight loss in CsA mice

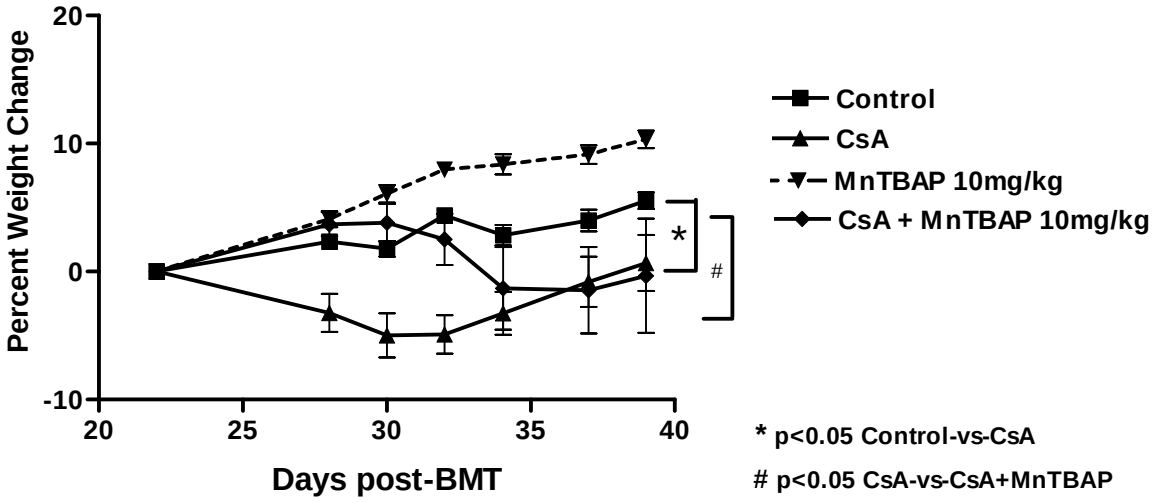

B. Delayed disease induction in MnTBAP treated mice

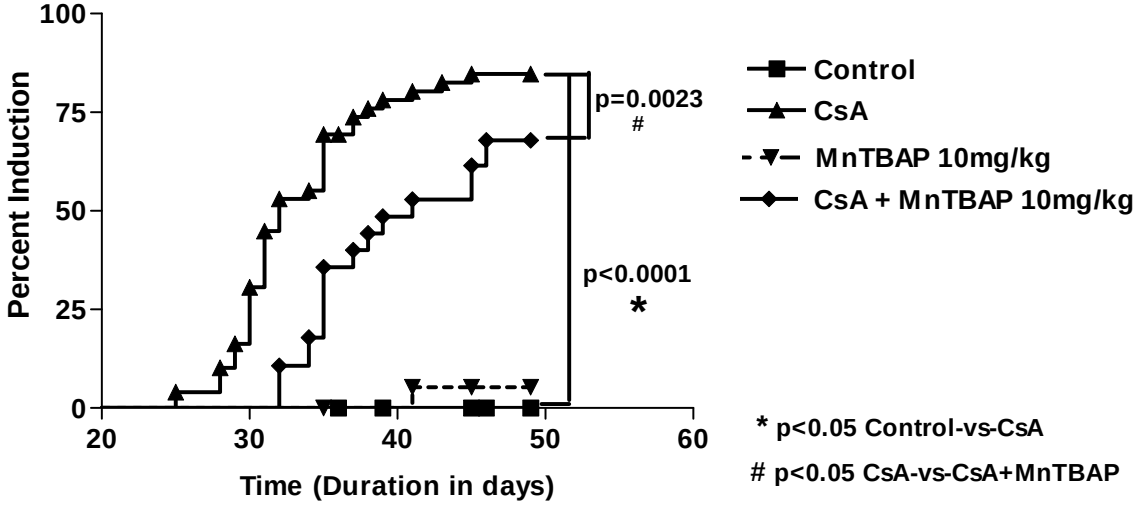

Figure 3.4 (Cont.) MnTBAP treatment delayed the development of SGVHD

C. Decreased SGVHD total induction after MnTBAP therapy

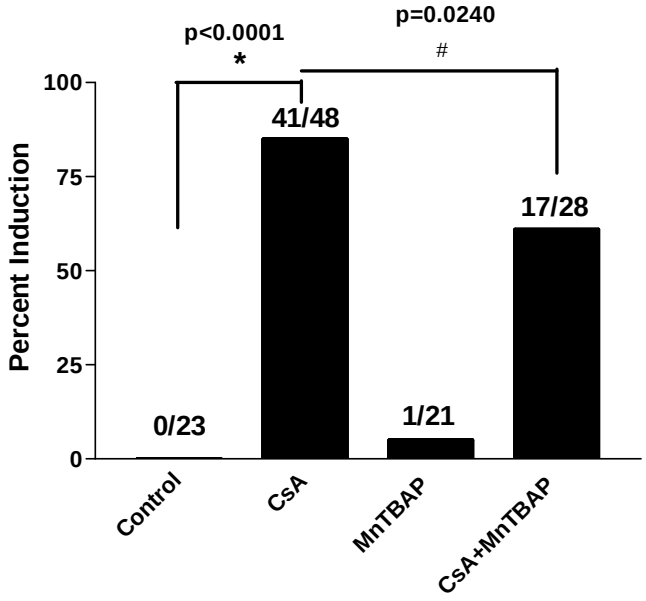

Figure 3.4 MnTBAP treatment delayed the development of SGVHD. Disease was induced in C3H/HeN mice, as described. Groups of control or CsA-treated mice were given 10 mg/kg of MnTBAP twice a day starting 2 days prior to BMT and every day for 21 days. The animals were then monitored for SGVHD induction (weight loss, diarrhea and/or mortality). (A) Animals were weighed individually 3x per week starting on day 21 post-BMT. Data presented represent pooled data from 2 experiments, plotted as average ± SEM of percent weight change for each treatment group (n = 16); (B) Animals were followed for induction and plotted as average ± SEM for the time to induction after BMT. Data presented represent pooled data from 4 experiments (n = 16); (C) Analysis for induction measured 49 days post-BMT, with the number of animals with SGVHD/total number of animals within each group presented above each bar. Data presented are pooled from four experiments.

Figure 3.5 MnTBAP therapy resulted in decreased colonic iNOS and TNF-α

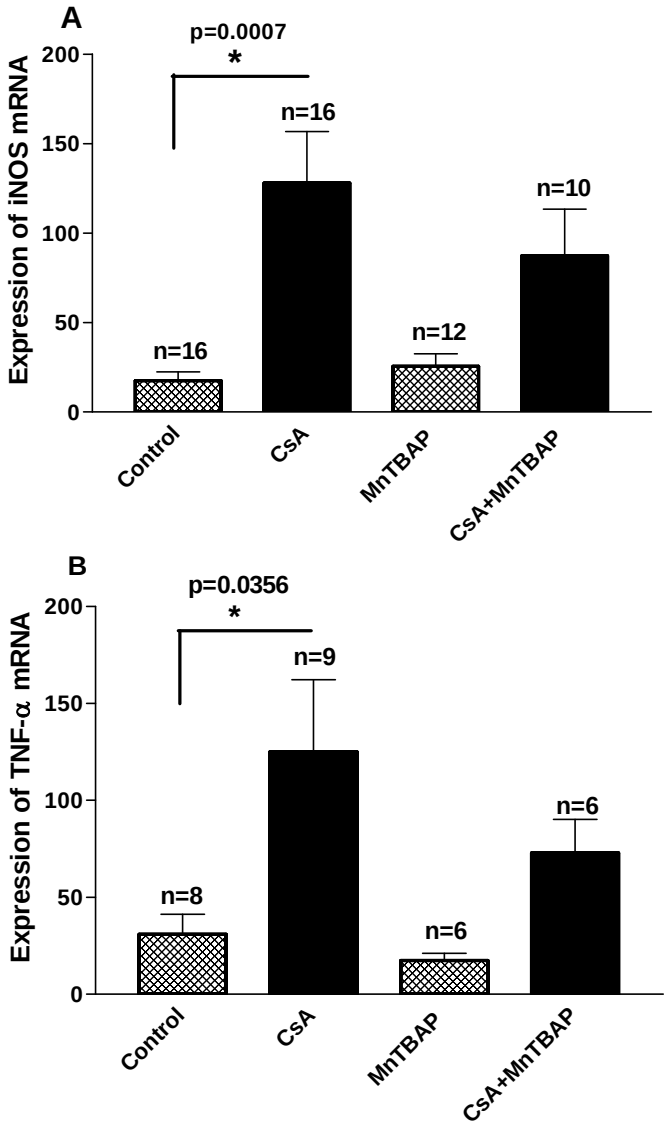

Figure 3.5 MnTBAP therapy resulted in decreased colonic (A) iNOS and (B) TNF-α. C3H/HeN mice were induced for SGVHD and treated with MnTBAP as described. On the day after the last MnTBAP treatment, the colon was removed from control, CsA-treated, MnTBAP-control, and MnTBAP-CsA-treated animals. Messenger RNA was isolated and analyzed by real time RT-PCR. Data presented are pooled from three individual experiments, *n* represents the number of mice per group.

Figure 3.6 MnTBAP therapy did not reduce IL-12 or IFN-γ mRNA levels

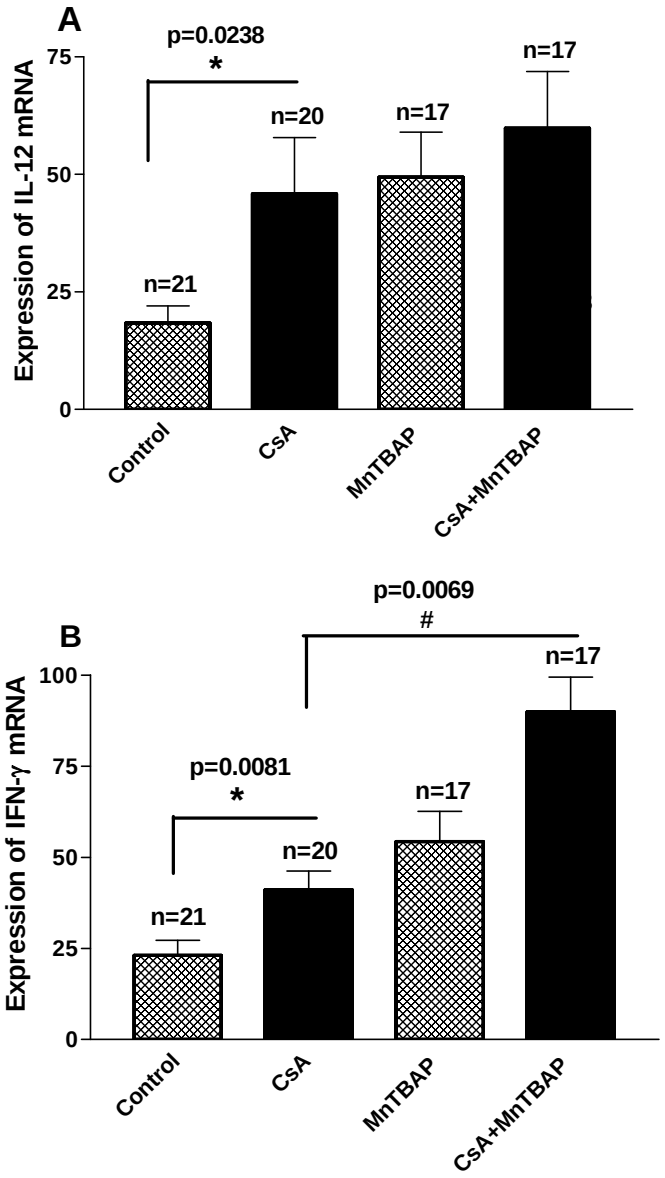

Figure 3.6 MnTBAP therapy did not reduce IL-12 or IFN-γ mRNA levels. SGVHD was induced as described and mRNA was isolated from the colons of control, CsA, MnTBAP and CsA+MnTBAP treated animals at day 21 post-BMT. Real time RT-PCR was performed for IL-12 (A) and IFN-γ (B). Data presented are the mean ± SEM, from pooled samples of four independant experiments, *n* represents the number of mice per group.

Figure 3.7 Reduced nitrotyrosine staining after antioxidant therapy

A. Immunohistochemistry staining of nitrotyrosine at day 21 post-BMT

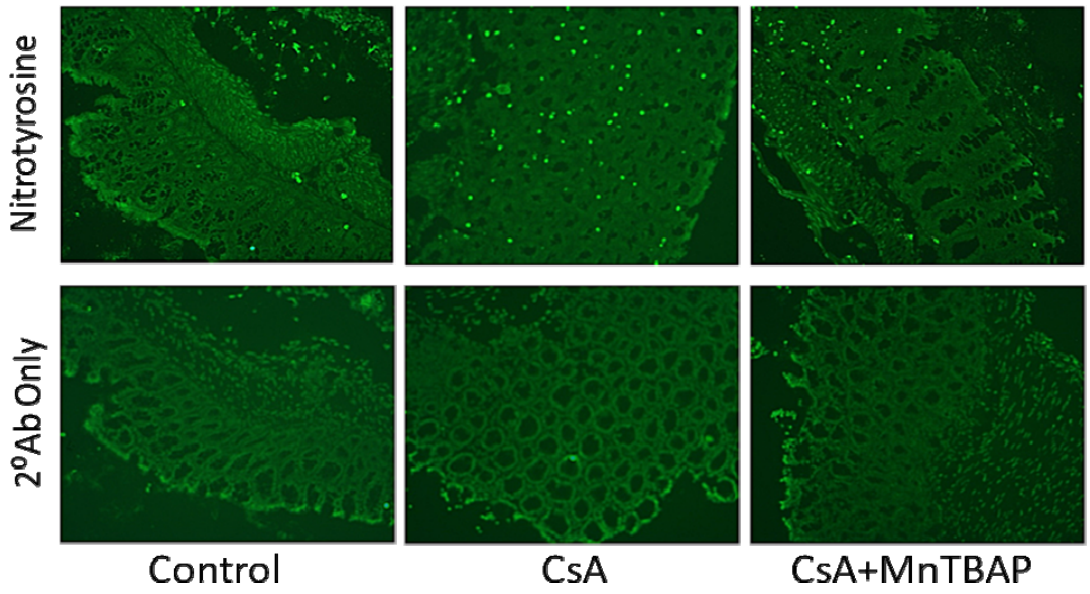

B. Quantitative measure of nitrotyrosine staining on day 21 colonic tissue

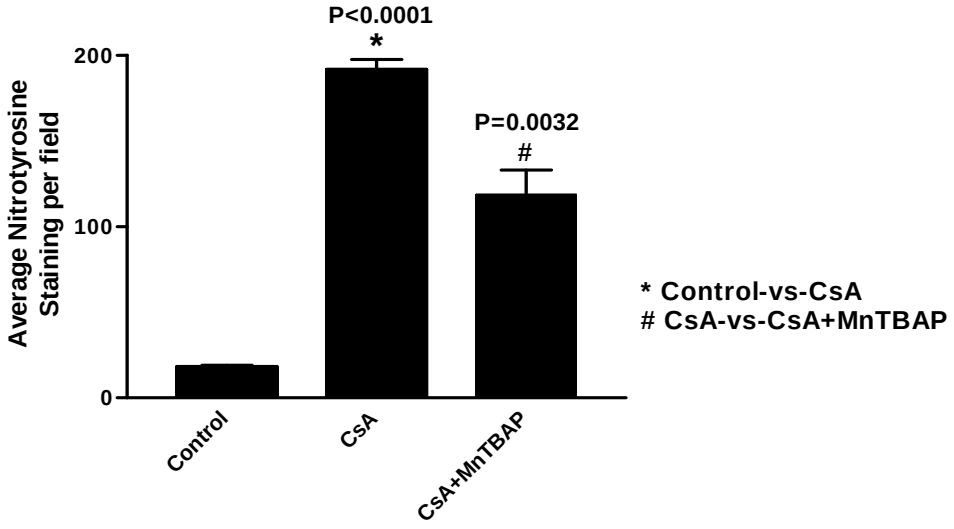

Figure 3.7 Reduced nitrotyrosine staining after antioxidant therapy. Colons of C3H/HeN mice were removed at day 21 post-BMT and frozen sections were analyzed by immunohistochemistry techniques for the presence of nitrotyrosine (A). Slides were visualized under 100x magnification and staining per field was quantified (B). The data presented are representative of samples from four mice from two individual experiments.

Figure 3.8 Delayed SGVHD after MnTBAP treatment post-CsA

A. Antioxidant therapy reduced weight loss in CsA mice

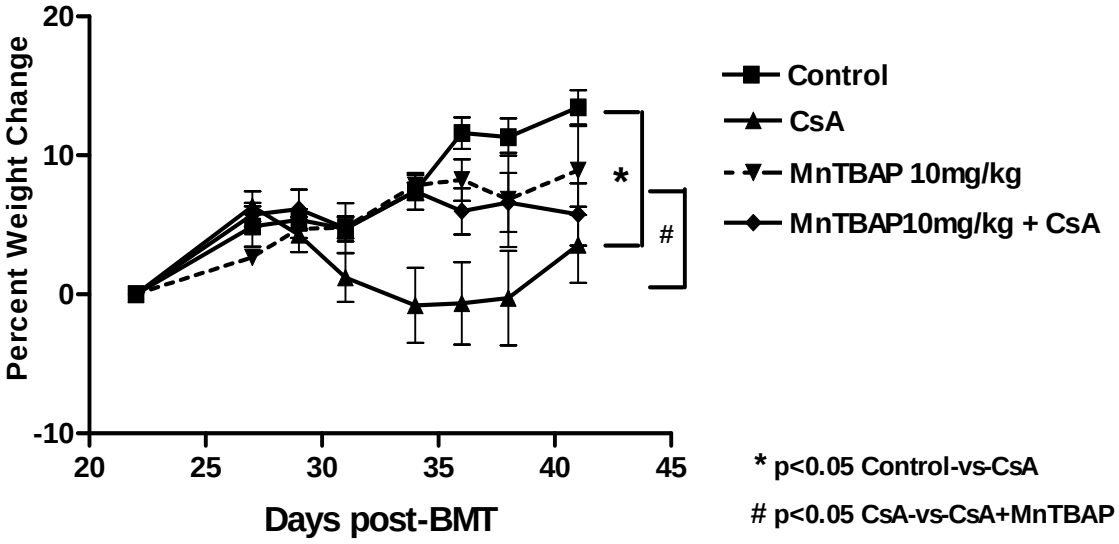

B. Delayed disease induction in MnTBAP treated mice

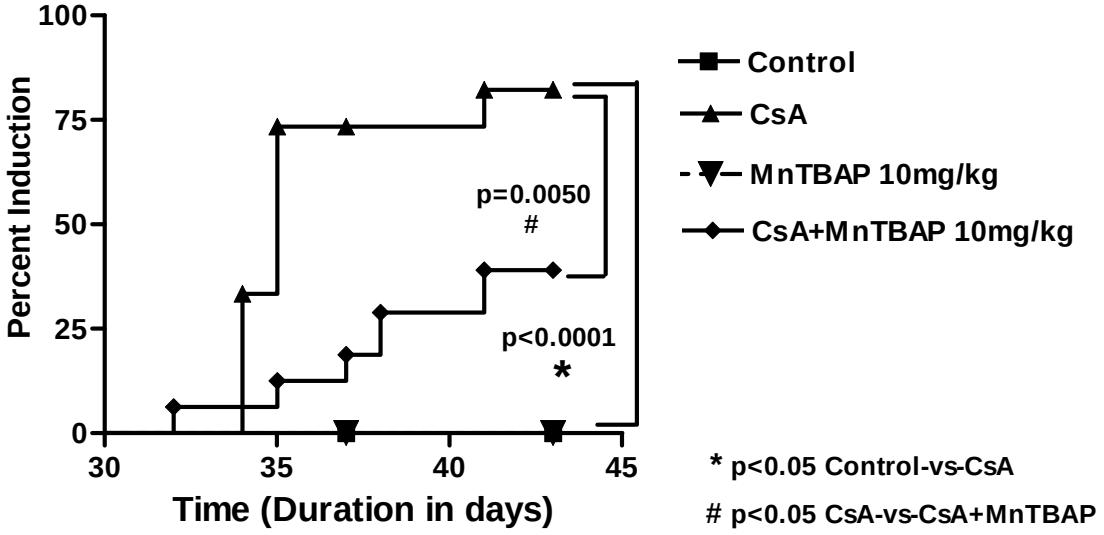

Figure 3.8 (Cont.) Delayed SGVHD after MnTBAP treatment post-CsA

C. Decreased SGVHD total induction after MnTBAP therapy

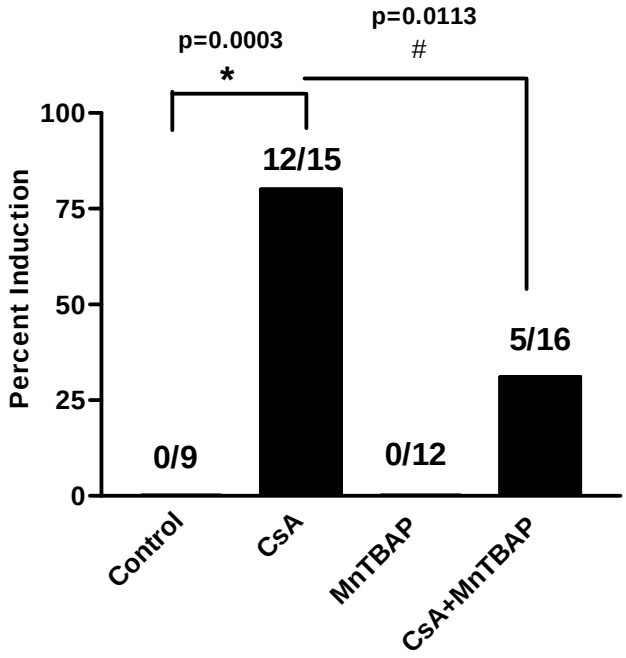

Figure 3.8 Delayed SGVHD after MnTBAP treatment post-CsA. Disease was induced in C3H/HeN mice, as described and groups of control or CsA-treated mice were given 10 mg/kg of MnTBAP twice a day beginning on day 21 post-BMT and every day up to 2-3 weeks, when the majority (> 80%) of the CsA animals had developed SGVHD. Animals were monitored for clinical symptoms of SGVHD. (A) Animals were weighed individually 3x per week starting on day 21 post-BMT and plotted as average ± SEM of percent weight change for each treatment group. (B) Animals were followed for induction and plotted as average ± SEM for the time to induction after BMT. (C) Analysis for induction measured 43 days post-BMT, with the number of animals with SGVHD/total number of animals within each group presented above each bar. Data presented are pooled from two experiments. Control $n = 9$, CsA $n = 15$, MnTBAP $n = 12$ and CsA+MnTBAP $n = 16$.

Figure 3.9 MnTBAP therapy reduced mRNA levels of iNOS

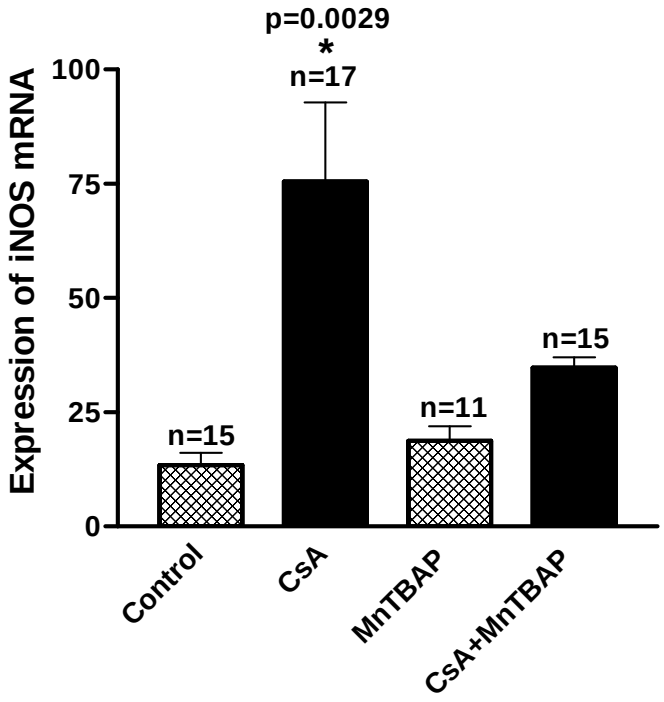

Figure 3.9 MnTBAP therapy reduced mRNA levels of iNOS. C3H/HeN mice were induced for SGVHD, as described and treated with MnTBAP post-CsA therapy. On the day after the last MnTBAP treatment, the colon was removed from each experimental group and mRNA was isolated from the colonic tissue. Real time RT-PCR was performed for iNOS. Data presented are pooled from two independent experiments, *n* represents the number of animals analyzed.

Figure 3.10 Decreased RNS in colon of CsA-treated mice after MnTBAP therapy

A. Immunohistochemistry staining of nitrotyrosine at day 21 post-BMT

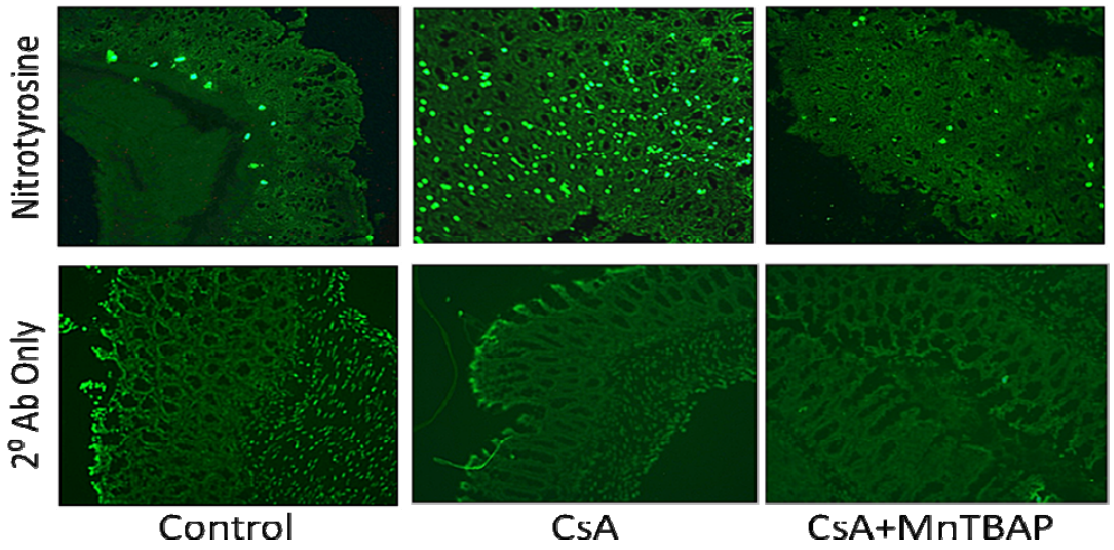

B. Quantitative measure of nitrotyrosine on SGVHD mice

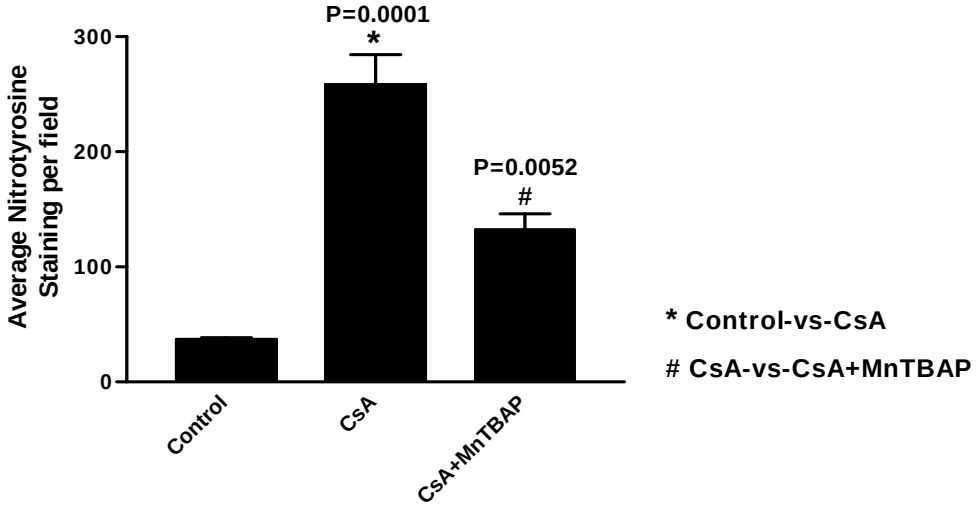

Figure 3.10 Decreased RNS in colon of CsA-treated mice after MnTBAP therapy. Immunohistochemistry analysis of colonic tissue during diseased stage revealed increased nitrotyrosine staining in colons of CsA-treated mice compared to control BMT and reduced staining in CsA after antioxidant therapy (A). Quantification of nitrotyrosine staining (B). Data is pooled from 2 experiments and represents *n*=4 mice per group.

Figure 3.11 Colon pathology was not altered by MnTBAP treatment

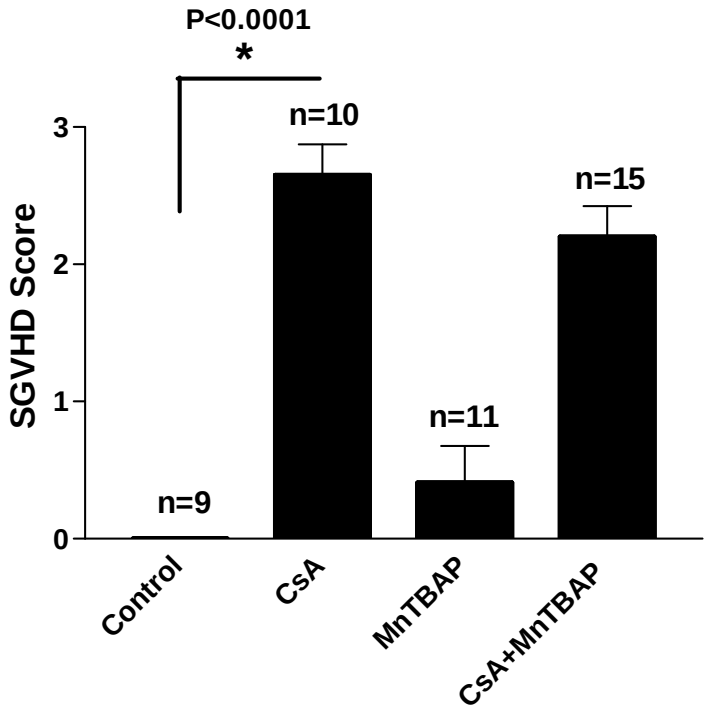

Figure 3.11 Colon pathology was not altered by MnTBAP treatment. Histological examination of SGVHD colons shows no difference after antioxidant therapy. Colon tissue was isolated during clinical symptoms of SGVHD, typically 3–4 weeks post-CsA treatment. The tissues were stained using H&E staining procedure and pathology grading was performed as described in Materials and Methods. Data represents mean grade ± SEM, *n* represents the number of mice per experimental group pooled from two independent experiments.

Figure 3.12 Migration of T cells into the colon was not reduced by MnTBAP

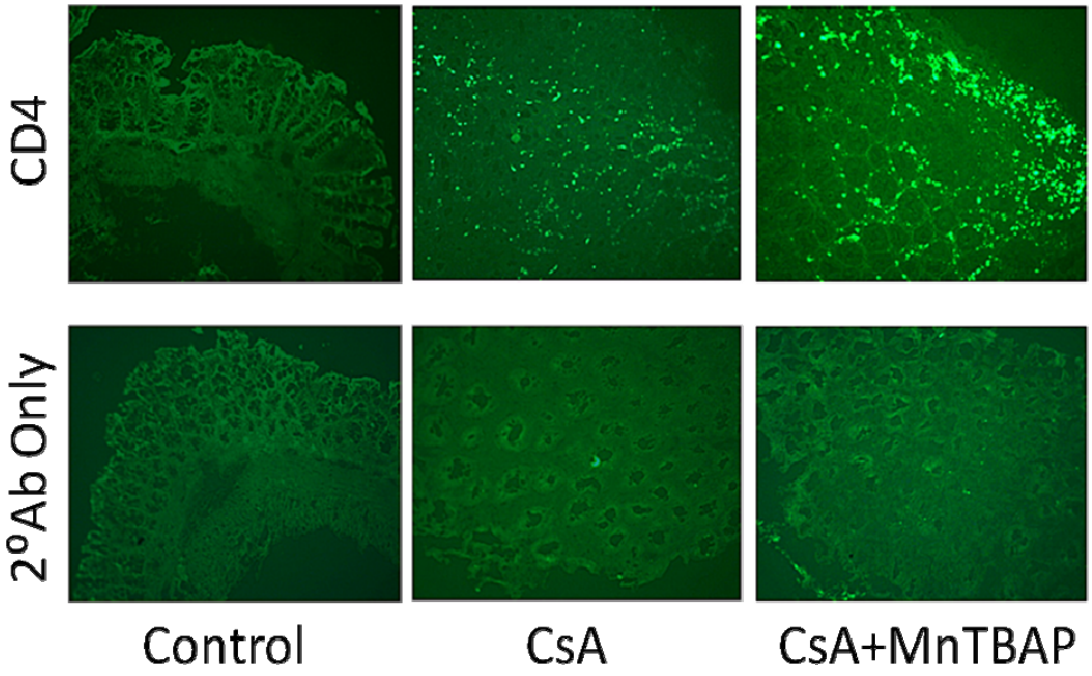

Figure 3.12 Migration of T cells into the colon was not reduced by MnTBAP. Immunohistochemistry staining of $CD4^+$ T cells in colonic tissue of SGVHD mice. Colon tissue from control BMT, CsA and CsA-MnTBAP treated animals was collected at day 43 post-BMT and frozen sections were stained for the presence of $CD4^+$ T cells. Colons from CsA animals show increased levels of CD4 staining compared to control BMT but MnTBAP treatment had no effect on inhibiting T cell migration into the colon of CsA-treated mice. The data presented are representative of *n*=4 from two individual experiments.

CHAPTER FOUR: ROLE OF T CELL HOMING IN SGVHD

4.1 Synopsis

Histological studies have demonstrated severe colonic tissue damage in SGVHD mice caused by massive infiltration of inflammatory cells, particularly $CD4^+$ T cells, into the colon of CsA-treated mice [55, 78, 80, 83, 100, 139]. Bryson et al. demonstrated a role for $CD4^+$ T cells in the induction of colitis observed in murine SGVHD. Increased $CD4^+$ but not $CD8^+$ T cells were observed in the colons of diseased animals. Additionally, *in vivo* depletion of $CD4^+$ T cells during CsA therapy inhibited significantly the induction of SGVHD [78] and SGVHD can be adoptively transferred with $CD4^+$ T cells from diseased animals into secondary recipients [58]. Previously published studies have demonstrated that an increase in colonic $CD4^+$ T cells was observed in CsA-treated mice by day 21 post-BMT, suggesting that enhanced T cell migration into the colon occurred during the CsA treatment period [78]. Studies were then undertaken to follow the migration of T cells at the early stages after BMT and investigate the mechanism that could result in the increased intestinal migration of CD4 effector T cells during the induction of SGVHD. Tissues from C3H/HeN mice were taken at various time points during CsA treatment and analyzed for the presence of $CD4^+$ T cells, CAM, chemokines and proinflammatory cytokines associated with T cell homing into the gut. *In vivo* studies were performed using a CFSE-labeled SGVHD $CD4^+$ T cell line to investigate where these T cells preferentially migrate. These investigations allowed us to gain a better understanding of the functional mechanisms that take place, during the 21 days of

induction/immunosuppression therapy, that result in the increased homing of effector T cells into colons of CsA-treated mice.

4.2 Enhanced $CD4^+\alpha\beta TCR^+$ T cells in colons of CsA-treated mice compared to control BMT

Previous studies have shown significant increases in colonic $CD4^+$ T cells isolated from SGVHD mice at 2–4 weeks post-CsA (5–7 weeks post-BMT) relative to transplant control animals [78]. In addition, a 2-fold increase in $CD4^+$ T cells was also observed in the IEL isolated from CsA versus BMT control mice 21 days after transplant, at the end of CsA therapy [78]. These studies suggested that increased numbers of $CD4^+$ T cells migrated into the colon of CsA-treated mice during CsA therapy. Studies were therefore initiated to follow the migration of T cells into the colon during the CsA treatment period (days 0-21 post-BMT). For these experiments, colons were isolated from control and CsA-treated mice at several time points during the 21 days of CsA therapy and the IEL and LPLs were isolated and analyzed by flow cytometry for various T cell markers. As shown in **Figure 4.1, A** an increased percentage of $CD4^+\alpha\beta TCR^+$ T cells was found in the colons of CsA-treated mice as early as day 14 post-BMT (P=0.0288) and they maintained this increase through day 21 post-BMT (P=0.0001). Lamina propia lymphocytes isolated from CsA versus control also showed an increased percent of $CD4^+\alpha\beta TCR^+$ T cells as well (**Figure 4.1, B**). Intraepithelial lymphocytes and LPL were also analyzed during active disease and confirmed previous results in which SGVHD mice had increased infiltration of $CD4^+$ T cells into their large intestine compared to control BMT animals (**Fig 4.1, A, B**). Immunohistochemistry analysis was performed to

confirm the flow cytometry analysis of isolated cells. *In situ* analysis demonstrated increased $CD4^+$ T cell staining in the colonic tissue of CsA-treated mice compared to control BMT at days 14 and 21 post-BMT (**Figure 4.2**).

4.3 Increased proinflammatory mediators and cell adhesion molecules (CAM) during SGVHD

Total body irradiation (TBI) can affect the severity of many diseases by amplifying the dysregulation of inflammatory cytokines. Irradiation along with allogeneic immune cells can damage the gastrointestinal (GI) tract, which allows for increased translocation of lipopolysaccharide (LPS) into the systemic circulation leading to increased levels of TNF-α [140]. Radiation has also been shown to stimulate macrophage production of proinflammatory cytokines in a dose dependant manner [141]. Using the murine model of SGVHD, Bryson et al. observed a significant increase in the migration of $CD4^+$ T cells into colons of CsA-treated animals during active disease [78]. Several *in vivo* and *in vitro* studies have demonstrated that endothelial cells (EC) respond to stimuli such as irradiation, LPS and TNF-α by either becoming activated or undergoing apoptosis [140, 142]. Additionally, early interactions between allogeneic lymphocytes and vascular endothelial cells correlate with up-regulated mRNA levels of adhesion molecules, as well as TNF-α, which can result in lymphocyte adherence and EC injury [143]. TNF-α is an inflammatory cytokine capable of inducing cell adhesion molecules such as VCAM-1, ICAM-1[119] and MAdCAM-1 [120]. Studies were therefore designed to examine the levels of adhesion molecules, TNF-α and proinflammatory chemokines in colonic tissue of CsA and control BMT mice. Real time RT-PCR assays were performed to determine if

increases in mRNA for TNF-α and CAM could be detected in the colon of CsA-treated animals. Results from a time course study revealed significantly increased mRNA levels for TNF-α at days 14 and 21 post-BMT in colonic tissue of CsA mice compared to BMT control (*P*=0.0009 at day 14 post-BMT; P=0.0387 at day 21 post-BMT; **Figure 4.3**).

Concomitant with this increase in proinflammatory cytokine production, colons of CsA mice had increased mRNA levels of CAM as early as day 14 post-BMT compared to control mice (**Figure 4.4**). MAdCAM-1 mRNA analyzed by real time RT-PCR revealed significantly increased levels at days 14 and 21 post-BMT in CsA-treated mice compared to BMT control mice (*P*=0.0358 at day 14; P=0.0006 at day 21 post-BMT **Figure 4.4, A**). Similar results were observed for VCAM-1 (*P*=0.0179 at day 14; P=0.0478 at day 21 post-BMT **Figure 4.4, B**) and ICAM-1 (*P*=0.0347 at day 14; P=0.0070 at day 21 post-BMT **Figure 4.4, C**). Immunohistochemistry staining of MAdCAM-1 expression confirmed the elevated levels of CAM in colonic tissue of CsA-treated mice. Increased levels of MAdCAM-1 were observed as early as day 14 post-BMT in colons of CsA-treated mice compared to control BMT and this expression was sustained during the time course study up to the period of active disease for SGVHD (**Figure 4.5**).

Chemokines play an important role in lymphocyte trafficking to specific sites, regulating immune responses and homeostasis. Radiation therapy is capable of disrupting the epithelial integrity leading to an inflammatory response and hence increased expression of proinflammatory cytokines and chemokines [140, 142, 144]. The constitutive presence of these regulators allows for the trafficking of lymphocytes into the gastrointestinal mucosal compartment disrupting the physiological balance and

contributing to pathogenesis like inflammatory bowel diseases (IBD) [111, 112]. Since many studies have confirmed increases in proinflammatory chemokines (i.e. CCL20, CCR6, CCR5, CCL5) during gut inflammation [111-113], experiments were performed to investigate if chemokines associated with mucosal homing were up-regulated during CsA treatment. **Figure 4.6** shows significant increases in mRNA levels of CCL20 (**Figure 4.6, A**; p=0.0089), CCR5, its ligand CCL5 (**Figure 4.6, B**; p=0.0150 and **Figure 4.6, C**; p=0.0406) and its ligand CCL3 (data not shown), in the gut of CsA-treated mice compared to controls at day 21 post-BMT. This significant increase in mediators and ligands were present in CsA-treated versus control BMT mice, suggesting a role for these molecules in the enhanced migration of $CD4^+$ T cells into the colon of CsA-treated animals.

4.4 Increased homing of labeled SGVHD T cells into the colons of CsA-treated mice

An increase in the migration of $CD4^+$ T cells was observed into the colons of CsA-treated mice compared to control BMT as early as day 14 post-BMT and this increase correlated with an increase in CAM and chemokines associated with mucosal homing. Studies were undertaken to determine if increases in these molecules was indeed functional. Since increased homing of $CD4^+$ T cells were observed in the colonic tissue of CsA-treated mice, along with increased β_7 integrin expression (preliminary data), we hypothesized that the most likely CAM involved in the trafficking of these lymphocytes to the gut is MAdCAM-1, which has been previously implied to be up-regulated in gut inflammation [109, 116]. For these experiments, a long term microbial

Ag-specific $CD4^+$ T cell line isolated from SGVHD animals was used to study the homing of lymphocytes into several organs of control and CsA-treated mice. Phenotypically the $CD4^+$ T cell line (SG6) was β_7 $integrin^+$ (**Figure 4.7**) and had an activated phenotype ($CD62L^-$, $CD44^{hi}$; data not shown). Stimulation of the SG6 cells with APC pulsed with bacterial Ag resulted in a significant proliferative response compared to APC alone (**Figure 4.8**). Similar responses have been observed in primary $CD4^+$ T cells isolated from SGVHD mice compared to those from BMT control animals [58]. To determine if these $CD4^+\beta_7 integrin^+$ SGVHD T cells would migrate at a higher frequency to the colon of CsA-treated mice versus that of control animals, SG6 cells labeled with CFSE were injected i.v. into the tail of control and CsA-treated mice at day 21 post-BMT. At this time point post-BMT increased expression of CAM and chemokines is present in CsA-treated mice (**Figures 4.4-4.6**). Tissues were isolated 24 h after SG6 injection and analyzed by fluorescent microscopy. Increased levels of SG6-labeled cells migrated into the colons of CsA-treated mice compared to control BMT (**Figure 4.9, A**). Similar increases in migration were also observed in the liver as well (data not shown). When the number of labeled SG6 were enumerated, a significant increase in the migration of these labeled $CD4^+$ T cells into the colonic tissue of mice treated with CsA ($P=0.0038$) was observed compared to control BMT animals (**Figure 4.9, B**), supporting the observation that increases in CAM were functional for the migration of $CD4^+$ T cells observed in the colons of CsA-treated mice.

4.5 $CD4^+$ T cell migration into the liver

The liver, along with the colon, represent the main target organs affected by the development of murine SGVHD. Histological evaluation of tissue samples from SGVHD mice have demonstrated increased lymphocytic infiltration of the colon and liver of CsA-treated compared to control BMT animals. Studies from this laboratory have demonstrated that there was a 100% correlation between liver and colon inflammation. In addition, the adoptive transfer of $CD4^+$ T cells from SGVHD mice into secondary recipients, not only resulted in colon pathology, but liver inflammation as well that was identical to *de novo* SGVHD [58]. The chronic liver inflammation that occurs during the development of murine SGVHD is very similar to that observed during the early stages of primary sclerosing cholangitis (PSC). Primary sclerosing cholangitis is a chronic inflammatory process of intra- and extra-hepatic bile ducts [145-147] and has been frequently associated with inflammatory bowel disease (IBD) [148, 149]. In addition, expression of MAdCAM-1 and CCL25, which are typically restricted to the endothelium of the gut mucosa have been shown to be upregulated on the portal endothelium of the liver, allowing the recruitment of $\alpha_4\beta_7^+$, $CCR9^+$, $CD4^+$ memory T cells to the liver from the gut [150]. Given the similarities between IBD, SGVHD and chronic liver inflammation, preliminary studies were initiated to monitor $CD4^+$ T cell migration into the livers of control BMT and CsA-treated animals. Immunohistochemistry analysis of liver samples at several time points after BMT revealed that while these $CD4^+$ T cells are observed as early as day 14-post BMT in the colon of CsA mice (**Figure 4.2**), they are not present in the liver until active disease (**Figure 4.10**). Furthermore, mRNA analysis of liver samples for MAdCAM-1 at day 14 post-BMT revealed no difference between

CsA and control mice, but a slight increase at day 21 pos-BMT (**Figure 4.11**) and significant difference during active disease (data not shown). In addition, as stated above, similar to murine colitis models, our results have demonstrated enhanced responsiveness of SGVHD $CD4^+$ T cells against antigens isolated from cecal bacterial preparations. These studies suggest that there is an ordered migration of T cells reactive against bacterial antigens from the gut into the liver during the development of SGVHD.

4.6 Summary

The data in this chapter represents the first demonstration that the $CD4^+$ T cells responsible for the pathogenesis observed in murine SGVHD are increased as early as day 14 post-BMT in the colons of CsA-treated mice compared to BMT controls, suggesting that during the 21 days of immunosuppressive therapy these $CD4^+$ T cells are either migrating or expanding into the intestines of these animals in a CsA-resistant manner. Concurrent with these findings, elevated expression of CAM, chemokines and proinfllammatory cytokines, shown to be involved in gut inflammation, were also elevated in the colon of CsA-treated mice. Finally, *in vivo* homing studies using $CD4^+$ T cells from SGVHD animals confirmed increased migration of these effector cells into the colon of CsA-treated mice, suggesting a functional role for the increased CAM expression observed in CsA-treated animals.

Figure 4.1 Enhanced numbers of $CD4^+$ IEL and LPL isolated from CsA-treated animals

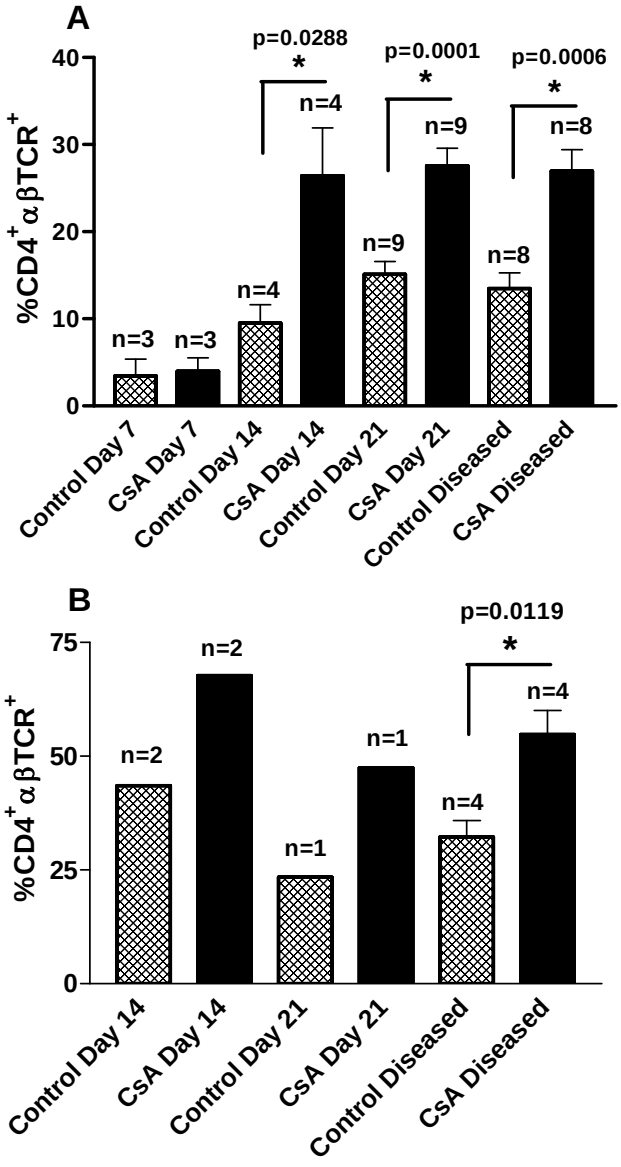

Figure 4.1 Enhanced numbers of $CD4^+$ IEL and LPL isolated from CsA-treated animals. C3H/HeN mice were lethally irradiated, reconstituted with syngeneic BM and treated for 21 days with 15 mg/kg of CsA i.p. At times after BMT, colons from mice were isolated and pooled within each experimental group. After isolation, (A) IEL and (B) LPL cells were stained with mAb for CD4 and αβTCR and analyzed by flow cytometry. Data is presented as the mean ± SEM, with *n* representing the number of experiments performed.

Figure 4.2 Elevated CD4 expression in colonic tissue of CsA-treated mice compared to control BMT

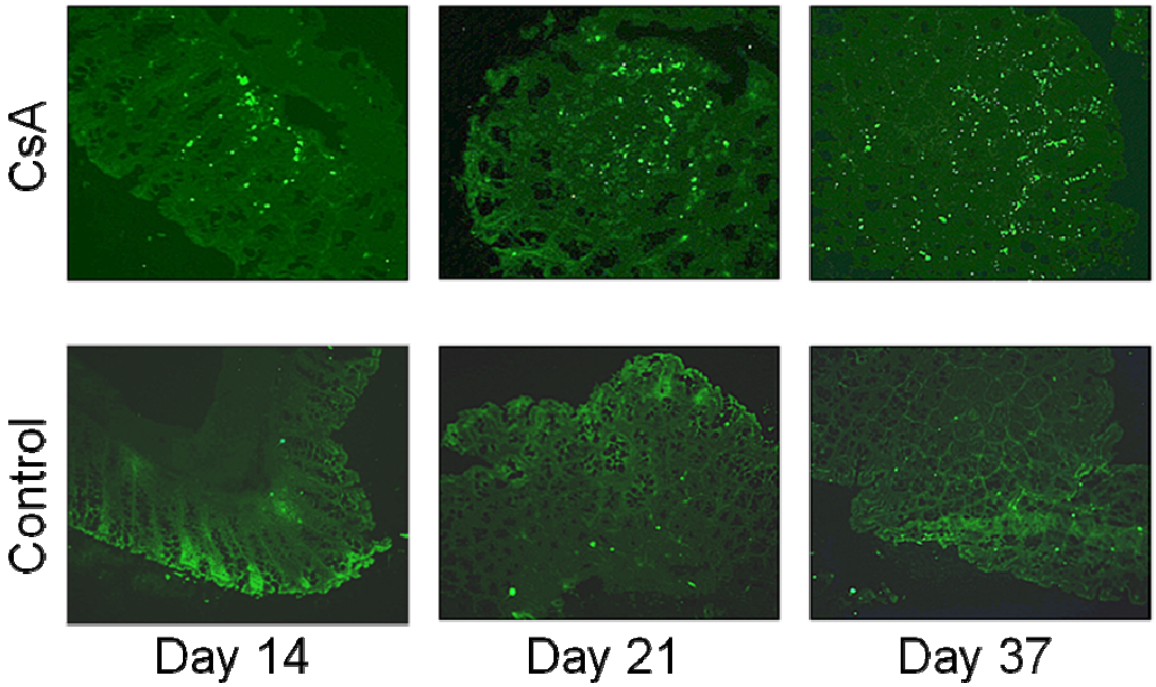

Figure 4.2 Elevated CD4 expression in colonic tissue of CsA-treated mice compared to control BMT. Immunohistochemistry staining revealed increased $CD4^+$ T cells in colonic tissue of CsA-treated mice. Colon tissue from control BMT and CsA animals was collected at several time points (Days 14, 21 and 37) and frozen sections were stained for the presence of $CD4^+$ T cells. Colons from CsA animals (top panel) show increased levels of CD4 staining compared to control BMT (lower panel). The data presented are representative of n=6 from two individual experiments.

Figure 4.3 Increased production of TNF-α in colonic tissue of CsA-treated mice

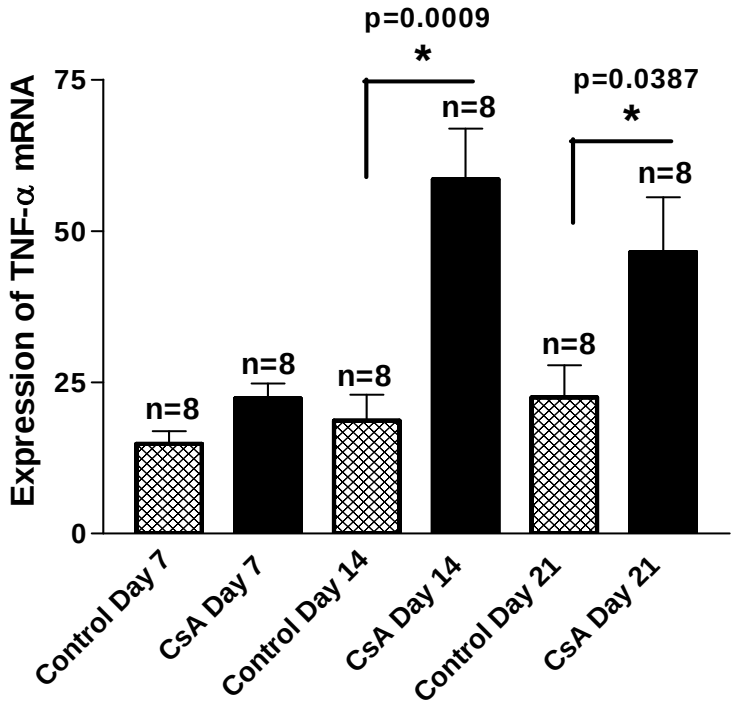

Figure 4.3 Increased production of TNF-α in colonic tissue of CsA-treated mice. C3H/HeN mice were induced for SGVHD as described. Tissue isolated from the distal colon was taken at the indicated time points during CsA treatment and analyzed by real time RT-PCR for the presence of mRNA for TNF-α. Data presented are the mean ± SEM, with *n* representing the number of animals analyzed in each group pooled from two independent experiments.

Figure 4.4 Elevated levels of CAM mRNA in the colon of CsA-treated mice compared to control BMT

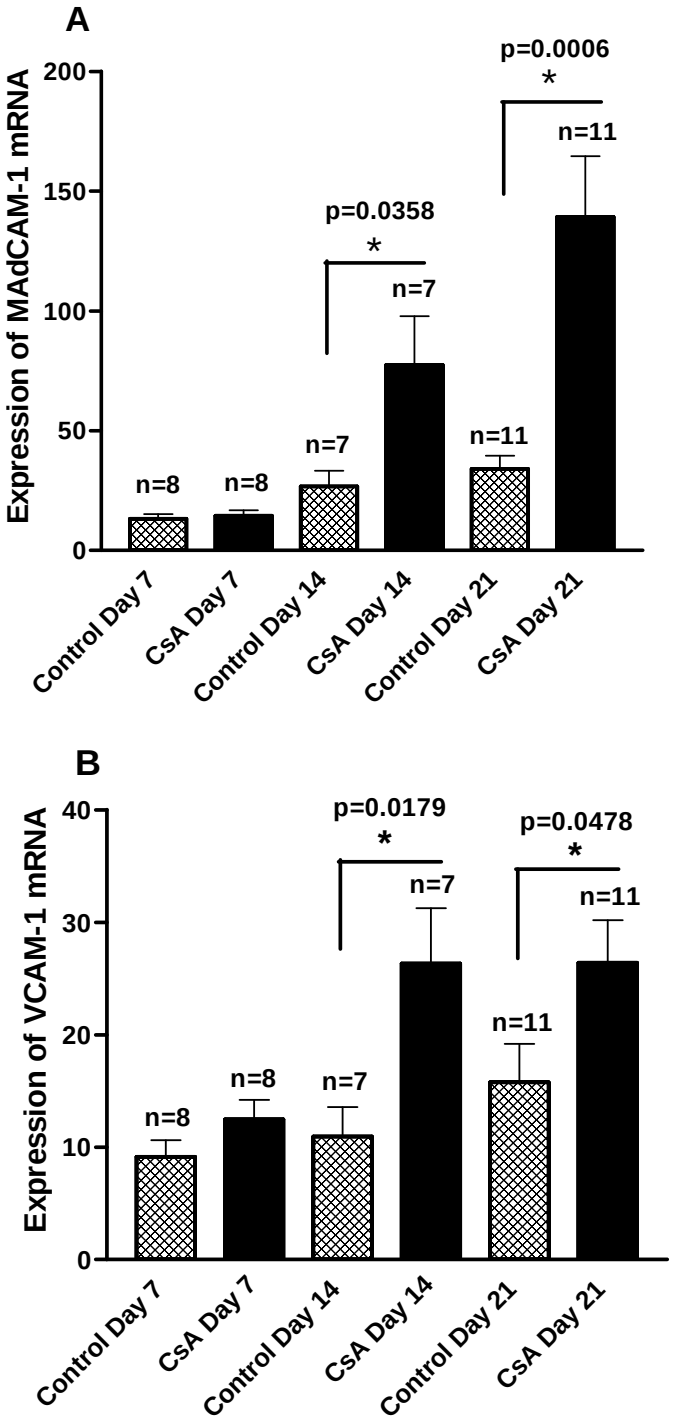

Figure 4.4 (Cont.). Elevated levels of CAM mRNA in the colon of CsA-treated mice compared to control BMT

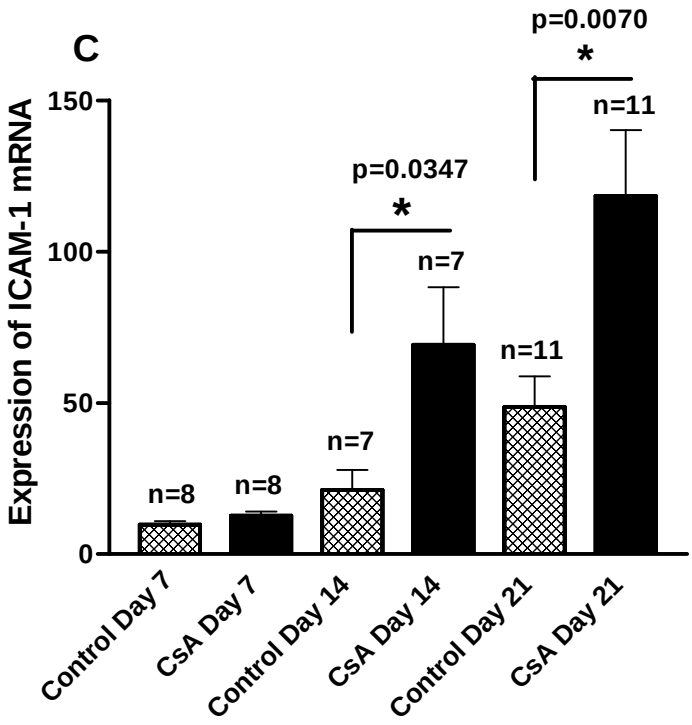

Figure 4.4 Elevated levels of CAM mRNA in the colon of CsA-treated mice compared to control BMT. RNA was isolated from the colons of control BMT and CsA-treated animals at the indicated time points. Real time RT-PCR was performed for (A) MAdCAM-1, (B) VCAM-1 and (C) ICAM-1. Data represents pooled results of two experiments and is shown as the mean ± SEM, with *n* representing the number of animals analyzed in each group.

Figure 4.5 Increased presence of MAdCAM-1 in colonic tissue of CsA-treated mice compared to control BMT

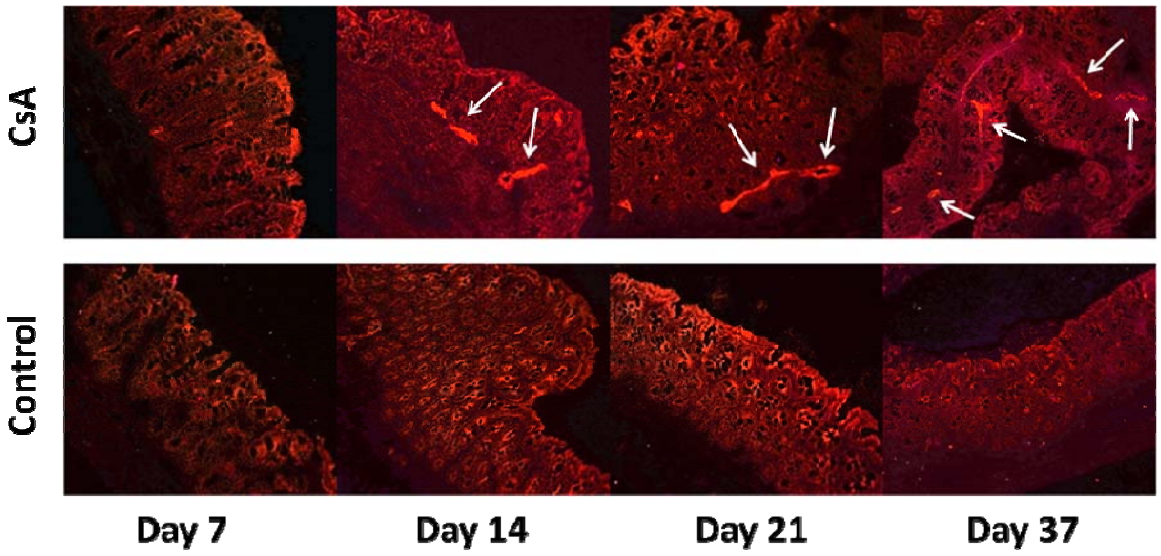

Figure 4.5 Increased presence of MAdCAM-1 in colonic tissue of CsA-treated mice. Colon tissue was isolated at days 7, 14, 21 and 37 after BMT, snap frozen and sections from control BMT and CsA-treated mice were stained by immunohistochemistry techniques for the presence of MAdCAM-1 (100x). The data presented are representative of *n*=9 from three independent experiments.

Figure 4.6 SGVHD induction results in increased production of proinflammatory chemokines in the colon

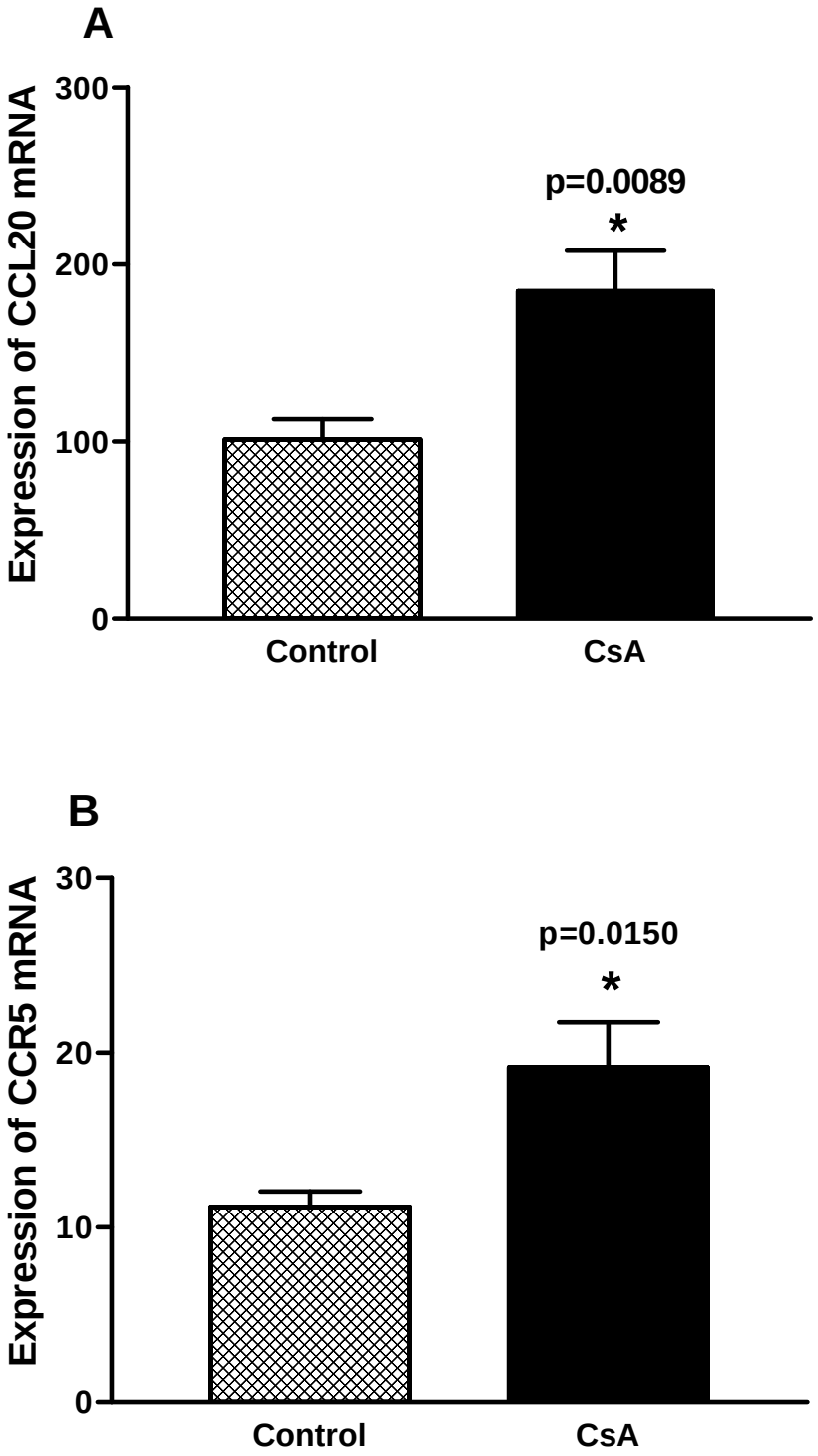

Figure 4.6 (Cont.) SGVHD induction results in increased production of proinflammatory chemokines in the colon

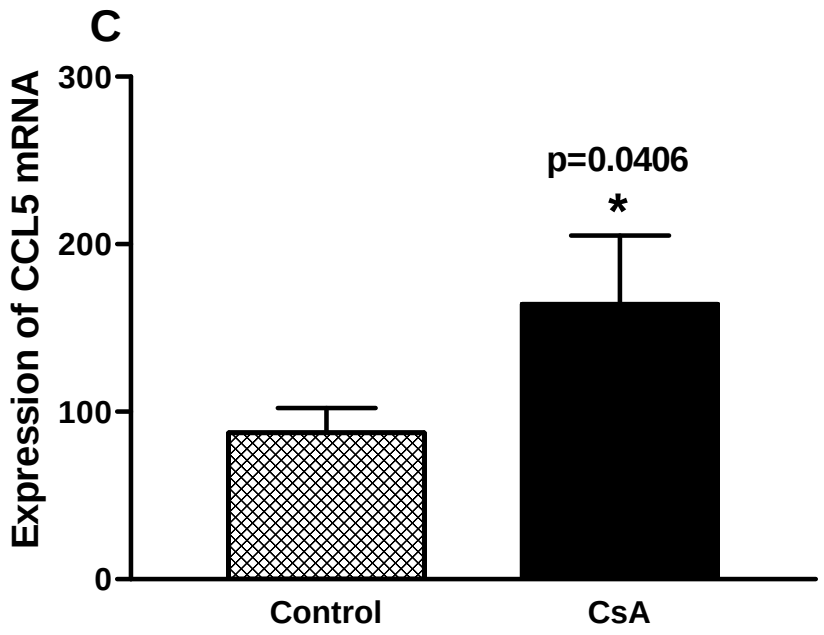

Figure 4.6 SGVHD induction results in increased production of proinflammatory chemokines in the colon. Messenger RNA was isolated from the colons of control BMT and CsA animals at day 21 post-BMT. Real time RT-PCR was performed for CCL20 (A), CCR5 (B) and CCL5 (C). Data presented are the mean ± SEM, from pooled samples from 2 experiments, with *n*=6.

Figure 4.7 SGVHD T cell line express a $CD4^{+}\beta_7integrin^{+}$ phenotype

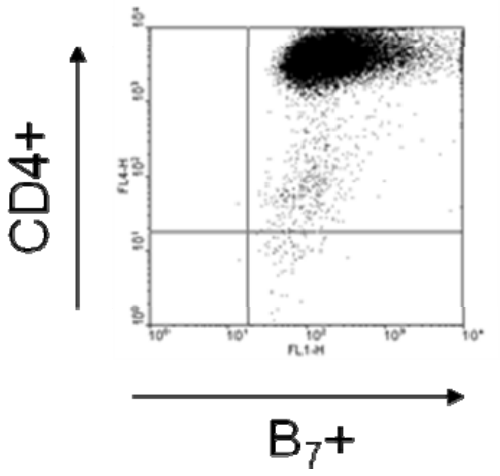

Figure 4.7 SGVHD T cell line express a $CD4^{+}\beta_7integrin^{+}$ phenotype. SGVHD T cell line or SG6 was harvested over Ficoll and analyzed by 2-color flow cytometry for CD4 and $\beta_7$integrin. Markers were set using unstained cells. Data are representative of three independent experiments.

Figure 4.8 SGVHD CD4$^+$ T cell line proliferates against bacterial-Ag pulsed DC

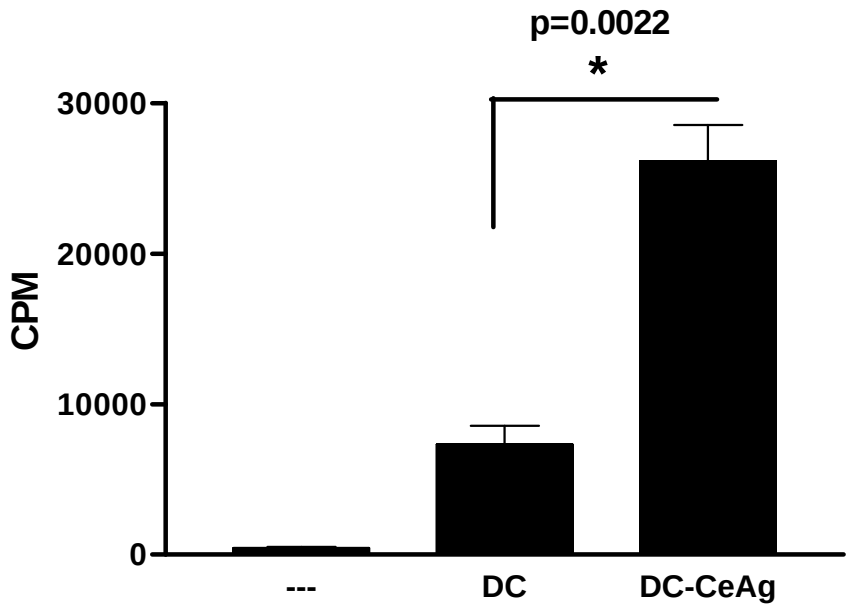

Figure 4.8 SGVHD CD4$^+$ T cell line proliferates against bacterial-Ag pulsed DC. SG6 cells were harvested 8-10 days after initiation of culture and 1-2 x 10^5 cells were cultured in 96-well flat-bottomed microtiter plates with 1 x 10^4 antigen-pulsed DC. Proliferation was measured by the addition of [^{3}H]-thymidine during the last 18 h of a 96 h culture.

Figure 4.9 Increased homing of $CD4^+$ T cells into the gut of CsA-treated mice

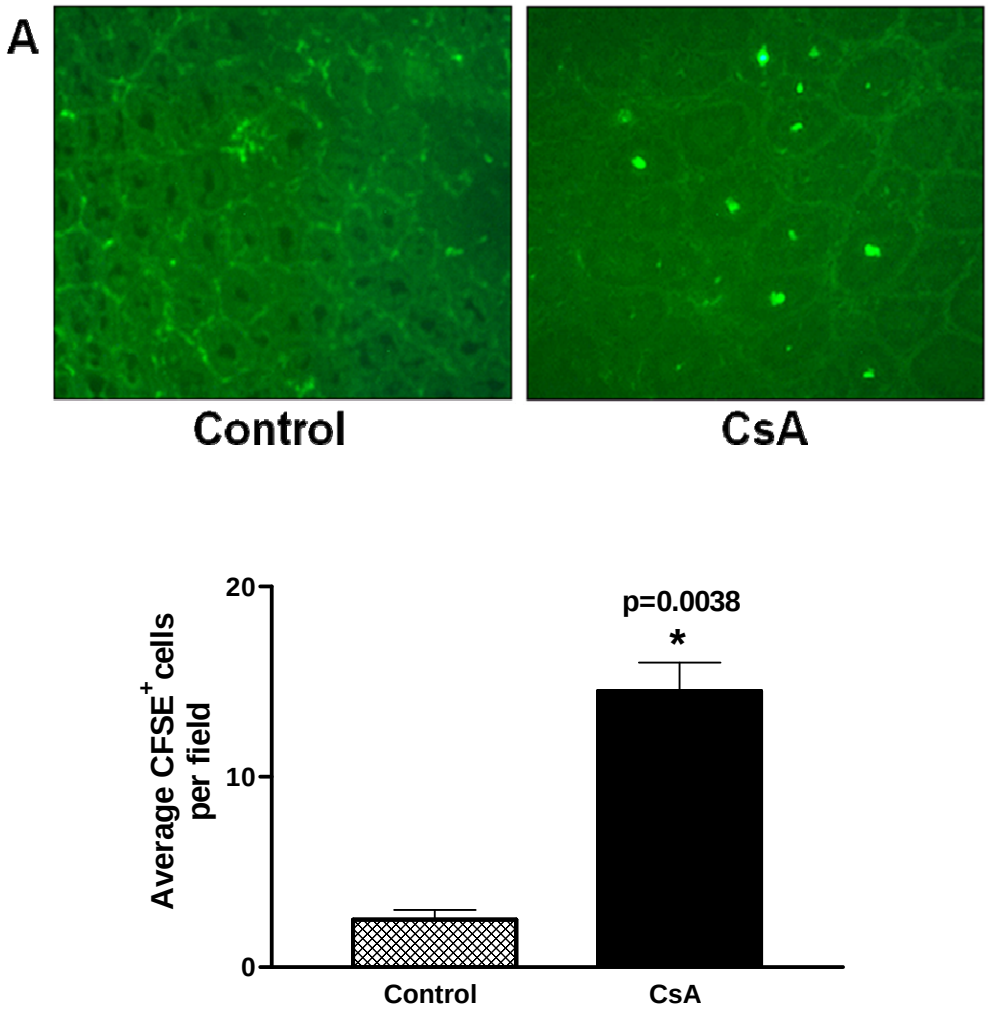

Figure 4.9 Increased homing of $CD4^+$ T cells into the colon of CsA-treated animals. SG6 cells were labeled with CFSE and injected (i.v.) into the tail of control or CsA-treated animals at day 21 post-BMT. After 24 hr, their distribution into the colon was visualized under a fluorescent microscope (A). Labeled SG6 cells were counted, within a microscope field, over a 100x magnification (B). The mean values and their standard error were determined from two independent experiments containing a total of four animals per experimental group.

Figure 4.10 Elevated $CD4^+$ T cell expression in liver tissue of SGVHD mice

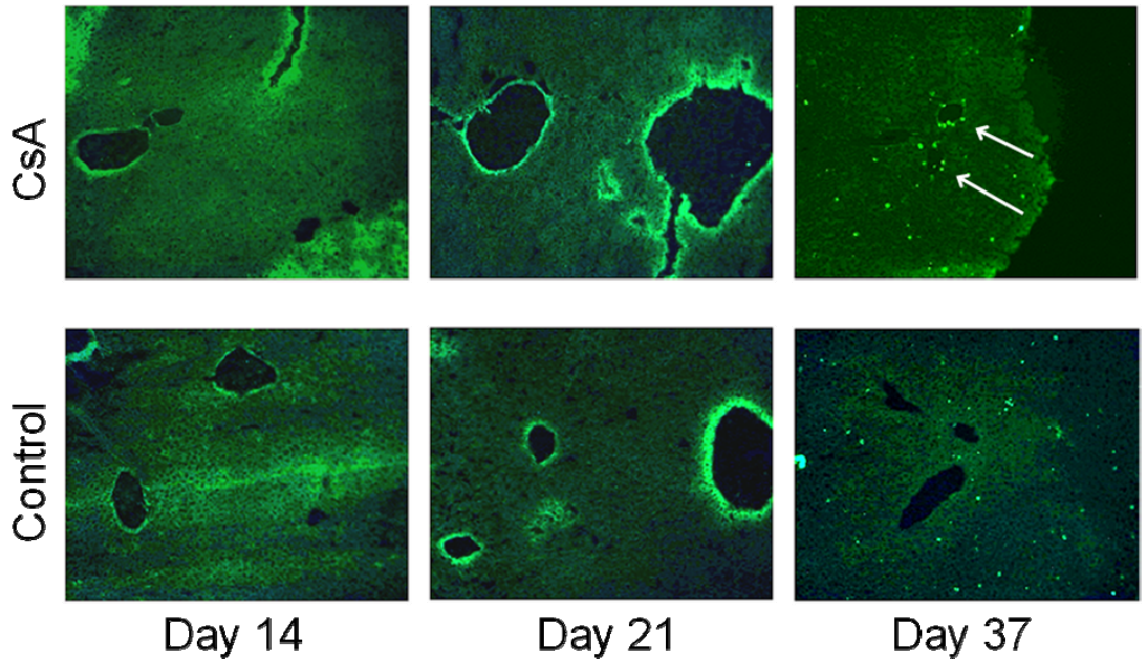

Figure 4.10 Elevated $CD4^+$ T cell expression in liver tissue of SGVHD mice. Immunohistochemistry staining revealed increased $CD4^+$ T cells in colonic tissue of SGVHD mice (day 37). Colon tissue from control BMT and CsA animals was collected at several time points (Days 14, 21 and 37) and frozen sections were stained for the presence of $CD4^+$ T cells. Colons from CsA-treated animals (top panel) showed increased levels of CD4 staining at day 37 post-BMT compared to control BMT (lower panel). The data presented are representative of n=4 at days 14, 21 and n=6 at day 37 from two individual experiments.

Figure 4.11 MAdCAM-1 mRNA expression post-BMT in liver tissue

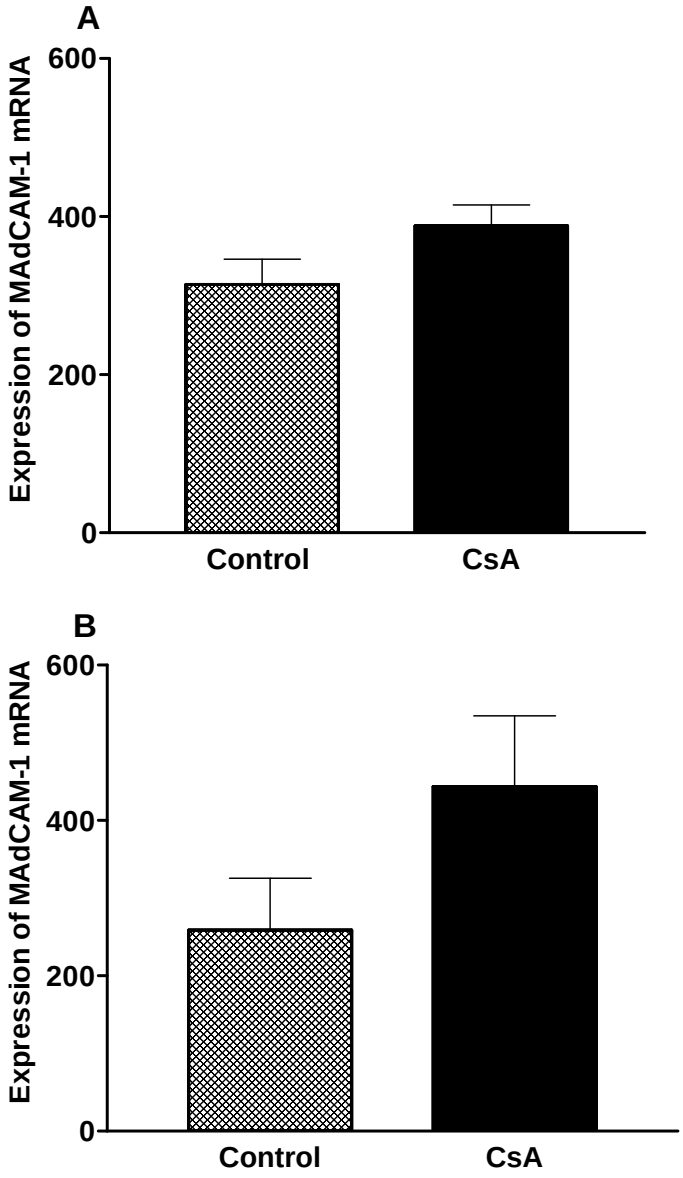

Figure 4.11 MAdCAM-1 mRNA expression post-BMT in liver tissue. BMT was performed as described. At times after BMT, control and CsA-treated animals were killed, livers were removed and RNA prepared. Expression of MAdCAM-1 was determined at day 14 (A) and day 21 (B) post-BMT by real time RT-PCR and normalized to GAPDH. Data presented are the mean ± SEM from 1 experiment, with *n*=8.

CHAPTER FIVE: DISCUSSION

5.1 Synopsis

Syngeneic GVHD can be induced in mice by reconstituting lethally irradiated animals with syngeneic BM cells followed by a 21 day treatment with the immunosuppressive agent CsA [55]. Clinical symptoms of the disease, which include weight loss and diarrhea, appear 2 to 3 weeks after cessation of CsA therapy and SGVHD-associated inflammation occurs primarily in the colon and liver [55]. Both radiation and CsA are preconditioning requirements for the development of SGVHD [57, 85] and participate in the induction of oxidative stress [65, 86-88]. SGVHD development is a multi step process resulting from the cooperative interaction of various effector cell populations including NK cells [80], T cells [78, 97] and macrophages [83], along with T_H1 cytokines that result as a consequence of the preconditioning regimens of this disease [80, 83]. A proposed mechanism of action of these proinflammatory mediators in SGVHD is via their stimulation of oxidative stress. The role of oxidative stress, specifically NO during active disease has been previously studied. Inhibition of iNOS resulted in decreased development of SGVHD [100]. These findings, along with the implication of oxidative stress production by the conditioning regimens, led us to hypothesize that CsA-treated mice produce elevated levels of ROS/RNS compared to control BMT and to investigate the role of oxidative stress in the induction of SGVHD. Since previous studies have demonstrated a role for $CD4^+$ T effector cells in the induction of murine SGVHD [58, 78], studies were undertaken to follow the migration of T cells at

the early stages after BMT and investigate the mechanism that could result in the increased migration of CD4 effector cells during the induction protocol of SGVHD.

5.2 Role of oxidative stress in SGVHD

In Chapter Three of this dissertation we examined the role of oxidative stress in SGVHD. This inducible disease was first described by Glazier et al. as a GVHD-like syndrome that developed in rats following syngeneic BMT and CsA treatment [16]. Both irradiation and CsA treatment are required for disease induction [57, 85] and participate in the production of oxidative stress [86-90]. We became interested in studying oxidative stress in the murine model of SGVHD since previous work had demonstrated a significant role for oxidative stress mediators during active disease [100]. Flanagan et al. determined the contribution of NO to the development of SGVHD by demonstrating that *in vivo* inhibition of iNOS with the inhibitor aminoguanidine (AG), starting on day 21 post-BMT for up to 2 weeks (post-CsA therapy), significantly reduced the development of disease. In their studies, iNOS inhibition resulted in the abrogation of clinical symptoms, tissue pathology and cytokine (IL-12 and IFN-γ) production associated with the development of SGVHD [100]. In accordance, Garside et al. [105] showed that inhibition of iNOS with L-NG-monomethyl arginine (L-NMMA), in their experimental model of mice GVHD, resulted in decreased intestinal pathology. In addition to these studies looking at the effect of post-CsA iNOS inhibition, studies in allogeneic GVHD have shown that inhibition of NO production at early stages following BMT can lead to mortality [98, 106], suggesting that NO levels could affect alloengraftment [98] or have a protective effect during this period [106]. For this reason we decided to treat mice with the antioxidant MnTBAP, since it can scavenge a broad spectrum of reactive oxygen as

well as nitrogen species [126, 135, 136, 151]. Experiments were designed to investigate the role of oxidative stress during the induction of SGVHD by treating mice with MnTBAP during the CsA treatment period after BMT (days 0-21), as well as during the post-CsA period.

In the immediate post-BMT period, conditioning and CsA treatment resulted in elevated production of inflammatory mediators. It was demonstrated that mice treated with CsA had increased levels of oxidative stress shown by increased levels of the ROS probe DCFH-DA. Staining of spleen lymphocytes taken from control BMT and CsA-treated mice at day 21 post-CsA (**Figure 3.1, A**) and 2-3 weeks post-CsA therapy (**Figure 3.1, B**) revealed increased levels of this ROS marker in CsA-treated mice compared to transplant controls. Reactive nitrogen species were also elevated in the CsA-treated animals compared to their control. Real time RT-PCR analysis revealed elevated mRNA levels of iNOS in colons of CsA-treated mice (**Figure 3.2, A**) and analysis of the serum showed elevated circulating nitrate in CsA animals (**Figure 3.2, B**) compared to control BMT. Along with increases in oxidative stress, our group has shown increased mRNA levels of TNF-α in the colons of CsA-treated mice compared to control BMT at several time points during and post-CsA therapy (**Figure 4.3**). It is known that irradiation can trigger TNF-α expression in many cell types and reports show that TNF-α signaling is associated with increased oxidative stress [94, 152]. Collectively, our results confirm that CsA-treated mice produce increased levels of oxidative stress compared to control transplanted mice.

Simmonds et al. previously published a direct correlation between increased production of ROS and increased pathogenesis in colorectal biopsy specimens of patients

with inflammatory bowel disease [153]. Similarly, Rachmilewitz et al. also reported increased concentrations of RNS (i.e. NO) in ulcerative colitis and Crohn's disease patients [154]. Thus, evidence exists of increased oxidative stress intermediates in IBD which could participate in the cellular damage and chronic inflammation observed in intestinal inflammation. Such findings point to the potential of antioxidant therapy as a possible curative option to ameliorate the deleterious effects caused by oxidative stress. Several studies have concentrated on the use of antioxidant therapy as an option to treat colitis and results reveal positive outcomes [155, 156]. The use of antioxidants to promote graft acceptance in animal models has also been successful, supporting the role of ROS/RNS in rejection [157]. In addition, antioxidant therapy in a murine model [158] as well as in a clinical trial [62] of GVHD has also been shown to improve disease outcome. These studies led us to the hypothesis that antioxidant therapy could ameliorate the inflammatory response observed in the colons of SGVHD animals.

The potential and beneficial effect of SOD mimetics have been demonstrated in many studies, highlighting the importance of antioxidant compounds as potential therapeutic treatment for many pathologies (i.e. renal and myocardial ischemia and reperfusion (I/R) injury, inflammatory conditions, pulmonary diseases) [126, 133-135, 151]. Therapy of CsA-treated mice with MnTBAP either during (**Figure 3.4**) or post-CsA (**Figure 3.7**) treatment resulted in the reduction of clinical symptoms and total disease induction. The use of antioxidant therapy in the murine model of SGVHD also reduced mRNA levels of iNOS (**Figures 3.5, A and 3.8**) and TNF-α (**Figure 3.5, B**) along with decreased nitrotyrosine staining (**Figures 3.6, 3.9**) in colonic tissue of CsA-treated mice compared to mice receiving CsA alone. These results demonstrated that MnTBAP

therapy of CsA-teated mice was capable of reducing RNS (i.e. iNOS and $ONOO^-$), avoiding the possible damage caused by their elevated levels and/or their downstream products (i.e. radical-driven oxidative events). Peroxynitrite has been shown to change cell membrane rigidity and permeability as well as to induce cell death in renal epithelial cells [159]. A reduction in peroxynitrite could explain why MnTBAP treatment delayed the clinical symptoms of SGVHD by reducing $ONOO^-$ induced damage to epithelial cells, resulting in reduction in diarrhea and weight loss. In addition to reducing proinflammatory mediators, MnTBAP therapy during CsA treatment also reduced the levels of CAM (data not shown) which contribute to the inflammatory response observed in this inducible disease (discussed in Chapter Four of this dissertation), The link that exists between CAM and lymphocyte homing to the site of inflammation has been documented in many pathologies [109, 113, 116, 160]. Thus MnTBAP-induced downregulation of CAM could affect lymphocyte homing to the inflamed gut observed in SGVHD.

Since the role of $CD4^+$ T cells has been well established in the pathogenesis observed in murine SGVHD [78, 161] and MnTBAP is capable of reducing CAM which contribute to T cell homing into the gut [109, 110, 116] (Chapter Four and discussed below), it could be hypothesized that antioxidant treatment could reduce the migration of $CD4^+$ effector T cells into the colon of CsA-treated animals prior to development of disease. However, our results showed that the cellular inflammatory response observed in the colon of SGVHD was not reduced by MnTBAP treatment (**Figure 3.10**) and $CD4^+$ T cells still migrated into the colons of CsA-treated mice after antioxidant therapy (**Figure 3.11**). These interesting findings suggest that while MnTBAP decreased some

inflammatory mediators (i.e. iNOS, TNF-α and CAM), as well as reduced clinical symptoms and delayed disease induction, treatment of mice with this antioxidant was not enough to prevent the histological changes observed in the SGVHD colon. Since the effector cytokines and CAM were not significantly reduced by MnTBAP, these changes may not have been enough to alter the migration of effector cells into the gut, but may reduce the negative effects of oxidative stress on the development of clinical symptoms. The pathophysiology caused by $ONOO^-$ on gut inflammation (i.e. IBD) has been difficult to predict since there are many oxidative mediators present during intestinal inflammation and neutralization of a specific mediator has been difficult. However, evidence does exist that both ROS and RNS are elevated in IBD, but their exact contribution remains unclear due to the lack of specificity of these scavengers [99].

MnTBAP has been commercially sold as an SOD mimetic and there is some recent evidence that it may not be a specific scavenger of superoxide [133, 137]. Experiments using this compound suggested that commercial MnTBAP is unable to dismutate superoxide *in vivo* and has been reported to likely scavenge peroxynitrite and carbonate radicals [133]. In our attempt to discover the mechanism of action by which MnTBAP delayed the development of SGVHD, we analyzed mRNA levels of antioxidant enzymes including: SOD, catalase, glutathione reductase (GPx) and NADPH reductase. Real time RT-PCR results revealed that MnTBAP treatment had no effect on any of these antioxidant enzymes (data not shown) in the murine model of SGVHD. These results were surprising since other publications have shown that MnTBAP treatment induces upregulation of antioxidant enzymes [162, 163]. However, there is also evidence that the preconditioning requirements (irradiation and CsA) of SGVHD by themselves can

downregulate antioxidant enzyme activity [66, 164, 165], thus it is possible that the regimens induced oxidative stress via the downregulation of antioxidant defenses which could not be overcome by MnTBAP treatment. Analysis of nitrotyrosine deposition revealed decreased immunohistochemical staining of this marker, suggesting that MnTBAP antioxidant action may be through inhibiting tyrosine nitration rather than scavenging super oxide [133]. In addition, Cooke et al. showed that under oxidative stress, $ONOO^-$ formation is enhanced, resulting in a positive loop that increases iNOS through the activation of NF-κB. The possibility exists that MnTBAP treatment scavenged $ONOO^-$ resulting in the reduction of NF-κB-induced expression of iNOS that we observed in the murine model of SGVHD [166]. This could explain why MnTBAP treatment both during and post-CsA period was able to reduce iNOS mRNA levels in colonic tissue of CsA-treated mice. Flanagan et al. demonstrated that SGVHD can be reduced following treatment with the iNOS inhibitor AG during the post-CsA period [100]. In their studies, AG therapy of CsA-treated mice resulted in decreased tissue pathology along with reduced mRNA levels of proinflammatory cytokines (i.e. IL-12 and IFN-γ). Surprisingly, in our studies, antioxidant therapy of CsA-treated mice with MnTBAP did not have the same effect.

Differences between these therapies may rely in their mode of action. Aminoguanidine specifically inhibits iNOS [104] by causing covalent modifications of the iNOS protein and the heme residue at the active site resulting in inactivation of iNOS [167]. Meanwhile, MnTBAP has been reported to scavenge a broader spectrum of oxidative stress mediators. Thus, it is possible that while AG treatment was able to effectively shut down iNOS enzymatic activity and the generation of RNI, MnTBAP

therapy only decreased it partially through negative feedback loops [166] which resulted in a reduction in the production of NO and downstream generation of $ONOO^-$. Flanagan et al. demonstrated a role for NO in the pathogenesis observed in SGVHD but the mechanism of NO-induced inhibition remained unclear. It was unknown if AG action was via the reduction of cytotoxic processes or via the reduction of inflammatory cytokines. Tissues isolated from SGVHD animals treated with AG revealed decreased mRNA levels for IL-12 and IFN-γ, suggesting NO participated in the production of these cytokines [100]. This finding is consistent with the studies of Zhao et al. [168] showing that NO can upregulate the production of IL-12 by alveolar macrophages. Meanwhile in the current studies outlined in Chapter Three of this dissertation, MnTBAP therapy did not decrease mRNA levels of these proinflammatory cytokines (**Figure 3.6**), which are known to mediate disease induction [80]. It has been shown that NO enhances IL-12 production which in turn stimulates NK cells to produce IFN-γ [169], suggesting that NO is a prerequisite for cytokine signaling and function. Our results support the idea that NO acts upstream of the induction of these proinflammatory cytokines since iNOS mRNA levels are significantly upregulated as early as day 14 post-BMT whereas significant increases of IL-12 or IFN-γ are not detected until day 21 post-BMT [100]. This could explain why AG treatment was able to decrease tissue pathology, while MnTBAP treatment did not, by reducing NO-induction of proinflammatory cytokines. Thus, while MnTBAP can alter NO production and other processes associated with RNS, it may not be as effective as AG in altering SGVHD pathology.

The preconditioning regimen of SGVHD, which includes irradiation and CsA, are both known to participate in the generation of oxidative stress. The data presented in

Chapter Three of this dissertation confirms the hypothesis that SGVHD induction results in increased oxidative stress in CsA-treated mice compared to BMT controls. Treatment with a commercially available SOD mimetic, MnTBAP, during the 21 days of CsA period as well as post-CsA treatment resulted in delayed disease induction and clinical symptoms of SGVHD. However, based on the findings outlined in this dissertation, we conclude that the reduction of proinflammatory mediators and oxidative stress was not sufficient to completely ameliorate disease induction.

5.3 Role of T cell homing in SGVHD

Leukocyte homing from the blood to different compartments of the body is governed by complex signal cascades and interactions involving selectins and integrins, found on the inflamed tissue, and their respective ligands on the surface of lymphocytes [2]. A role for $CD4^+$ T cells in the development of SGVHD has clearly been established [58, 78]. First, tissue analysis revealed an increased percentage of $CD4^+$ T cells in the SGVHD colons and further characterization confirmed these findings [78]. *In vivo* depletion studies using a mAb containing a cocktail against T cells during the post-CsA period failed to inhibit disease [80] and subsequent analysis revealed that antibody treatment was able to remove peripheral $CD4^+$ T cells but not colonic T cells [78] thus not altering SGVHD induction. Expanding on these studies, the use of specific mAb against $CD4^+$ T cells, following myeloablative conditioning and during the 21 days of CsA therapy period, significantly reduced the induction of clinical symptoms as well as pathology associated with murine SGVHD [78]. Along these findings, there is also evidence that $CD4^+$ T cells isolated from SGVHD mice are capable of inducing disease when adoptively transferred into secondary recipients [58]. Taken together, these findings

demonstrate that the presence of $CD4^+$ T cells in the colons of CsA-treated mice during the induction period is critical for disease development. In Chapter Four of this dissertation, experiments were performed to follow up on the observation that $CD4^+$ T cells accumulate in the colon during CsA therapy [80] and to study potential mechanisms involved in trafficking of these cells into the colon of CsA-treated mice. Real time RT-PCR mRNA analysis revealed increased levels of the proinflammatory cytokine TNF-α (**Figure 4.3**), as well as CAM (**Figures 4.4 and 4.6**) in colonic tissue of CsA-treated mice compared to control BMT as early as day 14 post-BMT. In addition, chemokines associated with the migration of T cells into mucosal tissues were also significantly elevated in the CsA-treated mice by day 21 post-BMT (**Figure 4.6**). Concurrent with these results, lymphocytes isolated from the colons of CsA-treated mice showed a significant increase in the percentage of $CD4^+$ T cells compared to control animals (**Figures 4.1 and 4.2**).

The conditioning agents of SGVHD (CsA and irradiation) have been shown to damage the vascular endothelium [92, 170] resulting in the upregulation of proinflammatory cytokines such as TNF-α. It was proposed that this inflammatory cascade resulted in the upregulation of CAM, which in turn enhanced the recruitment of leukocytes to the site of inflammation. Numerous studies have shown the important function that CAM have in different pathologies, as well as their role in lymphocyte homing to the inflamed organ [108-110, 116, 117, 142, 160]. Since our studies concentrated on the colon, we focused on the expression of MAdCAM-1 because it has been previously demonstrated to be essential in the induction of intestinal GVHD [117]. The $\alpha_4\beta_7$ integrin serves as the ligand for MAdCAM-1 and their interaction has been

strongly implicated in directing the recruitment of lymphocytes to the inflamed intestine [117, 171]. Eyrich et al. have shown that irradiation enhances the expression of VCAM and ICAM, but not MAdCAM by three days after radiation conditioning and syngeneic BMT [117]. The expression of these molecules subsided by nine days after BMT. Additional signals involved in the induction of allogeneic GVHD were required for the upregulation of MAdCAM in these studies. These additional signals were likely generated as a result of the allogeneic T cell response associated with the development of allogeneic GVHD. Based on the sequential expression of CAM following allogeneic BMT and GVHD induction [117], and the enhanced migration of $CD4^+$ T cells into the colon during CsA treatment in the SGVHD model, studies were initiated to examine the expression of CAM after BMT, during the CsA treatment period (d0-d21). Analysis of colonic tissue revealed significantly increased mRNA levels of CAM as early as day 14 post-BMT in CsA-treated mice compared to control BMT (**Figures 4.4 and 4.5**). Concurrent with these findings, significantly elevated levels of $CD4^+$ T cells were also observed in the colon of CsA-treated mice at this early time point (**Figures 4.1 and 4.2**). It should be noted that in contrast to the CsA therapy of BMT mice, preliminary studies have shown that treatment of normal, non-irradiated animals with CsA did not induce the influx of $CD4^+$ cells into the colon (data not shown), further demonstrating the dual requirement for pretransplant conditioning and CsA treatment in the development of SGVHD [57, 85, 97]. In addition, TNF-α mRNA levels were also significantly elevated by day 14 post-BMT in the colon mice treated with CsA compared to transplant control (**Figure 4.3**). Since the level of this proinflammatory molecule was significantly elevated during the CsA period, preliminary experiments were performed to analyze the role that

TNF-α may have in the induction phase of SGVHD. However, attempts to decrease TNF-α, by *in vivo* neutralization, was associated with a high mortality rate in the treated animals. Similar results have been previously reported in which TNF-α neutralization in the early post-BMT period resulted in increased mortality in an allogeneic BMT model system [172]. These results suggest that TNF-α has a protective effect during the early stages after BMT and is essential for recipient survival.

Histological evaluation of colonic tissue during active disease, as well as analysis of isolated cells, has led to the recognition that the severe colonic tissue damage observed in SGVHD mice is caused by an infiltration of inflammatory $CD4^+$ T cells into the colon of CsA-treated mice [55, 78, 80, 83, 100, 139]. The mechanism by which effector T cells are recruited into the gut during the inflammatory response of SGVHD remains unclear but a potential contributor likely involves chemokine gradients. Chemokine interactions with their corresponding receptors have been implicated in many inflammatory processes via their ability to attract effector cells to the sites of inflammation [112, 113, 160]. Several studies have been able to characterize chemokines highly expressed during gut inflammation which include CCR5, CCL3, CCL5 and CCL20 [112, 113]. We therefore analyzed the mRNA expression of these chemokines in colonic tissue and similar to the elevated levels of $CD4^+$ T cells and CAM, these chemokines associated with gut inflammation were also significantly increased in the colon of CsA-treated mice by day 21 post-BMT compared to control (**Figure 4.6**). The mRNA levels of these chemokines were also evaluated at day 14 post-BMT but at this time point only CCR5, which is expressed on the surface of activated lymphocytes, was significantly elevated (data not shown). However, its ligands (CCL3 and CCL5) were only slightly, but consistently

elevated, when compared to control BMT. No difference was observed in mRNA levels of CCL20 by day 14 post-BMT. While activated lymphocytes expressing CCR5 were present by day 14 post BMT, its counterligands, released by the tissue, were not yet up-regulated at this early time point, suggesting that other ligand-receptor pairs may be involved in the early homing of these T cells into the intestines of CsA mice. Changes in the expression levels of homeostatic chemokines, including CCL19, CCL21, CCL25, CCL28, as well as CXCL13 have been shown to be increased in IBD [113]. Thus, we cannot discard the possibility that other mediators are involved in the recruitment of these $CD4^+$ T cells to the inflamed tissue since high levels of redundancy are involved in chemokine receptor function and inflammatory responses.

To determine if the increases in CAM and chemokines were functional during the SGVHD induction period, a long-term $CD4^+$ T cell line, originally isolated from diseased animals, was used for lymphocyte trafficking studies. Previous results [58] and unpublished data, have demonstrated that an increased frequency of $CD4^+$ T cells in lymphoid cells isolated from SGVHD animals are reactive against microbial antigens present in the cecum of normal mice. Phenotypic analysis of these cells showed that they express β_7 integrin, which is a type of integrin expressed on the cell surface of activated lymphocytes and allows for their interaction with cell adhesion molecules (MAdCAM-1, VCAM-1) present in the inflamed gut. Our results showed increased mRNA levels of these CAM in colonic tissue of CsA-treated mice compared to control BMT as early as day 14 post-BMT (**Figures 4.4 and 4.5**). Concurrent with these findings, preliminary studies on IEL, isolated from the colon of control and CsA-treated mice at several time points during the induction protocol, revealed a 2-fold increased in $CD4^+\beta_7^+$ lymphocytes

in the colons of CsA animals by day 14 pos-BMT (data not shown). These results allowed us to hypothesize that $CD4^+$ T cells, isolated from diseased animals and bearing the β_7 integrin, would preferentially migrate into the colon of CsA-treated mice which express elevated levels of CAM. Homing studies performed by i.v. inoculation of the labeled $CD4^+$ SGVHD T cell line at day 21 post-BMT, revealed their increased migration into the colon of CsA-treated mice compared to control BMT, suggesting a functional role for the increased CAM and inflammatory mediators present in the intestines of CsA-treated mice. In this study, the migration and distribution of these $CD4^+$ T cells was also analyzed in other tissues including the liver, spleen and lung. In addition to the intestine, increased numbers of these labeled $CD4^+$ T cells were also observed in liver tissue of CsA-treated mice compared to control BMT animals, although not to the extent observed in the colon (data not shown).

The results presented in the Chapter Four of this dissertation demonstrates that during the 21 days of immunosuppressive therapy there is an ordered increase in the expression of inflammatory mediators and CAM that is associated with the increased migration of $CD4^+$ T effector cells into the colon, leading to the development of the colonic inflammation associated with murine SGVHD.

5.4 Proposed mechanism underlying oxidative stress and T cell role in the pathogenesis observed in murine SGVHD

To summarize our findings, we propose the following mechanism for the involvement of oxidative stress and T cell homing in murine SGVHD. Total body irradiation is a preconditioning regimen required for the induction of SGVHD. It is known that it upregulates production of oxidative stress as well as proinflammatory cytokines. As a consequence, immune cells along with ROS/RNS mediate tissue damage and initiate a cascade of inflammatory responses. Damage to the gastrointestinal tract allows for increased translocation of LPS and other microbial molecules into the systemic circulation. These bacterial products can lead to the stimulation of macrophages to produce proinflammatory mediators like TNF-α, IL-12 and NO. Tumor necrosis factor-α can in turn activate NF-κB induction of gene transcription of proinflammatory molecules resulting in increased cytokines, adhesion molecules and oxidative stress mediators involved in immune and inflammatory responses. In turn, IL-12, also known as a T cell stimulating factor, can stimulate the growth/function of the $CD4^+$ T cells known to mediate SGVHD, resulting in the production of IFN-γ which can feed back and further enhance macrophage activation. Macrophages can produce NO via iNOS leading to inflammation by upregulation of oxidative stress mediators. Nitric oxide by itself is a weak free radical but its combination with other ROS, like superoxide (O_2^-), can result in the formation of peroxynitrite ($\cdot O_2^- + \cdot NO \rightarrow ONOO^-$), a very toxic and reactive product capable of mediating several cytotoxic processes. CsA, another preconditioning agent of SGVHD, is also involved in upregulation of oxidative stress and its proposed mechanism is via the down regulation of antioxidant enzymes leading to the accumulation of

ROS/RNS. All these proinflammatory mediators can then act in concert to induce the lesions and pathology observed in the colon of SGVHD mice.

In addition, the elevated inflammatory signals (TNF-α, oxidative stress mediators/products) can also upregulate CAM on the surface of HEV present in the epithelium, allowing for the homing and extravasation of lymphocytes into the gut. APC present at the site of inflammation migrate into the MLN were they present microbial antigens and activate $CD4^+$ T cells. Once activated, these $CD4^+$ T cells express in their surface β_7 integrin which allows for their interaction with CAM present in the inflamed colonic tissue. Chemokines released by the tissue serve to attract these $CD4^+$ T cells to the site of inflammation. The colonic $CD4^+$ T cells can further enhance other effector cells, expanding the inflammatory response leading to tissue damage. Activation of $CD4^+$ T cells in the MLN/colon leads to an IBD-like disease that moves from the colon to the liver by aberrant expression of CAM (MAdCAM-1) and chemokines (CCL25) that are typically restricted to the epithelium of the gut mucosa. These $CD4^+$ T cells, as well as other inflammatory cells (macrophages, Kuppfer cells, dendritic cells (DC)), work together to mediate intra- and extra-hepatic liver inflammation that develops subsequent to the colonic inflammation (**see Figure 5.1**).

5.5 Future directions

The studies performed in this dissertation offer new findings that contribute to the understanding of the IBD-like colitis observed in murine SGVHD. Besides the contributing knowledge that these results provide they also give rise to further questions which require additional studies for their analysis.

In Chapter Three of this dissertation the role of oxidative stress in the development of SGVHD is discussed. Even though treatment with the antioxidant MnTBAP delayed disease induction it was not sufficient to inhibit disease or the contributing effector cells and cytokines associated with the pathology observed in SGVHD animals. The usage of this antioxidant at a higher dose (20 mg/kg, twice a day) but still under the safe concentration to be used following a toxicological report, resulted in increased mortality of mice (data not shown). Suggesting that combined treatment of CsA along MnTBAP had a toxic effect on mice, which was confirmed by increased pathology in colon and liver samples. In addition, MnTBAP action on scavenging ROS/RNS mediators has been somehow controversial and could result in misleading conclusions. It is evident that oxidative stress is increased in CsA-treated mice compared to control BMT but its exact contribution to the development of murine SGVHD during the 21 days of immunosuppression therapy remains unclear, thus requiring further studies to better analyze this matter. This approach can be studied by the use of a more specific antioxidant, like M40403, which is an SOD mimetic that specifically scavenges super oxide anions at a high rate, inhibiting its interaction with other biological oxidizing agents. This could provide a better understanding and specificity of the role of super oxide in SGVHD.

The role of T cell homing in SGVHD was discussed in the fourth chapter of this dissertation leading to the findings that there are mechanisms occurring during the period of CsA treatment that allow for increased migration of $CD4^+$ T cells into the colon of CsA-treated mice compared to control BMT. Cell adhesion molecules seem to be implicated in the homing of these T cells into the gut, specifically MAdCAM-1 via its interaction with $\alpha_4\beta_7^+$ present in the surface of activated T cells. Although significant increases in both CAMs and β_7^+ were present in colonic tissue of CsA-treated mice immunoblockade studies were not undertaken to confirm the role of these mediators in murine SGVHD. Further *in vivo* studies either blocking MAdCAM-1 or $\alpha_4\beta_7^+$ are required to study their effect on T cell migration and SGVHD outcome.

Figure 5.1 Role of oxidative stress and T cell homing in murine SGVHD

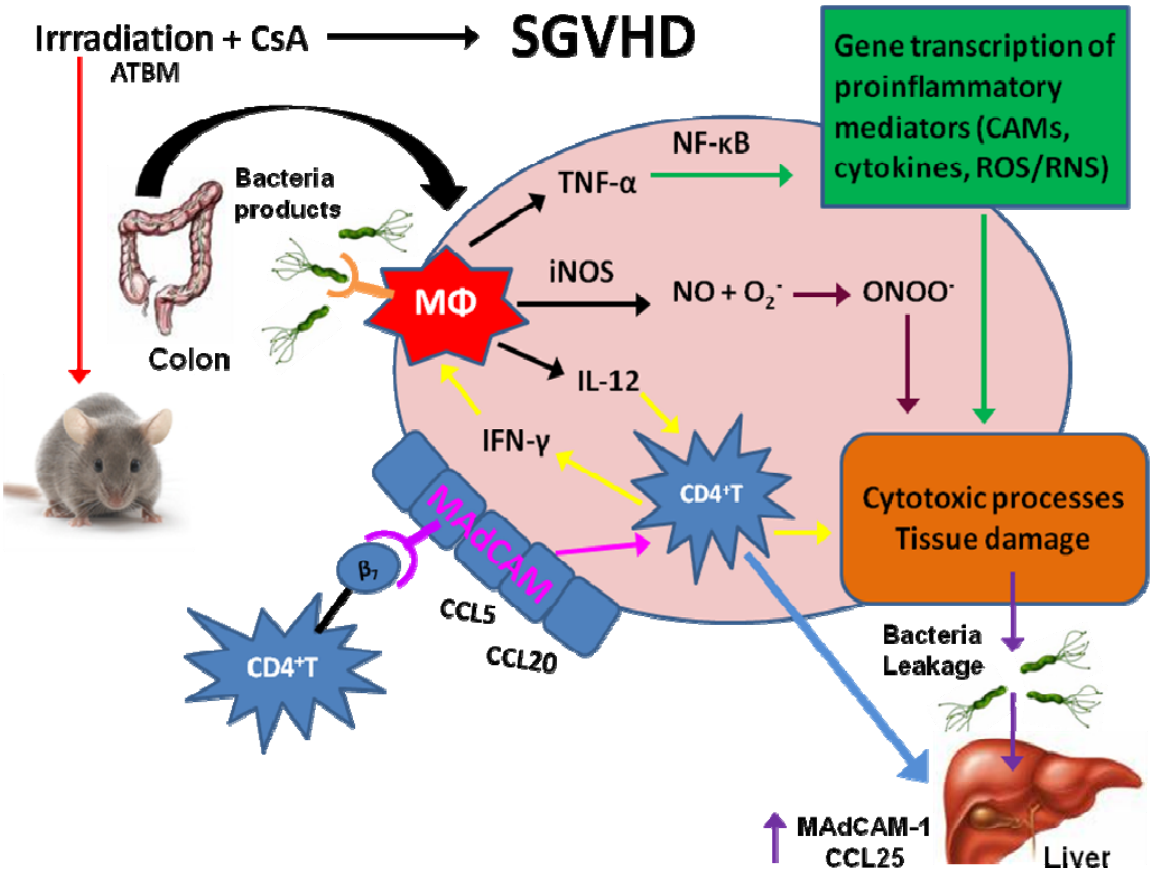

Figure 5.1 Role of oxidative stress and T cell homing in murine SGVHD. Irradiation and CsA treatment upregulate the production of oxidative stress as well as proinflammatory cytokines. Damage to the GI tract allows for increased translocation of bacteria products which stimulate MΦ to produce proinflammatory mediators. Chemokines released by the tissue serve to attract bacterial-specific $CD4^+$ T cells to the site of inflammation, expanding the inflammatory response and leading to further tissue damage. Activated $CD4^+$ T cells move from the colon into the liver by aberrant expression of MAdCAM-1 and CCL25 that act in concert with other inflammatory cells to mediate the liver inflammation that develops subsequent to the colonic inflammation.

Appendix. Reagent Preparation

Phosphate Buffer Saline (PBS) Solution:

For a 10X solution:

1. Add 92 g of NaH_2PO_4 (dibasic) to 4 liters of distilled water
2. Heat solution to 60°C in a water bath, stirring periodically to dissolve
3. While solution is still stirring, add 16 g of KH_2PO_4
4. Adjust pH to 7.2
5. Add 654.4 g NaCl to the stirring solution
6. Bring total volume to 8 liters with distilled water
7. Store at room temperature

For a 1X solution:

1. Combine 100 ml of 10X PBS with 900 ml distilled water

Paraformaldehyde solution:

For a 1% paraforlmaldehyde solution:

1. Combine 1 g paraformaldehyde with 25 ml of distilled water and incubate in a 56°C water bath, stirring occasionally until dissolved
2. Add 5 ml of 10X PBS and 20 ml distilled water to the solution and mix
3. Add 5 ml of 10X PBS and 45 ml distilled water to the solution and mix
4. Adjust pH to 7.4
5. Filter solution and place in a 100 ml bottle
6. Store at 4°C refrigerator

For a 3% paraforlmaldehyde solution:

1. Prepare 1 liter of 0.1M PBS by mixing 3.58 g $NaH_2PO_4 \bullet 2H_2O$ (monobasic) + 10.94 g NaH_2PO_4 (dibasic) and complete to 1 liter with distilled water
2. Add 30 g of paraformaldehyde to 900 ml of PBS
3. Heat solution to 60°C in a water bath, stirring periodically, until solution is clear
4. Allow solution to cool to room temperature
5. Adjust pH to 7.2-7.4
6. Bring total volume to 1 liter with PBS
7. Store at 4°C

Tris-buffer stock:

1. Dissolve 20.59 g of Triza Base into 800 ml distilled water
2. Adjust pH to 7.2
1. Bring total volume to 1 liter with distilled water
3. Autoclave 20 min, slow exhaust to sterilize
4. Store at room temperature

Tris-buffered ammonium chloride:

2. Dissolve 8.3 g of NH_4Cl in 800 ml of distilled water by stirring
3. Add 100 ml of Tris-buffer stock, pH 7.2
4. Adjust pH to 7.2
5. Bring total volume to 1 liter with distilled water
6. Dispense into 100 ml bottles and autoclave 20 min, slow exhaust to sterilize
7. Store at room temperature

Heat Activate Fetal Bovine Serum (FBS):

1. Take out FBS from -20°C and allow flask to thaw in a 37°C water bath, stirring occasionally
2. Once thawed, transfer FBS to 60°C water bath for 45 minutes
3. Allow to cool down at room temperature
4. Store at 4°C

Complete Media (RPMI 1640):

1. Add Fetal Bovine Serum (FBS):
    - For 10% media: 50 ml of FBS for each 500 ml bottle of RPMI
    - For 5% media: 25 ml of FBS for each 500 ml bottle of RPMI
2. Add 5 ml of penicillin/streptomycin/glutamine (100X)
3. Add 5 mM 2-mercaptoethanol (2-ME)
4. Store at 37°C

Cytotoxic Media (RPMI 1640):

1. Add 5 ml of penicillin/streptomycin/glutamine (100X) and 20 ml of bovine serum albumin (BSA) to one bottle of 500 ml RMPI
2. Store at 37°C

Hepes Bicarbonate Buffer:

1. Combine 23.8 g of Hepes with 21 g of NaCl
2. Bring total volume to 1 liter with distilled water
3. Adjust pH to 7.2
4. Transfer into a sterile flask and store at room temperature

0.5 M EDTA Solution:

1. Dissolve 16.81 g of EDTA in 90 ml of distilled water
2. Adjust pH to 7.2
3. Bring total volume to 100 ml with distilled water
4. Autoclave 20 min, slow exhaust to sterilize
5. Store at room temperature

CMF Solution:

1. Combine 100 ml 10X Hanks (Ca^{2+}, Mg^{2+}free), 100 ml 10x Hepes bicarbonate buffer and 20 ml FBS
2. Bring total volume to 1000 ml with distilled water
3. Filter sterilize and store at 4°C

CMF/FBS/DTE/EDTA Solution;

1. Combine 184 ml CMF, 16 ml FBS, 0.2 ml DTT (1M) and 0.4 ml EDTA (0.5M)
2. Prepare fresh and place in 37°C water bath until use

10% Complete /Collagenase Type VIII/DNaseI Solution:

1. Combine 80 ml 10% complete RMPI, 69.3 mg Collagenase (277U/mg) and 0.080 mg DNaseI (2000U/mg)
2. Prepare fresh and place in 37°C water bath until use

Percoll Soutions:

1. Prepare a 1X stock solution by diluting 90 ml Percoll with 10 ml of 10X PBS
2. For a 44% Percoll solution: Mix 44 ml of 1X stock and 56 ml 5% complete medium
3. For a 67% Percoll solution: Mix 67 ml of 1X stock and 33 ml 5% complete medium
4. Adjust pH to 7.2
5. Prepare fresh and place on ice until use

FACS Staining Buffer:

1. Combine 5 ml FBS, 50 mg NaN_3 into a flask containing 500 ml 1X PBS and mix to dissolve
2. Store in 4°C

REFERENCES

1. Bach, F.H., Albertini, R.J., Joo, P., Anderson, J.L., Bortin, M.M. (1968) Bone-marrow transplantation in a patient with the Wiskott-Aldrich syndrome. *Lancet* **2**, 1364-6.
2. C.A. Janeway, P.T., M. Walport, M.J. Slomchik (2005) *Immunobiology*. Taylor & Francis, New York.
3. Mosmann, T.R., Coffman, R.L. (1989) TH1 and TH2 cells: different patterns of lymphokine secretion lead to different functional properties. *Annu Rev Immunol* **7**, 145-73.
4. McKenzie, B.S., Kastelein, R.A., Cua, D.J. (2006) Understanding the IL-23-IL-17 immune pathway. *Trends Immunol* **27**, 17-23.
5. Steinman, L. (2007) A brief history of T(H)17, the first major revision in the T(H)1/T(H)2 hypothesis of T cell-mediated tissue damage. *Nat Med* **13**, 139-45.
6. Ford, D., Burger, D. (1983) Precursor frequency of antigen-specific T cells: effects of sensitization in vivo and in vitro. *Cell Immunol* **79**, 334-44.
7. Kojima, M., Cease, K.B., Buckenmeyer, G.K., Berzofsky, J.A. (1988) Limiting dilution comparison of the repertoires of high and low responder MHC-restricted T cells. *J Exp Med* **167**, 1100-13.
8. Felix, N.J., Allen, P.M. (2007) Specificity of T-cell alloreactivity. *Nat Rev Immunol* **7**, 942-53.
9. Kernan, N.A., Dupont, B. (1996) Minor histocompatibility antigens and marrow transplantation. *N Engl J Med* **334**, 323-4.
10. Ichiki, Y., Bowlus, C.L., Shimoda, S., Ishibashi, H., Vierling, J.M., Gershwin, M.E. (2006) T cell immunity and graft-versus-host disease (GVHD). *Autoimmun Rev* **5**, 1-9.
11. Robertson, N.J., Chai, J.G., Millrain, M., Scott, D., Hashim, F., Manktelow, E., Lemonnier, F., Simpson, E., Dyson, J. (2007) Natural regulation of immunity to minor histocompatibility antigens. *J Immunol* **178**, 3558-65.
12. Graff, R.J. (1978) Minor histocompatibility genes and their antigens. *Transplant Proc* **10**, 701-5.
13. Perreault, C., Decary, F., Brochu, S., Gyger, M., Belanger, R., Roy, D. (1990) Minor histocompatibility antigens. *Blood* **76**, 1269-80.
14. Perreault, C., Jutras, J., Roy, D.C., Filep, J.G., Brochu, S. (1996) Identification of an immunodominant mouse minor histocompatibility antigen (MiHA). T cell response to a single dominant MiHA causes graft-versus-host disease. *J Clin Invest* **98**, 622-8.
15. Weisdorf, D., Haake, R., Blazar, B., Miller, W., McGlave, P., Ramsay, N., Kersey, J., Filipovich, A. (1990) Treatment of moderate/severe acute graft-versus-host disease after allogeneic bone marrow transplantation: an analysis of clinical risk features and outcome. *Blood* **75**, 1024-30.
16. Glazier, A., Tutschka, P.J., Farmer, E.R., Santos, G.W. (1983) Graft-versus-host disease in cyclosporin A-treated rats after syngeneic and autologous bone marrow reconstitution. *J Exp Med* **158**, 1-8.

17. Ferrara, J.L., Deeg, H.J. (1991) Graft-versus-host disease. *N Engl J Med* **324**, 667-74.
18. Green, C.J. (1988) Experimental transplantation and cyclosporine. *Transplantation* **46**, 3S-10S.
19. Atkinson, K. (2003) *Clinical bone marrow and blood stem cell transplantation*. Cambridge University Press, New York.
20. Armitage, J.O. (1994) Bone marrow transplantation. *N Engl J Med* **330**, 827-38.
21. Korngold, R., Sprent, J. (1985) Surface markers of T cells causing lethal graft-vs-host disease to class I vs class II H-2 differences. *J Immunol* **135**, 3004-10.
22. Santos, G.W. (1974) Immunosuppression for clinical marrow transplantation. *Semin Hematol* **11**, 341-51.
23. Billingham, R.E. (1966) The biology of graft-versus-host reactions. *Harvey Lect* **62**, 21-78.
24. Loiseau, P., Busson, M., Balere, M.L., Dormoy, A., Bignon, J.D., Gagne, K., Gebuhrer, L., Dubois, V., Jollet, I., Bois, M., Perrier, P., Masson, D., Moine, A., Absi, L., Reviron, D., Lepage, V., Tamouza, R., Toubert, A., Marry, E., Chir, Z., Jouet, J.P., Blaise, D., Charron, D., Raffoux, C. (2007) HLA Association with hematopoietic stem cell transplantation outcome: the number of mismatches at HLA-A, -B, -C, -DRB1, or -DQB1 is strongly associated with overall survival. *Biol Blood Marrow Transplant* **13**, 965-74.
25. Ho, V.T., Soiffer, R.J. (2001) The history and future of T-cell depletion as graft-versus-host disease prophylaxis for allogeneic hematopoietic stem cell transplantation. *Blood* **98**, 3192-204.
26. Martin, P.J., Schoch, G., Fisher, L., Byers, V., Anasetti, C., Appelbaum, F.R., Beatty, P.G., Doney, K., McDonald, G.B., Sanders, J.E., et al. (1990) A retrospective analysis of therapy for acute graft-versus-host disease: initial treatment. *Blood* **76**, 1464-72.
27. Ferrara, J.L. (2000) Pathogenesis of acute graft-versus-host disease: cytokines and cellular effectors. *J Hematother Stem Cell Res* **9**, 299-306.
28. Antin, J.H., Ferrara, J.L. (1992) Cytokine dysregulation and acute graft-versus-host disease. *Blood* **80**, 2964-8.
29. Xun, C.Q., Thompson, J.S., Jennings, C.D., Brown, S.A., Widmer, M.B. (1994) Effect of total body irradiation, busulfan-cyclophosphamide, or cyclophosphamide conditioning on inflammatory cytokine release and development of acute and chronic graft-versus-host disease in H-2-incompatible transplanted SCID mice. *Blood* **83**, 2360-7.
30. Leeuwenberg, J.F., Van Damme, J., Meager, T., Jeunhomme, T.M., Buurman, W.A. (1988) Effects of tumor necrosis factor on the interferon-gamma-induced major histocompatibility complex class II antigen expression by human endothelial cells. *Eur J Immunol* **18**, 1469-72.
31. Norton, J., Sloane, J.P. (1991) ICAM-1 expression on epidermal keratinocytes in cutaneous graft-versus-host disease. *Transplantation* **51**, 1203-6.
32. McGlave, P.B., De Fabritiis, P., Deisseroth, A., Goldman, J., Barnett, M., Reiffers, J., Simonsson, B., Carella, A., Aeppli, D. (1994) Autologous transplants for chronic myelogenous leukaemia: results from eight transplant groups. *Lancet* **343**, 1486-8.

33. Filipovich, A.H., Weisdorf, D., Pavletic, S., Socie, G., Wingard, J.R., Lee, S.J., Martin, P., Chien, J., Przepiorka, D., Couriel, D., Cowen, E.W., Dinndorf, P., Farrell, A., Hartzman, R., Henslee-Downey, J., Jacobsohn, D., McDonald, G., Mittleman, B., Rizzo, J.D., Robinson, M., Schubert, M., Schultz, K., Shulman, H., Turner, M., Vogelsang, G., Flowers, M.E. (2005) National Institutes of Health consensus development project on criteria for clinical trials in chronic graft-versus-host disease: I. Diagnosis and staging working group report. *Biol Blood Marrow Transplant* **11**, 945-56.
34. Cahn, J.Y., Klein, J.P., Lee, S.J., Milpied, N., Blaise, D., Antin, J.H., Leblond, V., Ifrah, N., Jouet, J.P., Loberiza, F., Ringden, O., Barrett, A.J., Horowitz, M.M., Socie, G. (2005) Prospective evaluation of 2 acute graft-versus-host (GVHD) grading systems: a joint Societe Francaise de Greffe de Moelle et Therapie Cellulaire (SFGM-TC), Dana Farber Cancer Institute (DFCI), and International Bone Marrow Transplant Registry (IBMTR) prospective study. *Blood* **106**, 1495-500.
35. Ringden, O., Paulin, T., Lonnqvist, B., Nilsson, B. (1985) An analysis of factors predisposing to chronic graft-versus-host disease. *Exp Hematol* **13**, 1062-7.
36. Atkinson, K., Horowitz, M.M., Gale, R.P., van Bekkum, D.W., Gluckman, E., Good, R.A., Jacobsen, N., Kolb, H.J., Rimm, A.A., Ringden, O., et al. (1990) Risk factors for chronic graft-versus-host disease after HLA-identical sibling bone marrow transplantation. *Blood* **75**, 2459-64.
37. Tsoi, M.S., Storb, R., Dobbs, S., Kopecky, K.J., Santos, E., Weiden, P.L., Thomas, E.D. (1979) Nonspecific suppressor cells in patients with chronic graft-vs-host disease after marrow grafting. *J Immunol* **123**, 1970-6.
38. Tsoi, M.S., Storb, R., Dobbs, S., Medill, L., Thomas, E.D. (1980) Cell-mediated immunity to non-HLA antigens of the host by donor lymphocytes in patients with chronic graft-vs-host disease. *J Immunol* **125**, 2258-62.
39. Sprent, J., Schaefer, M., Korngold, R. (1990) Role of T cell subsets in lethal graft-versus-host disease (GVHD) directed to class I versus class II H-2 differences. II. Protective effects of L3T4+ cells in anti-class II GVHD. *J Immunol* **144**, 2946-54.
40. Sprent, J., Schaefer, M., Gao, E.K., Korngold, R. (1988) Role of T cell subsets in lethal graft-versus-host disease (GVHD) directed to class I versus class II H-2 differences. I. L3T4+ cells can either augment or retard GVHD elicited by Lyt-2+ cells in class I different hosts. *J Exp Med* **167**, 556-69.
41. Korngold, R., Sprent, J. (1987) Variable capacity of L3T4+ T cells to cause lethal graft-versus-host disease across minor histocompatibility barriers in mice. *J Exp Med* **165**, 1552-64.
42. Allen, R.D., Staley, T.A., Sidman, C.L. (1993) Differential cytokine expression in acute and chronic murine graft-versus-host-disease. *Eur J Immunol* **23**, 333-7.
43. Rus, V., Svetic, A., Nguyen, P., Gause, W.C., Via, C.S. (1995) Kinetics of Th1 and Th2 cytokine production during the early course of acute and chronic murine graft-versus-host disease. Regulatory role of donor CD8+ T cells. *J Immunol* **155**, 2396-406.
44. Fialkow, P.J., Gilchrist, C., Allison, A.C. (1973) Autoimmunity in chronic graft-versus-host disease. *Clin Exp Immunol* **13**, 479-86.

45. Carlson, M.J., West, M.L., Coghill, J.M., Panoskaltsis-Mortari, A., Blazar, B.R., Serody, J.S. (2009) In vitro-differentiated TH17 cells mediate lethal acute graft-versus-host disease with severe cutaneous and pulmonary pathologic manifestations. *Blood* **113**, 1365-74.
46. Yi, T., Zhao, D., Lin, C.L., Zhang, C., Chen, Y., Todorov, I., LeBon, T., Kandeel, F., Forman, S., Zeng, D. (2008) Absence of donor Th17 leads to augmented Th1 differentiation and exacerbated acute graft-versus-host disease. *Blood* **112**, 2101-10.
47. Reisner, Y., Itzicovitch, L., Meshorer, A., Sharon, N. (1978) Hemopoietic stem cell transplantation using mouse bone marrow and spleen cells fractionated by lectins. *Proc Natl Acad Sci U S A* **75**, 2933-6.
48. Vallera, D.A., Soderling, C.C., Carlson, G.J., Kersey, J.H. (1981) Bone marrow transplantation across major histocompatibility barriers in mice. Effect of elimination of T cells from donor grafts by treatment with monoclonal Thy-1.2 plus complement or antibody alone. *Transplantation* **31**, 218-22.
49. Hale, G., Cobbold, S., Waldmann, H. (1988) T cell depletion with CAMPATH-1 in allogeneic bone marrow transplantation. *Transplantation* **45**, 753-9.
50. Storb, R., Pepe, M., Anasetti, C., Appelbaum, F.R., Beatty, P., Doney, K., Martin, P., Stewart, P., Sullivan, K.M., Witherspoon, R., et al. (1990) What role for prednisone in prevention of acute graft-versus-host disease in patients undergoing marrow transplants? *Blood* **76**, 1037-45.
51. Nash, R.A., Antin, J.H., Karanes, C., Fay, J.W., Avalos, B.R., Yeager, A.M., Przepiorka, D., Davies, S., Petersen, F.B., Bartels, P., Buell, D., Fitzsimmons, W., Anasetti, C., Storb, R., Ratanatharathorn, V. (2000) Phase 3 study comparing methotrexate and tacrolimus with methotrexate and cyclosporine for prophylaxis of acute graft-versus-host disease after marrow transplantation from unrelated donors. *Blood* **96**, 2062-8.
52. Ruutu, T., Niederwieser, D., Gratwohl, A., Apperley, J.F. (1997) A survey of the prophylaxis and treatment of acute GVHD in Europe: a report of the European Group for Blood and Marrow, Transplantation (EBMT). Chronic Leukaemia Working Party of the EBMT. *Bone Marrow Transplant* **19**, 759-64.
53. Barrett, J., Childs, R. (2000) The benefits of an alloresponse: graft-versus-tumor. *J Hematother Stem Cell Res* **9**, 347-54.
54. Beschorner, W.E., Shinn, C.A., Fischer, A.C., Santos, G.W., Hess, A.D. (1988) Cyclosporine-induced pseudo-graft-versus-host disease in the early post-cyclosporine period. *Transplantation* **46**, 112S-117S.
55. Bryson, J.S., Jennings, C.D., Caywood, B.E., Kaplan, A.M. (1989) Induction of a syngeneic graft-versus-host disease-like syndrome in DBA/2 mice. *Transplantation* **48**, 1042-7.
56. Sorokin, R., Kimura, H., Schroder, K., Wilson, D.H., Wilson, D.B. (1986) Cyclosporine-induced autoimmunity. Conditions for expressing disease, requirement for intact thymus, and potency estimates of autoimmune lymphocytes in drug-treated rats. *J Exp Med* **164**, 1615-25.
57. Fischer, A.C., Beschorner, W.E., Hess, A.D. (1989) Requirements for the induction and adoptive transfer of cyclosporine-induced syngeneic graft-versus-host disease. *J Exp Med* **169**, 1031-41.

58. Bryson, J.S., Jennings, C.D., Brandon, J.A., Perez, J., Caywood, B.E., Kaplan, A.M. (2007) Adoptive transfer of murine syngeneic graft-vs.-host disease by CD4+ T cells. *J Leukoc Biol*.
59. Kahan, B.D. (1989) Cyclosporine. *N Engl J Med* **321**, 1725-38.
60. Viola, J.P., Carvalho, L.D., Fonseca, B.P., Teixeira, L.K. (2005) NFAT transcription factors: from cell cycle to tumor development. *Braz J Med Biol Res* **38**, 335-44.
61. Cho, M.L., Ju, J.H., Kim, K.W., Moon, Y.M., Lee, S.Y., Min, S.Y., Cho, Y.G., Kim, H.S., Park, K.S., Yoon, C.H., Lee, S.H., Park, S.H., Kim, H.Y. (2007) Cyclosporine A inhibits IL-15-induced IL-17 production in CD4+ T cells via down-regulation of PI3K/Akt and NF-kappaB. *Immunol Lett* **108**, 88-96.
62. Cho, M.L., Kim, W.U., Min, S.Y., Min, D.J., Min, J.K., Lee, S.H., Park, S.H., Cho, C.S., Kim, H.Y. (2002) Cyclosporine differentially regulates interleukin-10, interleukin-15, and tumor necrosis factor a production by rheumatoid synoviocytes. *Arthritis Rheum* **46**, 42-51.
63. Elliott, J.F., Lin, Y., Mizel, S.B., Bleackley, R.C., Harnish, D.G., Paetkau, V. (1984) Induction of interleukin 2 messenger RNA inhibited by cyclosporin A. *Science* **226**, 1439-41.
64. Kronke, M., Leonard, W.J., Depper, J.M., Arya, S.K., Wong-Staal, F., Gallo, R.C., Waldmann, T.A., Greene, W.C. (1984) Cyclosporin A inhibits T-cell growth factor gene expression at the level of mRNA transcription. *Proc Natl Acad Sci U S A* **81**, 5214-8.
65. Lim, S.W., Li, C., Ahn, K.O., Kim, J., Moon, I.S., Ahn, C., Lee, J.R., Yang, C.W. (2005) Cyclosporine-induced renal injury induces toll-like receptor and maturation of dendritic cells. *Transplantation* **80**, 691-9.
66. Pari, L., Sivasankari, R. (2008) Effect of ellagic acid on cyclosporine A-induced oxidative damage in the liver of rats. *Fundam Clin Pharmacol* **22**, 395-401.
67. Hagar, H.H. (2004) The protective effect of taurine against cyclosporine A-induced oxidative stress and hepatotoxicity in rats. *Toxicol Lett* **151**, 335-43.
68. Yang, J.M., Zhu, B. (2002) Intrahepatic cholestasis after liver transplantation. *Hepatobiliary Pancreat Dis Int* **1**, 176-8.
69. Roman, I.D., Fernandez-Moreno, M.D., Fueyo, J.A., Roma, M.G., Coleman, R. (2003) Cyclosporin A induced internalization of the bile salt export pump in isolated rat hepatocyte couplets. *Toxicol Sci* **71**, 276-81.
70. Jenkins, M.K., Schwartz, R.H., Pardoll, D.M. (1988) Effects of cyclosporine A on T cell development and clonal deletion. *Science* **241**, 1655-8.
71. Beschorner, W.E., Suresch, D.L., Shinozawa, T., Santos, G.W., Hess, A.D. (1988) Thymic immunopathology after cyclosporine: effect of irradiation and age on medullary involution and recovery. *Transplant Proc* **20**, 1072-8.
72. Hess, A.D., Fischer, A.C., Beschorner, W.E. (1990) Effector mechanisms in cyclosporine A-induced syngeneic graft-versus-host disease. Role of CD4+ and CD8+ T lymphocyte subsets. *J Immunol* **145**, 526-33.
73. Hess, A.D., Bright, E.C., Thoburn, C., Vogelsang, G.B., Jones, R.J., Kennedy, M.J. (1997) Specificity of effector T lymphocytes in autologous graft-versus-host disease: role of the major histocompatibility complex class II invariant chain peptide. *Blood* **89**, 2203-9.

74. Hess, A.D., Thoburn, C., Horwitz, L. (1998) Promiscuous recognition of major histocompatibility complex class II determinants in cyclosporine-induced syngeneic graft-versus-host disease: specificity of cytolytic effector T cells. *Transplantation* **65**, 785-92.
75. Chaturvedi, P., Hengeveld, R., Zechel, M.A., Lee-Chan, E., Singh, B. (2000) The functional role of class II-associated invariant chain peptide (CLIP) in its ability to variably modulate immune responses. *Int Immunol* **12**, 757-65.
76. Fischer, A.C., Ruvolo, P.P., Burt, R., Horwitz, L.R., Bright, E.C., Hess, J.M., Beschorner, W.E., Hess, A.D. (1995) Characterization of the autoreactive T cell repertoire in cyclosporin-induced syngeneic graft-versus-host disease. A highly conserved repertoire mediates autoaggression. *J Immunol* **154**, 3713-25.
77. Chen, W., Thoburn, C., Hess, A.D. (1998) Characterization of the pathogenic autoreactive T cells in cyclosporine-induced syngeneic graft-versus-host disease. *J Immunol* **161**, 7040-6.
78. Bryson, J.S., Zhang, L., Goes, S.W., Jennings, C.D., Caywood, B.E., Carlson, S.L., Kaplan, A.M. (2004) CD4+ T cells mediate murine syngeneic graft-versus-host disease-associated colitis. *J Immunol* **172**, 679-87.
79. Bryson, J.S., Jennings, C.D., Lowery, D.M., Carlson, S.L., Pflugh, D.L., Caywood, B.E., Kaplan, A.M. (1999) Rejection of an MHC class II negative tumor following induction of murine syngeneic graft-versus-host disease. *Bone Marrow Transplant* **23**, 363-72.
80. Flanagan, D.L., Jennings, C.D., Bryson, J.S. (1999) Th1 cytokines and NK cells participate in the development of murine syngeneic graft-versus-host disease. *J Immunol* **163**, 1170-7.
81. Cong, Y., Brandwein, S.L., McCabe, R.P., Lazenby, A., Birkenmeier, E.H., Sundberg, J.P., Elson, C.O. (1998) CD4+ T cells reactive to enteric bacterial antigens in spontaneously colitic C3H/HeJBir mice: increased T helper cell type 1 response and ability to transfer disease. *J Exp Med* **187**, 855-64.
82. Brimnes, J., Reimann, J., Nissen, M., Claesson, M. (2001) Enteric bacterial antigens activate CD4(+) T cells from scid mice with inflammatory bowel disease. *Eur J Immunol* **31**, 23-31.
83. Flanagan, D.L., Gross, R., Jennings, C.D., Caywood, B.E., Goes, S., Kaplan, A.M., Bryson, J.S. (2001) Induction of syngeneic graft-versus-host disease in LPS hyporesponsive C3H/HeJ mice. *J Leukoc Biol* **70**, 873-80.
84. Trinchieri, G. (2003) Interleukin-12 and the regulation of innate resistance and adaptive immunity. *Nat Rev Immunol* **3**, 133-46.
85. Fischer, A.C., Laulis, M.K., Horwitz, L., Beschorner, W.E., Hess, A. (1989) Host resistance to cyclosporine induced syngeneic graft-versus-host disease. Requirement for two distinct lymphocyte subsets. *J Immunol* **143**, 827-32.
86. Ahmed, S.S., Napoli, K.L., Strobel, H.W. (1995) Oxygen radical formation during cytochrome P450-catalyzed cyclosporine metabolism in rat and human liver microsomes at varying hydrogen ion concentrations. *Mol Cell Biochem* **151**, 131-40.
87. Wang, C., Salahudeen, A.K. (1995) Lipid peroxidation accompanies cyclosporine nephrotoxicity: effects of vitamin E. *Kidney Int* **47**, 927-34.

88. Josephine, A., Amudha, G., Veena, C.K., Preetha, S.P., Varalakshmi, P. (2007) Oxidative and nitrosative stress mediated renal cellular damage induced by cyclosporine A: role of sulphated polysaccharides. *Biol Pharm Bull* **30**, 1254-9.
89. Sonntag, C.V. (1987) *Chemical Basis of Radiation Biology* Taylor & Francis, London.
90. Kuwabara, M., Asanuma, T., Niwa, K., Inanami, O. (2008) Regulation of cell survival and death signals induced by oxidative stress. *J Clin Biochem Nutr* **43**, 51-7.
91. Hill, E.J. (1994) *Radiobiology for the radiologist*. J.B. Lippincott Company, Philadelphia.
92. Gao, S.Z., Alderman, E.L., Schroeder, J.S., Hunt, S.A., Wiederhold, V., Stinson, E.B. (1990) Progressive coronary luminal narrowing after cardiac transplantation. *Circulation* **82**, IV269-75.
93. Navarro-Antolin, J., Hernandez-Perera, O., Lopez-Ongil, S., Rodriguez-Puyol, M., Rodriguez-Puyol, D., Lamas, S. (1998) CsA and FK506 up-regulate eNOS expression: role of reactive oxygen species and AP-1. *Kidney Int Suppl* **68**, S20-4.
94. Natarajan, M., Gibbons, C.F., Mohan, S., Moore, S., Kadhim, M.A. (2007) Oxidative stress signalling: a potential mediator of tumour necrosis factor alpha-induced genomic instability in primary vascular endothelial cells. *Br J Radiol* **80 Spec No 1**, S13-22.
95. Jobin, C., Hellerbrand, C., Licato, L.L., Brenner, D.A., Sartor, R.B. (1998) Mediation by NF-kappa B of cytokine induced expression of intercellular adhesion molecule 1 (ICAM-1) in an intestinal epithelial cell line, a process blocked by proteasome inhibitors. *Gut* **42**, 779-87.
96. Akira, S., Takeda, K. (2004) Toll-like receptor signalling. *Nat Rev Immunol* **4**, 499-511.
97. Bryson, J.S., Jennings, C.D., Caywood, B.E., Kaplan, A.M. (1993) Thy1+ bone marrow cells regulate the induction of murine syngeneic graft-versus-host disease. *Transplantation* **56**, 941-5.
98. Drobyski, W.R., Keever, C.A., Hanson, G.A., McAuliffe, T., Griffith, O.W. (1994) Inhibition of nitric oxide production is associated with enhanced weight loss, decreased survival, and impaired alloengraftment in mice undergoing graft-versus-host disease after bone marrow transplantation. *Blood* **84**, 2363-73.
99. McCafferty, D.M. (2000) Peroxynitrite and inflammatory bowel disease. *Gut* **46**, 436-9.
100. Flanagan, D.M., Jennings, C.D., Goes, S.W., Caywood, B.E., Gross, R., Kaplan, A.M., Bryson, J.S. (2002) Nitric oxide participates in the intestinal pathology associated with murine syngeneic graft-versus-host disease. *J Leukoc Biol* **72**, 762-8.
101. Sakurai, H., Kohsaka, H., Liu, M.F., Higashiyama, H., Hirata, Y., Kanno, K., Saito, I., Miyasaka, N. (1995) Nitric oxide production and inducible nitric oxide synthase expression in inflammatory arthritides. *J Clin Invest* **96**, 2357-63.
102. Kubes, P., McCafferty, D.M. (2000) Nitric oxide and intestinal inflammation. *Am J Med* **109**, 150-8.
103. Nathan, C., Xie, Q.W. (1994) Nitric oxide synthases: roles, tolls, and controls. *Cell* **78**, 915-8.

104. Hoffman, R.A., Nussler, N.C., Gleixner, S.L., Zhang, G., Ford, H.R., Langrehr, J.M., Demetris, A.J., Simmons, R.L. (1997) Attenuation of lethal graft-versus-host disease by inhibition of nitric oxide synthase. *Transplantation* **63**, 94-100.
105. Garside, P., Hutton, A.K., Severn, A., Liew, F.Y., Mowat, A.M. (1992) Nitric oxide mediates intestinal pathology in graft-vs.-host disease. *Eur J Immunol* **22**, 2141-5.
106. Hongo, D., Bryson, J.S., Kaplan, A.M., Cohen, D.A. (2004) Endogenous nitric oxide protects against T cell-dependent lethality during graft-versus-host disease and idiopathic pneumonia syndrome. *J Immunol* **173**, 1744-56.
107. Cuzzocrea, S., Caputi, A.P., Zingarelli, B. (1998) Peroxynitrite-mediated DNA strand breakage activates poly (ADP-ribose) synthetase and causes cellular energy depletion in carrageenan-induced pleurisy. *Immunology* **93**, 96-101.
108. Butcher, E.C., Scollay, R.G., Weissman, I.L. (1979) Lymphocyte adherence to high endothelial venules: characterization of a modified in vitro assay, and examination of the binding of syngeneic and allogeneic lymphocyte populations. *J Immunol* **123**, 1996-2003.
109. Berlin, C., Berg, E.L., Briskin, M.J., Andrew, D.P., Kilshaw, P.J., Holzmann, B., Weissman, I.L., Hamann, A., Butcher, E.C. (1993) Alpha 4 beta 7 integrin mediates lymphocyte binding to the mucosal vascular addressin MAdCAM-1. *Cell* **74**, 185-95.
110. Gironella, M., Molla, M., Salas, A., Soriano, A., Sans, M., Closa, D., Engel, P., Salas, A., Pique, J.M., Panes, J. (2002) The role of P-selectin in experimental colitis as determined by antibody immunoblockade and genetically deficient mice. *J Leukoc Biol* **72**, 56-64.
111. Kang, S.G., Piniecki, R.J., Hogenesch, H., Lim, H.W., Wiebke, E., Braun, S.E., Matsumoto, S., Kim, C.H. (2007) Identification of a chemokine network that recruits FoxP3(+) regulatory T cells into chronically inflamed intestine. *Gastroenterology* **132**, 966-81.
112. Scheerens, H., Hessel, E., de Waal-Malefyt, R., Leach, M.W., Rennick, D. (2001) Characterization of chemokines and chemokine receptors in two murine models of inflammatory bowel disease: IL-10-/- mice and Rag-2-/- mice reconstituted with CD4+CD45RBhigh T cells. *Eur J Immunol* **31**, 1465-74.
113. Zimmerman, N.P., Vongsa, R.A., Wendt, M.K., Dwinell, M.B. (2008) Chemokines and chemokine receptors in mucosal homeostasis at the intestinal epithelial barrier in inflammatory bowel disease. *Inflamm Bowel Dis* **14**, 1000-11.
114. Hammerschmidt, S.I., Ahrendt, M., Bode, U., Wahl, B., Kremmer, E., Forster, R., Pabst, O. (2008) Stromal mesenteric lymph node cells are essential for the generation of gut-homing T cells in vivo. *J Exp Med* **205**, 2483-90.
115. Ahrendt, M., Hammerschmidt, S.I., Pabst, O., Pabst, R., Bode, U. (2008) Stromal cells confer lymph node-specific properties by shaping a unique microenvironment influencing local immune responses. *J Immunol* **181**, 1898-907.
116. Steffen, B.J., Breier, G., Butcher, E.C., Schulz, M., Engelhardt, B. (1996) ICAM-1, VCAM-1, and MAdCAM-1 are expressed on choroid plexus epithelium but not endothelium and mediate binding of lymphocytes in vitro. *Am J Pathol* **148**, 1819-38.

117. Eyrich, M., Burger, G., Marquardt, K., Budach, W., Schilbach, K., Niethammer, D., Schlegel, P.G. (2005) Sequential expression of adhesion and costimulatory molecules in graft-versus-host disease target organs after murine bone marrow transplantation across minor histocompatibility antigen barriers. *Biol Blood Marrow Transplant* **11**, 371-82.
118. Nakache, M., Berg, E.L., Streeter, P.R., Butcher, E.C. (1989) The mucosal vascular addressin is a tissue-specific endothelial cell adhesion molecule for circulating lymphocytes. *Nature* **337**, 179-81.
119. Chen, X.L., Zhang, Q., Zhao, R., Ding, X., Tummala, P.E., Medford, R.M. (2003) Rac1 and superoxide are required for the expression of cell adhesion molecules induced by tumor necrosis factor-alpha in endothelial cells. *J Pharmacol Exp Ther* **305**, 573-80.
120. Sikorski, E.E., Hallmann, R., Berg, E.L., Butcher, E.C. (1993) The Peyer's patch high endothelial receptor for lymphocytes, the mucosal vascular addressin, is induced on a murine endothelial cell line by tumor necrosis factor-alpha and IL-1. *J Immunol* **151**, 5239-50.
121. Morello, F., Saglio, E., Noghero, A., Schiavone, D., Williams, T.A., Verhovez, A., Bussolino, F., Veglio, F., Mulatero, P. (2009) LXR-activating oxysterols induce the expression of inflammatory markers in endothelial cells through LXR-independent mechanisms. *Atherosclerosis*.
122. Steinbach, W.J., Reedy, J.L., Cramer, R.A., Jr., Perfect, J.R., Heitman, J. (2007) Harnessing calcineurin as a novel anti-infective agent against invasive fungal infections. *Nat Rev Microbiol* **5**, 418-30.
123. Vallance, P., Leiper, J. (2002) Blocking NO synthesis: how, where and why? *Nat Rev Drug Discov* **1**, 939-50.
124. Griendling, K.K., FitzGerald, G.A. (2003) Oxidative stress and cardiovascular injury: Part I: basic mechanisms and in vivo monitoring of ROS. *Circulation* **108**, 1912-6.
125. Kunkel, E.J., Butcher, E.C. (2003) Plasma-cell homing. *Nat Rev Immunol* **3**, 822-9.
126. Oury, T.D., Thakker, K., Menache, M., Chang, L.Y., Crapo, J.D., Day, B.J. (2001) Attenuation of bleomycin-induced pulmonary fibrosis by a catalytic antioxidant metalloporphyrin. *Am J Respir Cell Mol Biol* **25**, 164-9.
127. Saito, Y., Nishio, K., Yoshida, Y., Niki, E. (2005) Cytotoxic effect of formaldehyde with free radicals via increment of cellular reactive oxygen species. *Toxicology* **210**, 235-45.
128. Lefrancois, L., and N. Lycke. (1997) Isolation of mouse small intestinal intraepithelial lymphocytes, peyer's patch, and lamina propria cells. In *Current Protocols in Immunology* (A. M. K. J. E. Coligan, D. H. Margulies, E. M. Shevach, and a. W. Strober, eds), John Wiley & Sons Inc., Hoboken, NJ, p. 3.19.1-3.19.16.
129. Nathan, C. (2003) Specificity of a third kind: reactive oxygen and nitrogen intermediates in cell signaling. *J Clin Invest* **111**, 769-78.
130. Kroncke, K.D. (2003) Nitrosative stress and transcription. *Biol Chem* **384**, 1365-77.

131. Valko, M., Leibfritz, D., Moncol, J., Cronin, M.T., Mazur, M., Telser, J. (2007) Free radicals and antioxidants in normal physiological functions and human disease. *Int J Biochem Cell Biol* **39**, 44-84.
132. Xiong, J.H., Li, Y.H., Nie, J.L., Yu, X.Y. (2002) [Effects of nitric oxide on myocardial contraction function]. *Space Med Med Eng (Beijing)* **15**, 149-51.
133. Batinic-Haberle, I., Cuzzocrea, S., Reboucas, J.S., Ferrer-Sueta, G., Mazzon, E., Di Paola, R., Radi, R., Spasojevic, I., Benov, L., Salvemini, D. (2009) Pure MnTBAP selectively scavenges peroxynitrite over superoxide: comparison of pure and commercial MnTBAP samples to MnTE-2-PyP in two models of oxidative stress injury, an SOD-specific Escherichia coli model and carrageenan-induced pleurisy. *Free Radic Biol Med* **46**, 192-201.
134. Day, B.J., Batinic-Haberle, I., Crapo, J.D. (1999) Metalloporphyrins are potent inhibitors of lipid peroxidation. *Free Radic Biol Med* **26**, 730-6.
135. Day, B.J., Fridovich, I., Crapo, J.D. (1997) Manganic porphyrins possess catalase activity and protect endothelial cells against hydrogen peroxide-mediated injury. *Arch Biochem Biophys* **347**, 256-62.
136. Day, B.J., Shawen, S., Liochev, S.I., Crapo, J.D. (1995) A metalloporphyrin superoxide dismutase mimetic protects against paraquat-induced endothelial cell injury, in vitro. *J Pharmacol Exp Ther* **275**, 1227-32.
137. Reboucas, J.S., Spasojevic, I., Batinic-Haberle, I. (2008) Quality of potent Mn porphyrin-based SOD mimics and peroxynitrite scavengers for pre-clinical mechanistic/therapeutic purposes. *J Pharm Biomed Anal* **48**, 1046-9.
138. Garcia-Ruiz, I., Rodriguez-Juan, C., Diaz-Sanjuan, T., del Hoyo, P., Colina, F., Munoz-Yague, T., Solis-Herruzo, J.A. (2006) Uric acid and anti-TNF antibody improve mitochondrial dysfunction in ob/ob mice. *Hepatology* **44**, 581-91.
139. Brandon, J.A., Jennings, C.D., Perez, J., Caywood, B., Alapat, D., Kaplan, A.M., Bryson, J.S. (2007) Induction of Murine Syngeneic Graft-Versus-Host Disease by Cells of Recipient Origin. *Transplantation* **83**, 1620-1627.
140. Robaye, B., Mosselmans, R., Fiers, W., Dumont, J.E., Galand, P. (1991) Tumor necrosis factor induces apoptosis (programmed cell death) in normal endothelial cells in vitro. *Am J Pathol* **138**, 447-53.
141. Shan, Y.X., Jin, S.Z., Liu, X.D., Liu, Y., Liu, S.Z. (2007) Ionizing radiation stimulates secretion of proinflammatory cytokines: dose-response relationship, mechanisms and implications. *Radiat Environ Biophys* **46**, 21-9.
142. Eissner, G., Lindner, H., Behrends, U., Kolch, W., Hieke, A., Klauke, I., Bornkamm, G.W., Holler, E. (1996) Influence of bacterial endotoxin on radiation-induced activation of human endothelial cells in vitro and in vivo: protective role of IL-10. *Transplantation* **62**, 819-27.
143. Gerbitz, A., Nickoloff, B.J., Olkiewicz, K., Willmarth, N.E., Hildebrandt, G., Liu, C., Kobzik, L., Eissner, G., Holler, E., Ferrara, J.L., Cooke, K.R. (2004) A role for tumor necrosis factor-alpha-mediated endothelial apoptosis in the development of experimental idiopathic pneumonia syndrome. *Transplantation* **78**, 494-502.
144. Cantisani, V., Mortele, K.J., Viscomi, S.G., Glickman, J., Silverman, S.G., Ros, P.R. (2003) Rectal inflammation as first manifestation of graft-vs-host disease: radiologic-pathologic findings. *Eur Radiol* **13 Suppl 4**, L75-8.

145. Worthington, J., Cullen, S., Chapman, R. (2005) Immunopathogenesis of primary sclerosing cholangitis. *Clin Rev Allergy Immunol* **28**, 93-103.
146. O'Mahony, C.A., Vierling, J.M. (2006) Etiopathogenesis of primary sclerosing cholangitis. *Semin Liver Dis* **26**, 3-21.
147. Maggs, J.R., Chapman, R.W. (2007) Sclerosing cholangitis. *Curr Opin Gastroenterol* **23**, 310-6.
148. Broome, U., Hauzenberger, D., Klominek, J. (1996) Adhesion molecules in primary biliary cirrhosis and primary sclerosing cholangitis. *Hepatogastroenterology* **43**, 1109-12.
149. Farrant, J.M., Hayllar, K.M., Wilkinson, M.L., Karani, J., Portmann, B.C., Westaby, D., Williams, R. (1991) Natural history and prognostic variables in primary sclerosing cholangitis. *Gastroenterology* **100**, 1710-7.
150. Adams, D.H., Eksteen, B. (2006) Aberrant homing of mucosal T cells and extra-intestinal manifestations of inflammatory bowel disease. *Nat Rev Immunol* **6**, 244-51.
151. Szabo, C., Day, B.J., Salzman, A.L. (1996) Evaluation of the relative contribution of nitric oxide and peroxynitrite to the suppression of mitochondrial respiration in immunostimulated macrophages using a manganese mesoporphyrin superoxide dismutase mimetic and peroxynitrite scavenger. *FEBS Lett* **381**, 82-6.
152. Suematsu, N., Tsutsui, H., Wen, J., Kang, D., Ikeuchi, M., Ide, T., Hayashidani, S., Shiomi, T., Kubota, T., Hamasaki, N., Takeshita, A. (2003) Oxidative stress mediates tumor necrosis factor-alpha-induced mitochondrial DNA damage and dysfunction in cardiac myocytes. *Circulation* **107**, 1418-23.
153. Simmonds, N.J., Allen, R.E., Stevens, T.R., Van Someren, R.N., Blake, D.R., Rampton, D.S. (1992) Chemiluminescence assay of mucosal reactive oxygen metabolites in inflammatory bowel disease. *Gastroenterology* **103**, 186-96.
154. Rachmilewitz, D., Stamler, J.S., Bachwich, D., Karmeli, F., Ackerman, Z., Podolsky, D.K. (1995) Enhanced colonic nitric oxide generation and nitric oxide synthase activity in ulcerative colitis and Crohn's disease. *Gut* **36**, 718-23.
155. Ishihara, T., Tanaka, K., Tasaka, Y., Namba, T., Suzuki, J., Okamoto, S., Hibi, T., Takenaga, M., Igarashi, R., Sato, K., Mizushima, Y., Mizushima, T. (2009) Therapeutic effect of lecithinized superoxide dismutase against colitis. *J Pharmacol Exp Ther* **328**, 152-64.
156. Kruidenier, L., Verspaget, H.W. (2002) Review article: oxidative stress as a pathogenic factor in inflammatory bowel disease--radicals or ridiculous? *Aliment Pharmacol Ther* **16**, 1997-2015.
157. Roza, A.M., Cooper, M., Pieper, G., Hilton, G., Dembny, K., Lai, C.S., Lindholm, P., Komorowski, R., Felix, C., Johnson, C., Adams, M. (2000) NOX 100, a nitric oxide scavenger, enhances cardiac allograft survival and promotes long-term graft acceptance. *Transplantation* **69**, 227-31.
158. Amer, J., Weiss, L., Reich, S., Shapira, M.Y., Slavin, S., Fibach, E. (2007) The oxidative status of blood cells in a murine model of graft-versus-host disease. *Ann Hematol* **86**, 753-8.
159. Piao, X.L., Cho, E.J., Jang, M.H., Cui, J. (2009) Cytoprotective effect of lignans from Forsythia suspensa against peroxynitrite-induced LLC-PK1 cell damage. *Phytother Res* **23**, 938-42.

160. Butcher, E.C., Picker, L.J. (1996) Lymphocyte homing and homeostasis. *Science* **272**, 60-6.
161. Bryson, J.S., Jennings, C.D., Brandon, J.A., Perez, J., Caywood, B.E., Kaplan, A.M. (2007) Adoptive transfer of murine syngeneic graft-vs.-host disease by CD4+ T cells. *J Leukoc Biol* **82**, 1393-400.
162. Ferret, P.J., Hammoud, R., Tulliez, M., Tran, A., Trebeden, H., Jaffray, P., Malassagne, B., Calmus, Y., Weill, B., Batteux, F. (2001) Detoxification of reactive oxygen species by a nonpeptidyl mimic of superoxide dismutase cures acetaminophen-induced acute liver failure in the mouse. *Hepatology* **33**, 1173-80.
163. Malassagne, B., Ferret, P.J., Hammoud, R., Tulliez, M., Bedda, S., Trebeden, H., Jaffray, P., Calmus, Y., Weill, B., Batteux, F. (2001) The superoxide dismutase mimetic MnTBAP prevents Fas-induced acute liver failure in the mouse. *Gastroenterology* **121**, 1451-9.
164. Prasad, N.R., Menon, V.P., Vasudev, V., Pugalendi, K.V. (2005) Radioprotective effect of sesamol on gamma-radiation induced DNA damage, lipid peroxidation and antioxidants levels in cultured human lymphocytes. *Toxicology* **209**, 225-35.
165. Kumar, K.B., Kuttan, R. (2004) Protective effect of an extract of Phyllanthus amarus against radiation-induced damage in mice. *J Radiat Res (Tokyo)* **45**, 133-9.
166. Cooke, C.L., Davidge, S.T. (2002) Peroxynitrite increases iNOS through NF-kappaB and decreases prostacyclin synthase in endothelial cells. *Am J Physiol Cell Physiol* **282**, C395-402.
167. Bryk, R., Wolff, D.J. (1998) Mechanism of inducible nitric oxide synthase inactivation by aminoguanidine and L-N6-(1-iminoethyl)lysine. *Biochemistry* **37**, 4844-52.
168. Zhao, H., Ma, J.K., Barger, M.W., Mercer, R.R., Millecchia, L., Schwegler-Berry, D., Castranova, V., Ma, J.Y. (2009) Reactive oxygen species- and nitric oxide-mediated lung inflammation and mitochondrial dysfunction in wild-type and iNOS-deficient mice exposed to diesel exhaust particles. *J Toxicol Environ Health A* **72**, 560-70.
169. Diefenbach, A., Schindler, H., Rollinghoff, M., Yokoyama, W.M., Bogdan, C. (1999) Requirement for type 2 NO synthase for IL-12 signaling in innate immunity. *Science* **284**, 951-5.
170. Hill, G.R., Teshima, T., Gerbitz, A., Pan, L., Cooke, K.R., Brinson, Y.S., Crawford, J.M., Ferrara, J.L. (1999) Differential roles of IL-1 and TNF-alpha on graft-versus-host disease and graft versus leukemia. *J Clin Invest* **104**, 459-67.
171. Picarella, D., Hurlbut, P., Rottman, J., Shi, X., Butcher, E., Ringler, D.J. (1997) Monoclonal antibodies specific for beta 7 integrin and mucosal addressin cell adhesion molecule-1 (MAdCAM-1) reduce inflammation in the colon of scid mice reconstituted with CD45RBhigh CD4+ T cells. *J Immunol* **158**, 2099-106.
172. Cooke, K.R., Hill, G.R., Gerbitz, A., Kobzik, L., Martin, T.R., Crawford, J.M., Brewer, J.P., Ferrara, J.L. (2000) Hyporesponsiveness of donor cells to lipopolysaccharide stimulation reduces the severity of experimental idiopathic pneumonia syndrome: potential role for a gut-lung axis of inflammation. *J Immunol* **165**, 6612-9.

VITA

JACQUELINE PEREZ
Birthplace: Lebanon, Pennsylvania, USA
December 27, 1979

EDUCATION

B.S. in Biology, *Magna Cum Laude*, University of Puerto Rico, Rio Piedras, PR, June 2002

PROFESSIONAL BACKGROUND AND EXPERIENCE

1/04 – 9/02	Abbott Laboratory Inc, Barceloneta PR: Biochemical Laboratory Technician for ADI Supervisor: Leslie Raices
5/02 – 8/01	University of Puerto Rico: Teaching Assistant for the Animal Organismal (Zoology) Laboratory Major Professor: Omar Perez
8/01- 6/01	University of Kentucky: Undergraduate Summer Research Assistant, Graduate Center for Toxicology Major Profesor: Dr. Linda Dwoskin

GRANTS AND FUNDING

7/08-1/04	Toxicology Training Grant Recipient
8/01-6/01	NIEHS Environmental Toxicology-Short Term Training Grant

AWARDS AND HONORS

4/08	AAI Minority Scientist Travel Award-FASEB MARC Program
4/08	UK Graduate School Travel Award to 2008 Annual American Association of Immunologist (AAI) Meeting-Experimental Biology
11/07	John Wallace Diversity Scholarship
2002-1999	Who's who Among American Universities and College Students
2002-1999	Dean's Honor List
2002-1999	University of Puerto Rico Natural Sciences Honor Roll
05/98	Robert C. Byrd Scholarship

PROFESSIONAL ACTIVITIES

2006 – 2008	Treasurer of Toxicology Student Forum, Graduate Center for Toxicology, University of Kentucky

PUBLICATIONS

J. Perez, J.A. Brandon, C.D. Jennings, B.Caywood, A.M. Kaplan, and J.S. Bryson. "Role of oxidative stress in the development of murine Syngeneic Graft-Versus-Host Disease", Manuscript in preparation.

J. Perez, J.A. Brandon, C.D. Jennings, B.Caywood, A.M. Kaplan, and J.S. Bryson. "$CD4^+$ T cells accumulate in the colon of CsA-treated mice following myeloablative conditioning and bone marrow transplantation", 2009, Submitted for publication (Journal of Leuckocyte Biology).

J.A. Brandon, **J. Perez**, C.D. Jennings, A.M. Kaplan and J.S. Bryson. "Murine syngeneic graft-versus-host disease: A unique model for chronic liver", 2009, Submitted for publication (GUT Journal).

Bryson J.S, C.D. Jennings, J..A. Brandon, **J. Perez**, B.Caywood and A.M. Kaplan. "Adoptive Transfer of Murine Syngeneic Graft-Versus-Host Disease by $CD4^+$ T cells", **2007**, J. Leukoc. Biol. 82(6):1393-400.

J.A. Brandon, C.D. Jennings, **J. Perez**, B.Caywood, A.M. Kaplan and J.S. Bryson. "Recipient T Cells Participate in the Induction of Murine Syngeneic Graft-Versus-Host Disease (SGVHD)", **2007**, Transplantation 83(12):1620-7.

PRESENTATIONS

J. Perez, J.A. Brandon, C.D. Jennings, B.Caywood, A.M. Kaplan, J.S. Bryson. Treatment with antioxidant reduces intestinal pathology associated with Syngeneic Graft-Versus-Host Disease (SGVHD), Markey Cancer Center Research Day, October 30, 2008, University of Kentucky, Lexington, KY.

J. Perez, J.A. Brandon, C.D. Jennings, B.Caywood, A.M. Kaplan, J.S. Bryson. Treatment with antioxidant reduces intestinal pathology associated with Syngeneic Graft-Versus-Host Disease (SGVHD), Department of Microbiology, Immunology and Molecular Genetics 2nd Retreat, October 16, 2008, Four Point by Sheraton, Lexington, KY.

J. Perez, J.A. Brandon, C.D. Jennings, B.Caywood, A.M. Kaplan, J.S. Bryson. Reduction of Murine Syngeneic Graft-Versus-Host Disease (SGVHD) following treatment with superoxide dismutase mimetic MnTBAP, 95th Annual American Association of Immunologist (AAI) Meeting-Experimental Biology 2008, April 5-9, 2008, San Diego, CA.

J. Perez, J.A. Brandon, C.D. Jennings, B.Caywood, A.M. Kaplan, J.S. Bryson. Role of CsA induced Oxidative Stress in the Development of Syngeneic Graft-Versus-Host Disease (SGVHD), 36th Annual Autumn Immunology Conference, November 21-24, 2007, Chicago, IL.

J. Perez, J.A. Brandon, C.D. Jennings, B.Caywood, A.M. Kaplan, J.S. Bryson. Role of CsA induced Oxidative Stress in the Development of Syngeneic Graft-Versus-Host Disease (SGVHD), Department of Microbiology, Immunology and Molecular Genetics Retreat, October 5, 2007, Holiday Inn Lexington-North, Lexington, KY.

J. Perez, J.A. Brandon, C.D. Jennings, B.Caywood, A.M. Kaplan, J.S. Bryson. Role of CsA induced Oxidative Stress in the Development of Syngeneic Graft-Versus-Host Disease (SGVHD), Markey Cancer Center Research Day, September 27, 2007, University of Kentucky, Lexington, KY.

J.A. Brandon, C.D. Jennings, **J. Perez**, B.Caywood, A.M. Kaplan, J.S. Bryson. Recipient T Cells from Lethally Irradiated Bone Marrow Reconstituted Mice Participate in the Induction of Murine Syngeneic Graft-Versus-Host Disease (SGVHD), 35th Annual Autumn Immunology Conference, November 17-19, 2006, Chicago, IL

J. Perez, S.W. Goes, J.A. Brandon, C.D. Jennings, B.Caywood, A.M. Kaplan, J.S. Bryson. CD4+ Memory T cells Increase During Induction of Syngeneic Graft-Versus-Host Disease (SGVHD), 4th Annual Midwest Blood Club Symposium, April 6-7, 2006, Lexington, KY.

L.D. Palmer, **J. Perez**, S.W. Goes, B.E. Caywood, C.D. Jennings, A.M. Kaplan, and J.S. Bryson. "Cyclosporine A-Induced Increase in Liver NK Cells Following Syngeneic Bone Marrow Transplantation". 4th Annual Midwest Blood Club Symposium, April 6-7, 2006, Lexington, KY.

J.A. Brandon, C.D. Jennings, **J. Perez**, D. Alapat, B. Caywood, A.M. Kaplan, J.S. Bryson. "Induction of Murine Syngeneic Graft-versus-Host Disease (SGVHD) by Recipient T Cells". 4th Annual Midwest Blood Club Symposium, April 6-7, 2006, Lexington, KY.

J.A. Brandon, C.D. Jennings, **J. Perez**, D. Alapat, B. Caywood, A.M. Kaplan, J.S. Bryson. "Induction of Murine Syngeneic Graft-versus-Host Disease (SGVHD) by Recipient T Cells". ASBMT 2006 BMT Tandem Meeting, February 16-20, 2006. Honolulu, Hawaii.

J.A. Brandon, C.D. Jennings, **J. Perez**, B. Caywood, A.M. Kaplan, J.S. Bryson. Recipient T Cells Participate in the Induction of Murine Syngeneic Graft-Versus-Host Disease (SGVHD), 34th Annual Autumn Immunology Conference, November 19-21, 2005, Chicago, IL.

PROFESSIONAL SOCIETIES

2008	American Association of Immunologist
2001-Present	Golden Key International Honor Society